Smart PEV Charging Station Operation and Design Considering Distribution System Impact

by

Omar Hafez

A thesis
presented to the University of Waterloo
in fulfillment of the
thesis requirement for the degree of
Doctor of Philosophy
in
Electrical and Computer Engineering

Waterloo, Ontario, Canada, 2016

AUTHOR'S DECLARATION

I hereby declare that I am the sole author of this thesis. This is a true copy of the thesis, including any required final revisions, as accepted by my examiners.

I understand that my thesis may be made electronically available to the public.

Abstract

Penetration of plug-in electric vehicles (PEVs) into the market is expected to be large in the near future. Also, as stated by the Ontario Ministry of Transportation, the province is investing $20 million from Ontario's Green Investment Fund to build nearly 500 electric vehicle charging stations (EVCSs) at over 250 locations in Ontario by 2017. Therefore, estimating PEV charging demand at an EVCS with their complex charging behavior, their impact on the power grid, and the optimal design of EVCS need be investigated.

This thesis first presents a queuing analysis based method for modeling the 24-hour charging load profile of EVCSs. The queuing model considers the arrival of PEVs as a non-homogeneous Poisson process with different arrival rates over the day; considering customer convenience and charging price as the factors that influence the hourly arrival rate of vehicles at the EVCS. One of the main contributions of the thesis is to model the PEV service time considering the state-of-charge of the battery and the effect of the battery charging behavior. The impact of PEV load models on distribution systems is studied for a deterministic case, and the impact of uncertainties is examined using the stochastic optimal power flow and Model Predictive Control approaches.

The thesis presents a novel mathematical model for representing the total charging load at an EVCS in terms of controllable parameters; the load model developed using a queuing model followed by a neural network (NN). The queuing model constructs a data set of PEV charging parameters which are input to the NN to determine the controllable EVCS load model. The smart EVCS load is a function of the number of PEVs charging simultaneously, total charging current, arrival rate, and time; and various class of PEVs. The EVCS load is integrated within a distribution operations framework to determine the optimal operation and smart charging schedules of the EVCS. Objective functions from the perspective of the local distribution company (LDC) and EVCS owner are considered for studies. The performance of a smart EVCS vis-à-vis an uncontrolled EVCS is examined to emphasize the demand response (DR) contributions of a smart EVCS and its integration into distribution operations.

Finally, the thesis presents the optimal design of an EVCS with the goal of minimizing the life-cycle cost, while taking into account environmental emissions. Different supply options such as renewable energy technology based and diesel generation, with realistic inputs on their physical, operating and economic characteristics are considered, in order to arrive at the optimal design of EVCS. The charging demand of the EVCS is estimated considering real drive data. Analysis is also carried out to compare the economics of a grid-connected EVCS with an isolated EVCS and the optimal break-even distance is determined. Also, the EVCS is assumed to be connected to the grid as a smart energy hub based on different supply options.

Acknowledgments

First and foremost, I would like to thank and praise Allah for helping me through this work and for providing me with all the great ideas, patience and health necessary for completion my PhD degree.

Then, I would like to express my sincere gratitude to my supervisor Professor Kankar Bhattacharya, for his invaluable support, guidance and patience during the course of my PhD studies. It has truly been an honour and privilege to have completed my studies under his supervisions. His professionalism, thoughtful guidance, and positive feedback have helped me throughout my studies.

I owe my deepest gratitude to my PhD committee for their valuable comments, inputs, and suggestions, that helped improve this work: Professor Rajiv Varma from the Department of Electrical and Computer Engineering, Western University, London; Professor Sagar Naik, Dr. Mohamed Ahmed, and Dr. Tarek Abdelgalil from the Department of Electrical and Computer Engineering, University of Waterloo; Dr. Amir Hajimiragha from the Department of Chemical Engineering, University of Waterloo.

I gratefully appreciate the financial support from Saudi Cultural Bureau in Canada and my employer, Umm Al-Qura University, Saudi Arabia.

I would also thank all my colleagues in our labs for making them a friendly environment to work in, I really enjoyed it.

Many thanks also go to all technical and academic support provided by the Department of Electrical and Computer Engineering at the University of Waterloo.

A heartfelt gratitude to my family and in-laws for their unconditional support, encouragement, love, and care. To my beloved father, Abdul Aziz, you are my inspiration to excel in everything that I do, and I know that I get my passion for knowledge and learning from you. To my amazing mother, Ruhiyya, your endless love, and nurturing is the reason that I have been able to reach this point in my life, and for your patient and understanding, even though it meant being away from you. To my sister Summaiah, brothers, Mohammed, Yousef, and Abdullah, I am blessed to have you looking out for me always. Thank you for being there for me throughout my ups and downs.

To my beautiful and loving wife, Alaa, your endless love, and nurturing is the reason that I have been able to reach this point in my life, and no amount of thanks will be enough for the way you have supported and encouraged me in my passion to learn. To my beloved daughter, Lamar, and Taha (son), many thanks for your true endless love, patient and honest support which inspired me to work hard and achieve what we are now proud of. Whatever I am today, and where I stand today is because of all of you, and I shall always strive to make you proud.

To my wonderful in-laws, Tawfiq (father in-law), and Sanaa (mother in-law), I am truly blessed to have you in my life. There was no end to the encouragement I always received from all of you, and it always raised my spirits.

I dedicate this thesis to my parents, my family in-laws, sister, brothers, my wife Alaa Hakeem, my daughter Lamar and my son Taha with love and appreciation.

Table of Contents

List of Figures

List of Tables

List of Abbreviations

BCB	Battery Charging Behavior
BESS	Battery Energy Storage System
COE	Cost of Energy
CSCLE	Charging Station Controllable Load Estimator
DR	Demand Response
EVCS	Electric Vehicle Charging Station
FIT	Feed-In-Tariff
GHG	Green House Gas
HOMER	Hybrid Optimization of Multiple Energy Resources
LDC	Local Distribution Company
LF	Load Flow
MPC	Model Predictive Control
NHTS	National Household Travel Survey
NN	Neural Network
NPC	Net Present Cost
O&M	Operation and Maintenance
OPF	Optimal Power Flow
PEV	Plug-in Electric Vehicle
PV	Photovoltaic
SLF	Stochastic Load Flow
SOC	State-Of-Charge
SOPF	Stochastic Optimal Power Flow
TOU	Time-Of-Use
TTS	Transportation Tomorrow Survey
WISE	Waterloo Institute for Sustainable Energy

Chapter 1
Introduction

1.1 Motivation

The global demand for energy has been increasing rapidly, which impose a large burden on the existing energy resources, and adversely impacts the environment and global warming. As governments around the world move toward a green energy economy, Plug-in Electric Vehicles (PEVs) have an increasingly important role to play, because of their contribution to emissions reduction from the transport sector. In Canada, almost 35% of the total energy demand is from the transport sector and it is the second largest source of greenhouse gas (GHG) emissions [1]. By the end of the year 2025 most of the electricity generation in Ontario, Canada, is planned to be environmentally friendly. Figure 1.1 presents the planned supply mix in Ontario by 2025 [2].

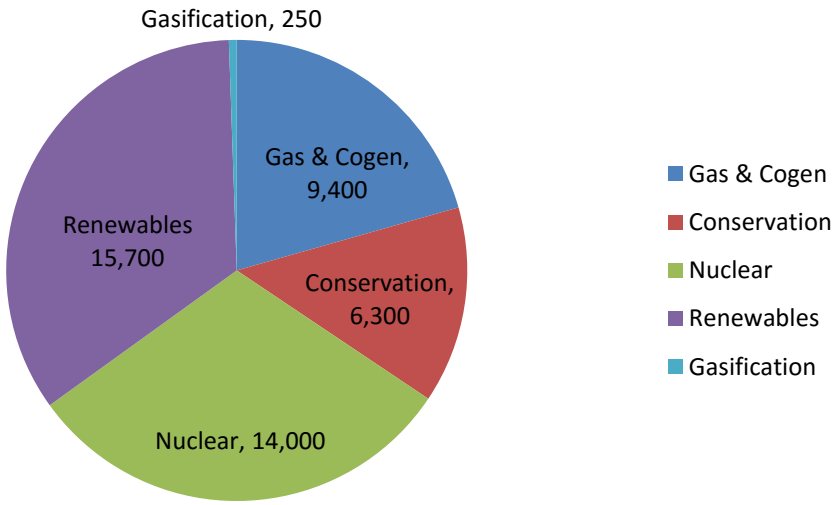

Figure 1.1: Ontario plan supply mix (in MW) by 2025 [2].

The Ontario Green Energy Act (GEA) of 2009 proposed to reduce the province's impact on GHG emissions, and create significant employment opportunities in a green economy [3]. The Government of Ontario chalked out a path to move toward a green energy economy through increased penetration of renewable energy sources and PEVs [2], which present significant potential of solving environmental and economic problems. GHG emission from gasoline vehicles is significantly higher than from Battery Electric Vehicles (BEV), Plug-in Hybrid Electric Vehicles (PHEV), and Hybrid Electric Vehicles (HEV), as shown in Figure 1.2 [4].

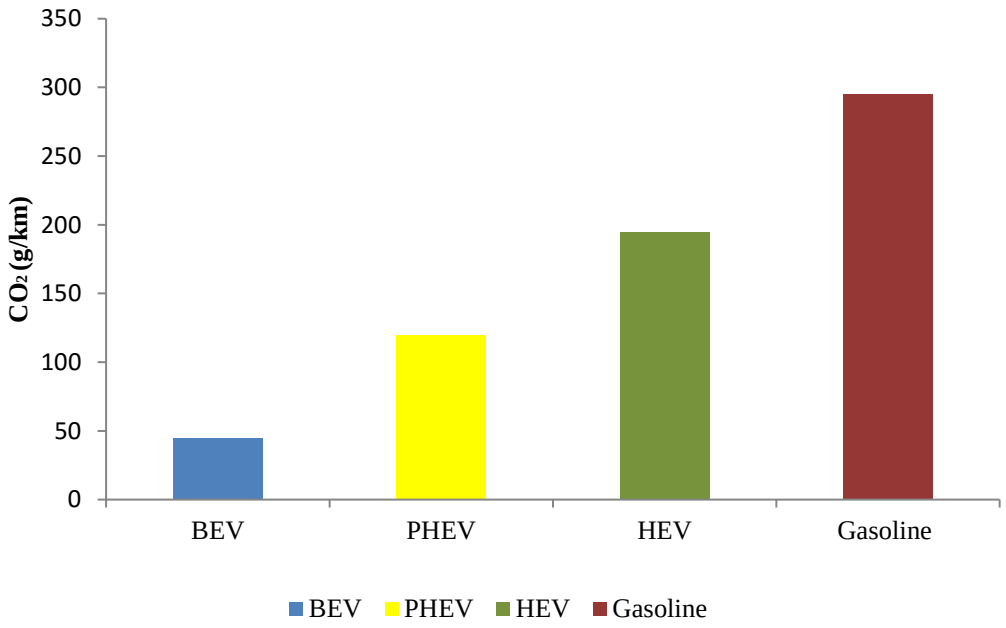

Figure 1.2: GHG emissions from electric vehicles vis-à-vis gasoline vehicles in Ontario [4].

The development and penetration of PEVs are strongly supported and encouraged by the governments because PEVs have minimal gasoline consumption and do not directly produce GHG emissions. For example, in Ontario, customers are eligible for up to $10,000 in rebates when purchasing certain BEVs or PHEVs [5]. Sales of PEVs are expected to accelerate rapidly over the next several years; Figure 1.3 presents the annual sales of light duty PEVs in different provinces of Canada and, it is noted that, Ontario is one of the top provinces with sales expected to reach over 50,000 vehicles by 2020 [6].

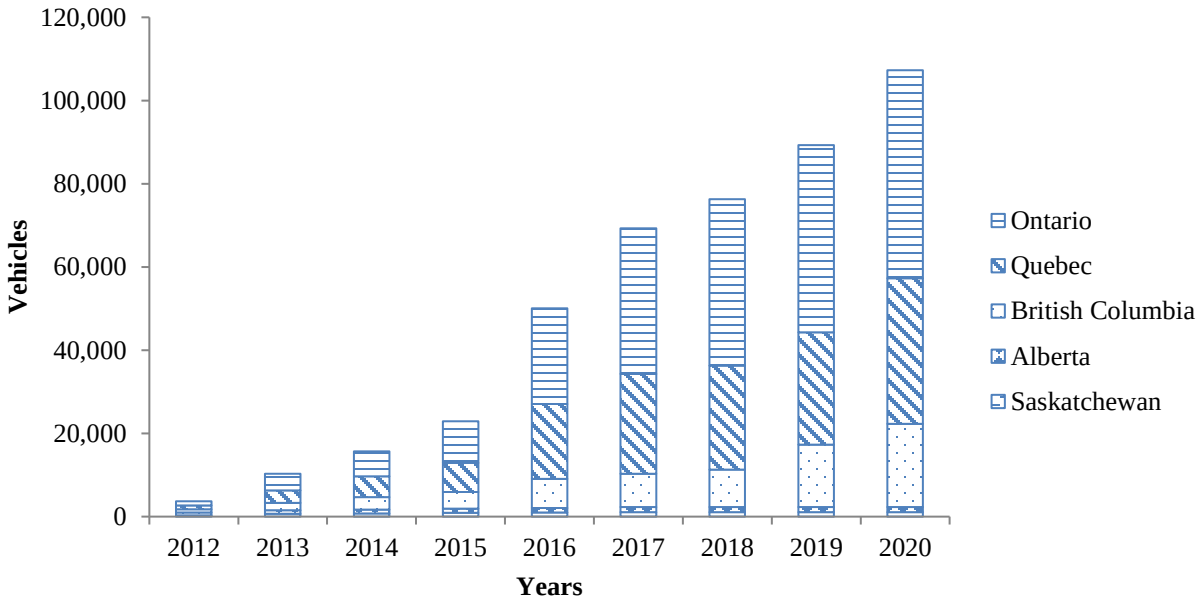

Figure 1.3: Annual light duty PEV sales in different provinces across Canada [6].

Penetration of PEVs into the market is expected to be large in the near future, and with their complex charging behavior, many technical problems related to their impact on the power grid need be investigated. Since the charging behavior of PEVs is dependent on a number of factors, their overall charging demand tends to be uncertain as well.

From the Local Distribution Company's (LDCs) perspective, meeting the increased demand arising from charging of the PEVs, while satisfying the distribution system operating constraints, and reducing the system losses, is a major challenge. On the other hand, the PEV charging demand will depend on the customers' convenience and their response to PEV charging price, *i.e.*, the peak PEV charging demand is expected when it is more convenient for customers to charge their PEVs or when the charging price is low. The PEV arrival rate at a charging station will vary accordingly. Therefore, the integration of the PEV customer behavior to estimate PEV charging demand is a critical issue which needs to be investigated.

Furthermore, it can be noted that the charging demand at an Electrical Vehicle Charging Station (EVCS) is affected by different factors, such as the number of PEVs arriving at an hour (λ), number of PEVs being charged simultaneously (N), the state of

charge (SOC) of the PEV battery, charging levels, battery capacity, charging duration, etc. Some of these parameters are independent processes, such as the arrival rate λ; and some are dependent on the PEV type, such as battery capacity, or battery charging behavior (BCB); while some others are dependent on the PEV driving patterns, such as the SOC of the PEV battery and the charging duration. Note that, some of the parameters of the EVCS can be controlled effectively, such as N, the number of PEVs charging simultaneously. However, in order to do so, there is a need to effectively model the EVCS load as a function of various input parameters and controllable variables. So far, to the best knowledge of the author there is no reported work that examines how the EVCS load can be modeled as a smart load, nor any attempt has been made to integrate the same, within a larger operations framework of the distribution system for demand response (DR) provisions.

Penetration of renewable energy sources into distribution systems are gradually being recognized as important alternatives and has been attracting the attention of policy makers and researchers because of their friendliness to the environment and potential to reduce dependence on fossil fuels. However, these sources, such as, wind and solar PV, are intermittent and increases the uncertainty in the distribution system operation. Also, the interactions between renewable energy sources and PEVs have complicated implications on distribution system operations and economics. As stated by the Ontario Ministry of Transportation, the province is investing $20 million from Ontario's Green Investment Fund to build nearly 500 EVCS at over 250 locations in Ontario by 2017 [5]. Therefore, the optimal design of EVCS in the presence of renewable energy sources need be discussed and their optimal coordination carefully determined.

1.2 Literature Review

1.2.1 PEV Load Modeling

Penetration of PEVs into the market is expected to be large in the near future, and with their complex charging behavior, their charging load models need be investigated. Since the charging behavior of PEVs is dependent on a number of factors, their overall charging

demand tends to be uncertain. Several research studies have considered modeling of PEV charging demand considering uncertainty.

An optimization model based on a simplified zonal model of Ontario's electricity-transmission network is presented in [7] that determines the optimal and maximum allowable penetration of PHEVs into Ontario's transport sector. It is noted that the present and projected electricity grid of Ontario can be optimally exploited for charging approximately 500,000 PHEVs without the need for any additional transmission or generation investments beyond those currently planned.

Analysis of the available load and transportation data to extract probability density functions (pdf) describing different uncertainties characterizing PEV charging, is presented in [8], and Monte Carlo simulation is carried out to take into account these uncertainties and predict the anticipated impacts of PHEVs on a representative test network.

An integrated agent based model combining power system models, agent based transport simulations, and models of specific vehicle technologies is developed in [9] to estimate the daily behavior of electric vehicles (EVs) and individual battery energy levels at different locations of the vehicles during the day. It is concluded that using control signals can mitigate network congestion.

In [10], a modified Latin hypercube sampling method is used to calculate the charging load of PEVs while considering their stochastic behavior. A two-stage optimization model determines the optimal charging states of PEVs on a given day. In the first stage, the peak load including the charging load of PEVs is minimized while the load fluctuation is minimized in the second-stage with peak load being fixed at the value obtained from the first stage. The developed PEV charging load model is used to determine the benefits and cost of PEV charging and discharging coordination strategies from a social welfare stand point.

Usage data from 76 vehicles over a one-year period from Winnipeg, Canada is analyzed in [11] to estimate the PEV charging profiles and their impact on utility load. It is observed that the proposed stochastic models with conditional pdfs can improve the accuracy of the predictions compared to a deterministic model.

The travel patterns of light-duty vehicles in the USA obtained from the 2009 National Household Travel Survey (NHTS) [12] is used in [13] to estimate the electrical energy and power consumption of PEVs for two uncontrolled charging scenarios.

A modeling methodology is proposed in [14], where detailed vehicle usage patterns are taken into account and statistical distributions of charging energies are produced to develop statistical charging load models of PHEVs considering the US NHTS data [12].

In [15], a PHEV home charging load model based on residential activity patterns is proposed. The developed load model is used to control PHEV usage and other residential electricity activities to hours with lower demand. From a comparison of the residential load standard deviation with and without PHEV charging it is noted that the most likely charging time is the afternoon, and the PHEV represents 1/3 of the total expected load during the peak load and around a fifth of the total daily electric energy used.

A decentralized random access framework considering the NHTS 2009 data [12] and the RELOAD database [16] is proposed in [17] to schedule PHEV charging considering grid constraints. Thereafter, the scheduled PHEV charging load is used to examine the impact on grid operations.

The optimal daily charging schedule of EVs considering both system and customer uncertainties is presented in [18], using a multi-period three-phase unbalanced load flow and rolling-horizon optimization method. The proposed model focusses on controlling the rate and times at which EVs charge over a 24-h time horizon, with a minimum cost objective, subject to certain constraints, and ensuring that individual phases are not overloaded.

The charging demand of PEVs is affected by different factors, such as the number of PEVs being charged simultaneously, their charging levels, battery capacity, and charging duration, all of which are uncertain. Monte Carlo simulation is used in [19] to generate virtual trip distances considering driving habits, different vehicle models, etc., and hence a novel annual energy consumption model is formulated for light duty fleet of PEVs.

A stochastic unit commitment model is used in [20] to study the impact of PHEV charging patterns on power system operations and scheduling. Coordination of thermal

generating units, PHEV charging loads, and large-scale wind penetration is considered. Daily charging demands of various types of PHEVs are estimated on the basis of a PHEV population projection and transportation survey. It is noted that a smart charging schedule for PHEVs can reduce the operating cost of the power system and compensate for the fluctuations in wind generation.

Three different charging strategies- uncontrolled, minimization of network losses, and minimization of the electricity cost paid by PEV owners, considering demographic data and the NHTS 2009 data base [12], is presented in [21] to estimate the impact of PEV charging in a real open-loop radial distribution system. The results show that the developed model reduces the impact of PEV charging on the residential distribution systems.

In [22], a decentralized PEV charging scheme is proposed where the system operator sends price-based signal to PEV aggregators. It also examines a simple price-only control signal based PEV charging mechanism and compares it with the price/quantity signal mechanism.

A decision support algorithm and market participation policy using dynamic programming based on New York Independent System Operator data is developed in [23] for a load aggregator which submits inflexible and flexible bids to a liberalized hour-ahead power market, while monitoring localized feeder and PEV rate constraints and manages the charging of PEVs connected at the distribution network.

A three level hierarchical control algorithm to determine the cooperation between PEVs and wind power is presented in [24]. Grid frequency is used as the feedback signal to control PEV charging, which thus, serves as an ancillary service to the grid. The grid frequency regulation is improved and overall cost is minimized using the proposed algorithm.

1.2.2 Queuing Models Based PEV Load Model and Smart PEV Charging

Modeling the PEV charging demand using queuing analysis considering different characteristics is discussed in several studies.

In [25], a max-weight PEV dispatch algorithm based on a queuing formulation, integrated with renewable energy sources is used to control PEV charging in order to avoid costly distribution system infrastructure upgrades.

A probabilistic constrained load flow problem with stochastic wind generation and EV demand is presented in [26] where customers are assumed to be served at the charging station in M/M/∞ queue, and the number of charged/discharged EVs is modelled by Poisson distribution and their service time follows an exponential distribution. The settings of discrete and continuous control variables in the probabilistic constrained load flow problem are determined using a hybrid learning automata system.

The spatial and temporal distribution of demand, based on fluid dynamic traffic model and M/M/s queuing is used to develop the charging demand model for a rapid charging station in [27]. The highway Poisson-arrival-location model is used to estimate the arrival rate of electrical vehicles at the charging station.

A probabilistic power flow is proposed in [28] to study the impact of PHEV charging on the power grid. Four different types of PHEVs are considered and the factors that affect their charging behavior such as, battery capacity, and charging level, are discussed. A single PHEV charging demand model is formulated and queuing theory is used to describe the behavior of multiple PHEVs at an EVCS and a local residential community.

A real-time load management algorithm based on maximum sensitivities selection is developed in [29] to improve the grid performance with high penetration of PEVs. The coordination of PEV charging is based on real-time cost minimization while maintaining voltage profiles and generation limits. It is noted that the proposed algorithm is able to reduce the overall system load and power peaks, thus resulting in energy savings and cost reduction.

In recent research, the Model Predictive Control (MPC) approach has been applied to various operational and control problems in the context of smart grids to consider the effect of uncertainties. In [30], a prediction based real-time charging method is proposed that considers the effect of future vehicles penetrating into the grid. In [31], a power dispatch problem using MPC based approach is formulated for a distribution system with a high

penetration of renewable energy resources and PEVs. The proposed MPC-based dispatch is able to accommodate the inherent uncertainty and variability of the PEV charging loads.

Most of the works on PEV charging demand modeling that use queuing analysis [26-28], consider the arrival rates as a Poisson process, which is a stochastic process that assumes the PEVs to have a constant arrival rate. Only a few researchers have modeled the arrival rate as a non-homogeneous Poisson process [32]. Moreover, the charging time is typically modeled by exponential distributions with given upper and lower limits, which are randomly assigned to each PEV, and the waiting time is assumed to be infinite. Furthermore, it should be noted that during the fast charging process, the charging power typically starts at a high rate, and drops off as the battery SOC approaches its full capacity, as per the BCB of PEVs [33].

Moreover, different charging facilities have been studied by researchers for example; day-time charging scenarios for PEVs at parking lots are studied in [34] using a two-stage approximate dynamic programming framework to determine the optimal charging strategies. A case study of a residential parking lot charging station [35] examines how many charging spots can be reduced by encouraging customers to charge at off-peak hours, while in [36], an online management strategy is proposed that enables aggregators in public parking lots to dynamically manage PEV charging to maximize the owners' interests.

In the literature, two broad strategies for smart charging of PEVs are reported. In decentralized smart charging, the charging strategy is determined by individual PEV owners [37] while centralized smart charging strategy is generally determined by the LDC considering its own objectives and the charging schedule is communicated to the PEV owners [38]. In [39] a strategy for optimizing the charging rates of EVs based on a local control charging method is proposed to deliver the maximum amount of energy to the EVs while maintaining the network within acceptable operating limits. In the local control charging method, the optimal charging rates of the EVs is determined individually based on local network conditions and their battery SOC. A comparison between the centralized and

decentralized charging strategies is made; and the advantages and disadvantages of each are presented.

In [40], it is noted that the integration of large number of EVs in the system can be managed without the need for grid reinforcements by the adoption of advanced centralized EV charging control strategies. Additionally, the adoption of these charging schemes allow operating the networks in less stressed conditions, with improved voltage profiles and lower congestion levels. Also, the impact of EV charging on a medium-voltage network and the LDC's benefits arising from the use of smart charging schemes are discussed.

1.2.3 Impact of PEV Penetration on the Distribution System

As we move toward a greener future, the PEVs have an increasingly important role to play, because of their contribution to emissions reduction from the transport sector. However, increased numbers of PEVs can have a significant impact on the power distribution system performance. Several studies show that the power distribution grid can be significantly impacted by high penetration levels of PEVs.

An optimal load management strategy based on a quadratic cost formulation is presented in [41]. It is noted that EV charging will likely coincide with the system peak demand and thus, in order to avoid overloading of the distribution feeders, adequate load management schemes need be in place.

The impact of uncoordinated PHEV charging on system peak load, losses, voltage and system load factor are discussed in [42] and is noted to have adversely affected the efficiency of the distribution grid. An optimal coordinated charging strategy to minimize the power losses and maximize the grid load factor is proposed.

Three optimal coordinated PHEV charging algorithms with the objectives of minimizing the load factor and load variance are proposed in [43] to study the impact of PHEV charging on the distribution system. Coordinated charging of PHEVs is also considered and it is shown that low penetration of PHEVs may cause unacceptable variations

in voltage profiles if there are no regulations on charging, while coordinated charging can reduce system peak load, losses, and mitigate the impacts of uncoordinated charging in the distribution system.

In [44], a comprehensive study to assess the implications arising from adoption of PEVs in Ontario, from the technical, consumer, policy, regulatory, and market points of view are presented and specific measures and approaches, and policy initiatives relevant to Ontario are discussed. Moreover, the study identifies barriers and issues that need to be addressed, provides recommendations where gaps exist in the knowledge base, and finally identifies the R&D needs.

Schedule and dispatch the PEV load by aggregators of PEV fleets using the proposed algorithm while reducing their energy cost is presented in [45], using information about the forecasted charging demand for the coming day. Moreover, the impacts of PEV fleets on the bulk power system are estimated using the proposed algorithms based on realistic vehicle travel patterns from [12].

A modeling framework that incorporates the operation and coordinated charging of PEV loads in a three-phase unbalanced, residential, distribution system is proposed in [46] to minimize the total energy drawn from the substation, total losses, and the total cost of PEV charging, and hence to examine the impact of PEVs on the overall system load profile, bus load profiles, feeder currents, voltages, taps and capacitor switching.

Different penetrations of PEVs considering real data of residential load, ambient conditions, and vehicle parameters is examined in [47] to predict the final SOC of daily driving for PEVs and to study their effect on the transformer insulation life. Different charging scenario studies reported in [47] concludes that PEVs significantly increase the demand side uncertainties and can potentially reduce the distribution transformer insulation life.

In [48] a new smart charging algorithm is presented that manages PEV charging, the transformer temperatures are estimated and hence the impact of PEV charging on overhead distribution transformers is studied. Detailed travel data from [12] is used and several

different schemes for mitigating overloads by shifting PEV charging times (smart charging) are discussed.

1.2.4 Integration of Renewable Energy Sources with PEVs

Renewable energy sources combined with PEVs present significant potential in solving environmental and economic problems. However, the operational challenges associated with PEVs and renewable energy sources need to be studied. Several studies discussed the integration of PEVs with renewable energy sources in the context of system operations.

A multi-year, multi-objective planning model which minimizes GHG emissions and system costs over the planning horizon is proposed in [49]. The model is solved using a non-dominated sorting genetic algorithm considering uncertainties to determine the optimal level of PEV penetration as well as the location, size, and year of installation of renewable DG units. This helps the LDC better assess the expected impacts of PEVs on their networks and on proposed renewable DG connections.

A two-stage stochastic operations model for a microgrid is developed in [50] to determine the optimal energy scheduling for DGs and distributed energy storage devices while accommodating the intermittent renewable energy resources and considering battery degradation costs. The impact of PEVs on microgrid energy scheduling under various charging schemes is also discussed.

In [51], the expected grid operation cost is minimized while considering the random behavior of PEVs in a stochastic security-constrained unit commitment model. The coordinated integration of aggregated PEV fleets and wind energy sources in power systems is studied. It is concluded that power systems can mitigate the variability of renewable energy sources and reduce grid operation costs by smart coordination of the storage capability of PEVs.

A conceptual framework and an optimization methodology for designing grid-connected systems that integrate PEV chargers, renewable energy, and Li-ion storage is

presented in [52]. It is shown that solar PV generation can be more cost effective while Li-ion storage technology and micro wind turbines are not cost effective yet, as compared to alternative solutions.

A PEV charging policy, which makes economic charging decisions every five minutes based on real-time market price signal, that considers transmission and distribution integration issues and solar PV output, is proposed in [53]. It is shown that the PEVs provide voltage support to the distribution system and allow increased penetration of distributed solar PV arrays and can therefore defer distribution network upgrades.

The optimal size of local energy storage for a PHEV charging facility and control strategy for its integration with PHEV charging stations and a solar PV system is proposed in [54]. The local energy storage sizing method minimizes a cost function based on the average value of kilowatt-hour, solar PV irradiance, and PHEVs' usage patterns. It provides general guidance and pathways to solve two major technical challenges- local energy storage device sizing and system control strategies.

A mathematical model based on particle swarm optimization and interior point method is formulated to address an economic dispatch problem, taking into account the uncertainties of PEVs and wind generators [55]. To study the probability distributions of the charge/discharge behaviors of PEVs a simulation based approach is developed first. Also, assuming that the wind speed follows the Rayleigh distribution the probability distribution of wind power is also derived.

An aggregated battery storage model in load frequency control simulations is used in [56] to investigate the application of PEV as a regulation power provider with high wind power penetrations. It is noted that optimal charge/discharge of PEVs can minimize their energy costs, and provide regulation power for both high and low wind speed days.

To optimize the wind capacity in order to minimize the total cost that includes customer interruption cost and annual generation cost, a reliability/cost evaluation model is proposed in [57]. Different numbers of PEVs are considered to minimize the total distribution system cost. Monte Carlo simulation is used to simulate wind speed, load point

outage, and PEV charging/discharging numbers. It is concluded that the proposed reliability/cost model can help in planning of distribution systems considering renewable energy generation and PEVs.

1.3 Research Objectives

In view of the above discussions, the main objectives of the research presented in this thesis can be outlined as follows:

- Model the arrival rate of customers to charge their PEVs at the EVCS assuming it to be a continuous and random, non-homogeneous Poisson process. Two different arrival patterns will be considered- based on customers' convenience, and customers' response to PEV charging price. The first arrival rate profile will make use of the large database of mobility statistics available from the Waterloo Region Transportation Tomorrow Survey (TTS) [58]. The second arrival rate profile will consider the customers' response to PEV charging price, where the price data will be obtained from the winter Time-of-Use (TOU) prices applicable in Ontario, Canada [59].

- A detailed representation of the BCB of PEVs and the SOC, and the time taken to charge PEVs, including a finite waiting time will be considered for the first time to estimate the PEV charging load using queuing theory. These features will render the proposed queuing model more realistic and accurate and also more generic and universal, than the existing models. Such detailed models will provide accurate information of the charging load taking into account different classes of PEVs.

- Examine the impact on distribution system operation, and determine the optimal strategies for the LDC to improve its operational performance using load flow and OPF analysis. Thereafter, study the impact of such PEV load model on LDC operation in the presence of uncertainties, using stochastic load flow, stochastic OPF analysis, and MPC based analysis.

- Model the EVCS load as a smart load by proposing a Charging Station Controllable Load Estimator (CSCLE) comprising a queuing model, to construct the PEV charging

data set as an input to a NN; and a NN model, to estimate the smart charging demand profile of the EVCS as a function of different controllable variables.

- Determine the smart operational decisions at the EVCS from the perspectives of both the LDC and the EVCS owner, integrating the developed NN based smart load model of the EVCS within the distribution operations framework considering PEV smart charging constraints, and EVCS related constraints.
- The contribution of smart EVCS loads to DR and their integration in the distribution systems operation framework will be examined. To demonstrate the effectiveness and need for such a control scheme in smart grids the smart EVCS operations will be compared with an uncontrolled EVCS.
- Determine the optimal design of an EVCS considering various renewable energy technology options and diesel generation with realistic inputs on their physical, operating and economic characteristics.
- Determine the break-even distance for connection of the EVCS with the main grid and compare that with the cost of an isolated EVCS. Compare the same with an optimally designed EVCS with renewable energy based supply options and grid connected configuration.

1.4 Thesis Outline

The remainder of the thesis is organized as follows:

Chapter 2 presents a brief review of the background topics relevant to the research including PEVs, distribution system operation, queuing theory and NN.

Chapter 3 presents a queuing analysis based methodology for modeling the 24-hour charging demand profile of a PEV charging station. The impact of PEV load models on distribution systems is studied for a deterministic case, and the impact of uncertainties is examined and compared using the stochastic OPF and the MPC approaches.

Chapter 4 presents a novel approach to model the total charging load at an EVCS in terms of controllable variables, the load model developed using a queuing model followed by

a NN. The EVCS load is integrated within a distribution operations framework to determine the optimal operation and smart charging schedules of the EVCS. The performance of a smart EVCS vis-à-vis an uncontrolled EVCS is examined to emphasize the DR contributions of a smart EVCS and its integration into distribution operations.

Chapter 5 presents the optimal design and operation of a hybrid, renewable energy based EVCS minimizing the lifecycle cost, while taking into account environmental emissions. Different configurations including isolated EVCS, and a grid connected EVCS as a smart energy hub are designed, to compare and evaluate their economics, operational performance and environmental emissions. Analysis is also carried out to determine the break-even economics for a grid-connected EVCS. The well-known energy modeling software for hybrid renewable energy systems, HOMER, is used in the studies reported in this chapter.

Chapter 6 summarizes the research presented in the thesis, highlights the main contributions, and suggests directions for future research work.

Chapter 2
Background

2.1 Introduction

This chapter presents a background review of the main concepts and tools pertaining to the research presented in this thesis. First, a background on PEVs is presented in Section-2.2 discussing their categories and characteristics, PEV charging, and their levels of charging. Section-2.3 presents an overview of distribution system operations, followed by some concepts on queuing analysis and its applications to estimating PEV charging demand, in Section-2.4. Finally, Section-2.5 discusses the basics of NN modeling.

2.2 Plug-in Electric Vehicles (PEV)

The electric vehicle technology goes back to 1899, when Dr. Ferdinand Porsche and his team developed the first hybrid vehicle [60]. In the late 1960s, when General Motors developed a vehicle that could be plugged into an electrical wall outlet, the PEV concept was introduced. Since the turn of the 21st century, global warming, increase in gas price and poor air quality have become increasingly important issues that have driven the transport sector to move toward more fuel efficient vehicles. A best example of fuel efficient vehicle is the PEV.

There are three important categories of environmentally friendly PEVs as follows:

- Battery Electric Vehicle (BEV)- completely dependent on rechargeable battery. These vehicles have the capability to cut down overall emissions from the transport sector by 70% because no emission is produced by BEVs [61], [62].
- Hybrid Electric Vehicle (HEV)- combines internal combustion engine with an electric motor and battery. The battery is charged by utilizing energy from regenerative breaking and it reduces GHG smog by almost 90%.
- Plug-in Hybrid Electric Vehicle (PHEV)- uses gas and an external power outlet to charge its battery. The GHG emissions are reduced significantly and the overall efficiency of energy conversion is high. PHEVs are similar to HEVs but include a plug-in charger for drawing power from the external grid, and it is designed to operate on

electric power and reduce fuel consumption as much as possible. Therefore, the All Electric Range (AER) capability for the portion of a driving trip is significantly large as compared with other categories of PEVs. Furthermore, the AER is used to characterize PHEVs, for example, a PHEV-40 means a PHEV can drive 40 miles solely on electricity and the rest is driven on gasoline [44], [63]. Thus the AER can be defined as the distance that the PHEV travels during the day using the battery until the minimum allowable battery SOC level is reached.

Battery SOC represents the amount of charge remaining for use by the EV and it is expressed in percentage; for example, an SOC of 50% implies the battery is half-charged. The charging service time is affected by different factors, such as the charging level, battery capacity, battery SOC, and the BCB. The BCB plays a significant role in the battery charging time and rate. Also since minimum service time is one of the criteria that PEV customers seek, the BCB of PEVs need be taken into consideration. For example, the battery of a typical PEV during fast charging attains an SOC of 50% in 10 minutes, 75% in 15 minutes, beyond which there is a drop in the charging rate, as shown in Figure 2.1 [33]. Considering a maximum required SOC for the PEVs to be 85%, it is noted from Figure 2.1 that this is attained in 22 minutes; therefore, the service time depends on the BCB of the PEV.

The SOC of the battery depends on the daily recharge energy (E_C) and battery capacity, and can be stated as follows:

$$SOC = 1 - \frac{E_C}{C_{Bat}} \tag{2.1}$$

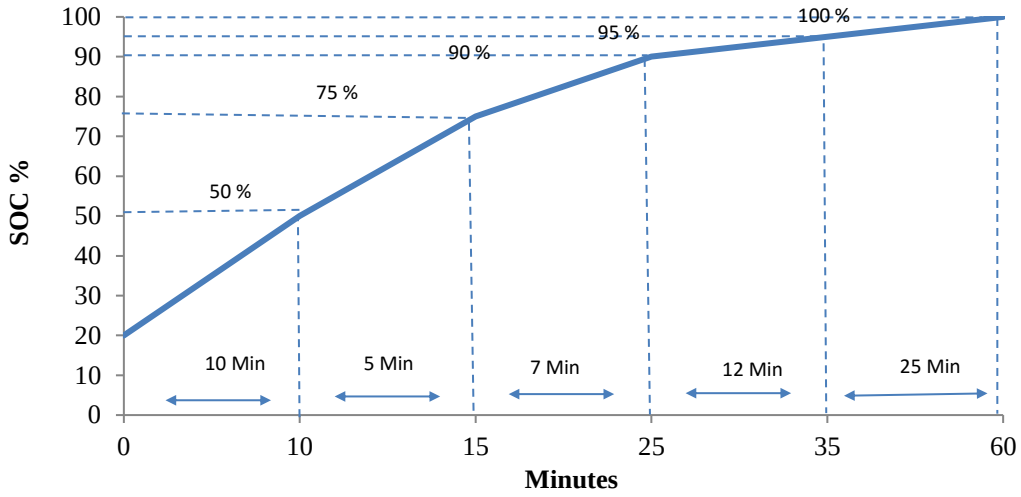

Figure 2.1: Typical BCB of a PEV during fast charging [33].

As of today, there are three levels of PEV charging available, as specified by the National Electric Code (NEC) and [45], described below:

- Level-1: Standard electrical outlet 120 V, single-phase, found in both residential and commercial buildings in Canada. The charging time is usually from 6 to 15 hours, depending on the size of the battery. The maximum power varies between 1.44 to 1.92 kW.
- Level-2: 240 V, single-phase ac supply, such outlets are found in many homes in Canada for electric cloth driers and electric ovens. The maximum power is limited to 7.2 kW because of the small charging system in the car which transfers the power from 120 V ac or 240 V ac outlets to dc voltages. The charging time is between 2 to 5 hours depending on the battery size.
- Level-3: 480-volt, three-phase supply which allows fast charging, and it is not likely to be used in a residential setting because of the expense of purchasing the technology, upgrading a home's electrical system and high voltage safety concerns. The fast charging stations use up to 600 V of dc power to recharge vehicles in a matter of minutes, typically about 15 minutes to reach an 80 percent SOC. These

types of charging stations are beginning to appear in commercial environment and are intended to function like a neighbourhood gas station.

2.3 Distribution System Operation

In general, the electrical interconnections linking the bulk electric power system to end-use customers, requiring energy services at voltage levels below that of transmission and sub-transmission systems, is known as distribution systems. The voltage level of the generated power is boosted up by a step-up transformer at the generating station to match the voltage level of the transmission system. Near to the customer end, a step-down transformer transforms the bulk power to lower voltage levels. To reach the local substations close to the demand center this power is further transferred over the sub-transmission system network. Finally, the power is transformed to a lower voltage level for distribution on a primary distribution feeder at the distribution substation [64]-[66]. Figure 2.2 presents a typical power system generation, transmission and distribution structure with different voltage levels.

The primary distribution feeder can have a radial, loop or primary network configuration. The most frequently and widely used configuration is the radial distribution system because it is the simplest and the least expensive system to build. Moreover, the operation and expansion of such distribution systems are simple because there is only one path for the power flow from the substation to the customer. However, it is considered to be a low reliability configuration because any fault occurring immediately after the substation will cause a power interruption on the downstream feeder.

In the traditional load flow problem, the solution provides the voltage magnitudes, angles, and line power flows through the network for a set of loads at different buses. The generation sources are considered as power sources, not voltage or current sources, and loads are usually represented as constant power loads.

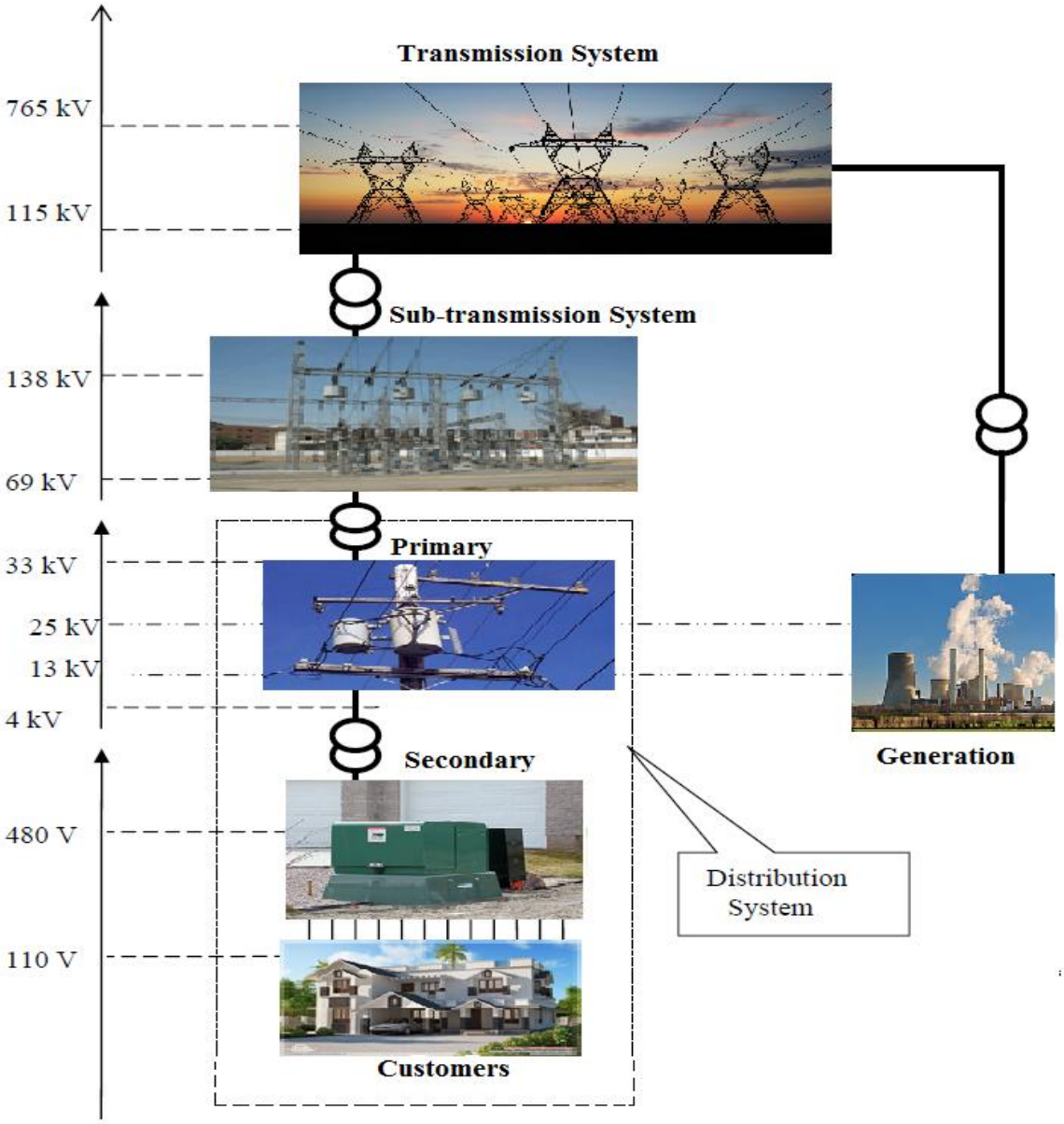

Figure 2.2: Typical power system with voltage levels.

In power system analysis, OPF models have been extensively used for various studies. These OPF models can have different objectives such as, minimizing cost, loss,

power drawn from substation *etc*, and are usually modeled as a non-linear programing (NLP) formulations [67]. In general, the OPF problem can be expressed in the following form:

$$\min \quad f(x) \tag{2.2}$$

$$s.t. \quad g(x) = 0 \tag{2.3}$$

$$h(x) \leq 0 \tag{2.4}$$

$$x \geq 0 \tag{2.5}$$

where x represents a vector of decision variables; $g(x)$ describes the power flow equations of the system and other relevant equality constraints; and $h(x)$ represents a vector of nonlinear functional and control variables, with lower and upper bounds characterizing the operational limits of the system, such as node voltage, and feeder current limits.

In traditional distribution load flow, the three-phase radial distribution system is assumed to be balanced and can be represented by an equivalent single-line diagram as shown in Figure 2.3 The line shunt capacitance can be neglected because it is small at the distribution voltage level. The substation bus is analogous to the transmission slack bus, providing for all the feeder losses.

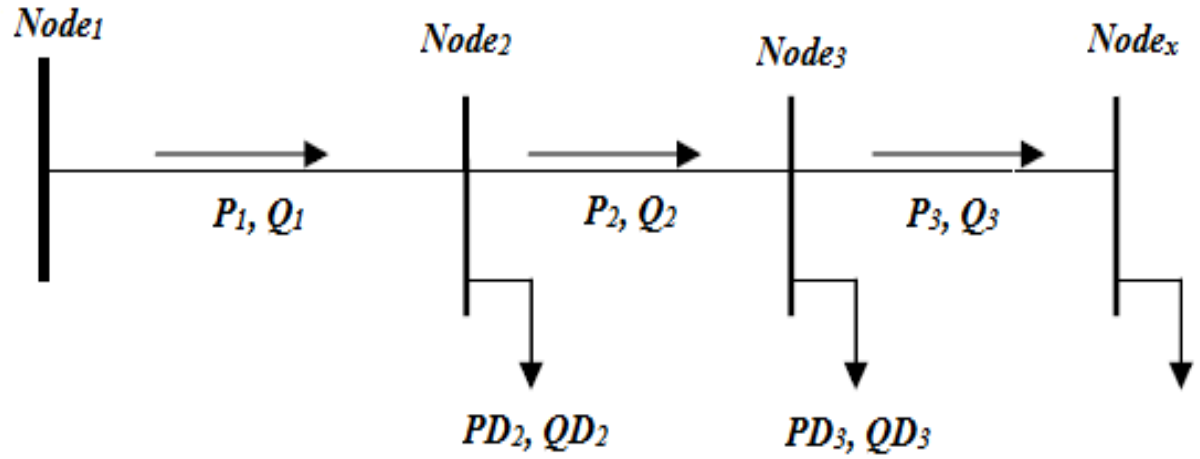

Figure 2.3: Radial distribution network single-line diagram.

As indicated in Figure 2.3, Node 1 is the distribution substation bus or slack bus, and is the only *PV* bus in the system, having a constant voltage, while the remaining buses are load buses (*PQ* buses). The general power flow equations can be written as follows:

$$P_i - PD_i = \sum_j V_i V_j Y_{i,j} \cos(\theta_{i,j} + \delta_j - \delta_i) \tag{2.6}$$

$$Q_i - QD_i = -\sum_j V_i V_j Y_{i,j} \sin(\theta_{i,j} + \delta_j - \delta_i) \tag{2.7}$$

In (2.6) and (2.7), $Y_{i,j}$ and $\theta_{i,j}$ are the magnitudes and corresponding angles of the Y-bus matrix elements respectively; and δ is the associated voltage angle at a bus. PD_i, and QD_i are the active and reactive power demand at bus *i*, respectively.

One of the most common objective functions used in OPF formulation is minimization of losses, as given below:

$$P_{Loss} = \frac{1}{2}\sum_{k=1}^{24}\left[\sum_{i=1}^{N}\sum_{j=1}^{N} G_{i,j}\left(V_{i,k}^2 + V_{j,k}^2 - 2V_{i,k}V_{j,k}\cos\left(\delta_{j,k} - \delta_{i,k}\right)\right)\right] \tag{2.8}$$

Subject to:

Substation Capacity Limits

$$PS_i^{Min} \le PS_i \le PS_i^{Max} \tag{2.9}$$

$$QS_i^{Min} \le QS_i \le QS_i^{Max} \tag{2.10}$$

Bus Voltage Limits

$$V_i^{Min} \le V_i \le V_i^{Max} \tag{2.11}$$

2.4 Queuing Theory

In our daily life queues are a usual phenomenon and have been experienced by all of us. Queuing theory is a mathematical model dealing with waiting times. The queue process begins when a customer arrives for a service, served if the server is empty, or waits for

service, and finally leaves the system after being served [68]. Queuing theory provides the tools needed to study different processes associated to queues such as, arriving at the queue, waiting, and finally leaving the system after being served. Moreover, queuing theory is also used to answer the system performance questions such as, what is the average arrival rate, what is the average service time, how many customers can be simultaneously served, what is the probability for serving this number of customers, and so on.

To understand queuing theory, in depth study of the characteristics that impact its performance need be carried out. For example, queuing analysis used in this research has examined the following aspects and considered them in modeling [69]:

- How do customers arrive at the PEV charging station? Are customer arrivals more during peak load hours or during off-peak?
- How much time do customers spend at the charging station?
- How many outlets should the PEV charging station ideally have, for servicing PEVs?

A typical queuing system with the three important characteristics of the queuing models- the arrival rate of PEV, service time, and number of PEVs being served, are presented in Figure 2.4.

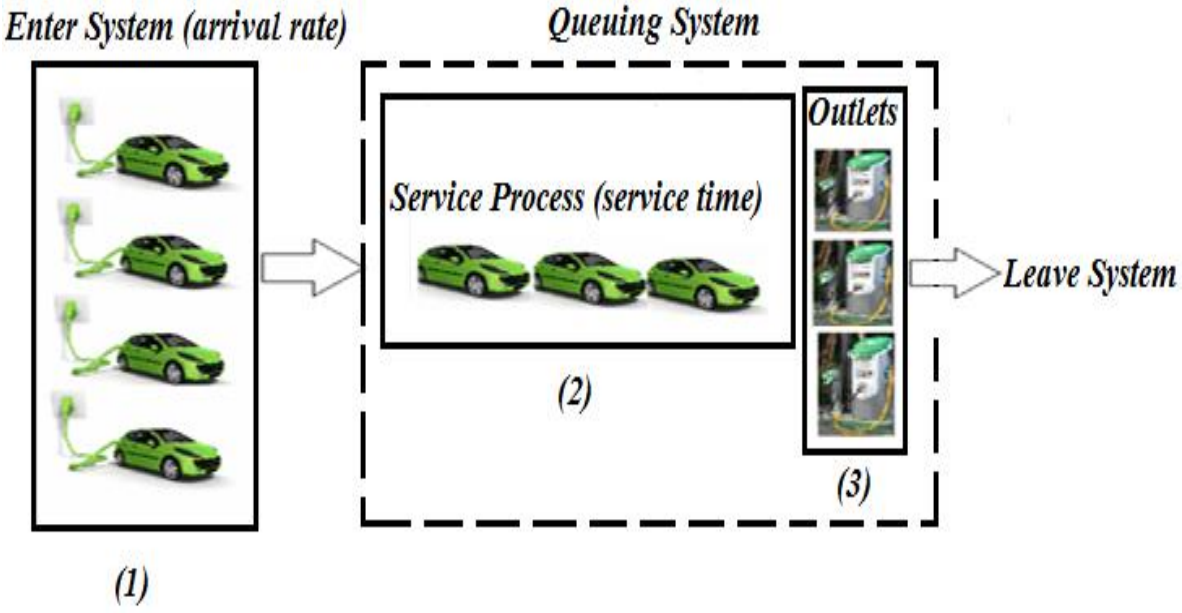

Figure 2.4: A typical queuing system.

The three most important characteristics of a queuing system are discussed below [68]:

- Arrival rate- In general, the arrival rate is modeled as a Poisson process and represented by an exponential distribution with a mean arrival time of $1/\lambda$, where λ is the arrival rate.
- Service time- The service time is generally modeled as an exponential distribution with a mean service time of $1/\mu$, where μ is the service time rate.
- Number of servers- The number servers available at an instant, and can be used.

Based on the above characteristics, queuing systems can be classified by the following convention:

A/B/C

Where *A* is the arrival rate, *B* is the service time and *C* is the number of servers. *A* and *B* can be one of the following [68]:

- M (Markov) Exponential probability density
- D (Deterministic) All customers have the same value
- G (General) Any arbitrary probability distribution

Examples of most common queuing systems that can be defined with this convention are:

M/M/1: This is the simplest queuing system to analyze. The arrival and service times are negative exponentially distributed Poisson processes. The system comprises only one server. This queuing system can be applied to a wide variety of problems as any system with a very large number of independent customers can be approximated as a Poisson process.

M/M/s: The arrival and service times are negative exponentially distributed Poisson processes. The system has *s* servers.

M/D/1: The arrival is represented by a negative exponentially distributed Poisson process while the service time is deterministic and can be assumed to be same for all customers. The system has only one server.

G/G/n: This is the most general queuing system where the arrival and service times are both arbitrary probability distributions. The system has *n* servers. No analytical solution is known for this queuing system [69].

M/M/s/K: In this representation, the arrival and service times are negative exponentially distributed Poisson processes. The system has *s* servers. The system has a maximum serving capacity, *K*; assuming $s \leq K$, and the maximum queue capacity is $K - s$.

2.5 Neural Networks

Neural networks (NN) have been widely applied in various engineering applications such as system identification, signal enhancement, and noise cancellation and defined as [70]: "An interconnected assembly of simple processing elements, units or nodes, whose functionality is loosely based on the animal neuron. The processing ability of the network is stored in the inter-unit connection strengths, or weights, obtained by a process of adaption to, or learning from, a set of training patterns".

The power system literature has seen many applications of NN; for example, in [71], the strategies to incorporate a NN-based load model into static and dynamic voltage stability are presented. In order to provide the forecasted load, NN is used in [72] to learn the relationship among past, current, and future temperatures and loads. One standard application of NN is its use as a function approximation tool.

2.5.1 NN Structure

The structure of a feed-forward NN is presented as follows:

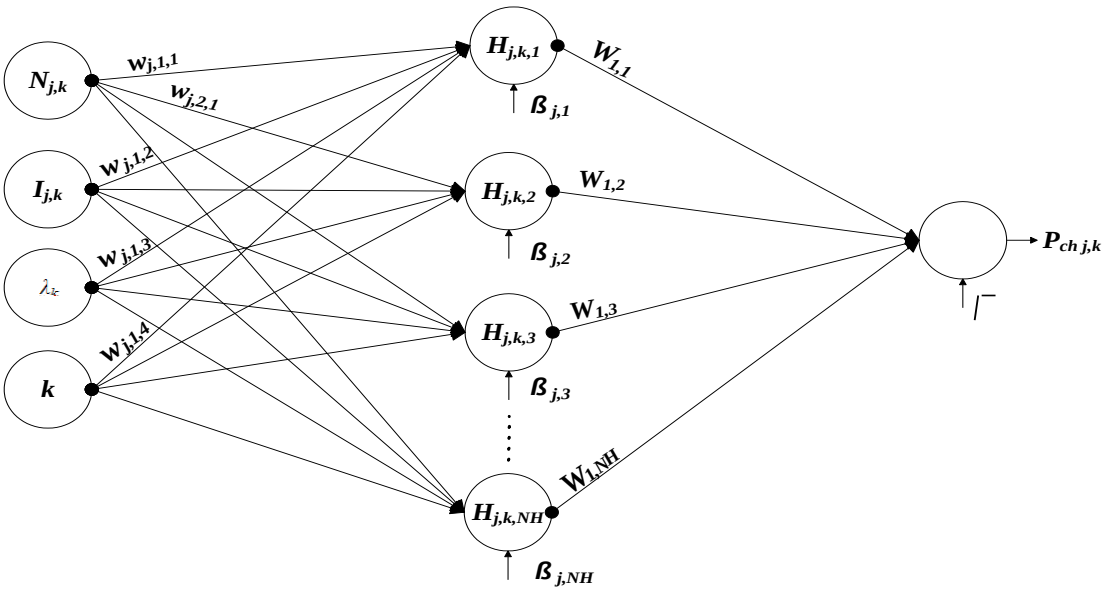

Figure 2.5: NN structure.

There are *x* input layer neurons and one output layer neuron in the NN structure in Figure 2.5. Furthermore, the considered NN has one hidden layer with NH number of neurons in the hidden layer. During the training process, NH is varied to arrive at the best fit for the load model. The NN is trained in MATLAB using the Levenberg-Marquardt algorithm for back propagation.

While training the NN, the entire dataset is divided into three subsets. The first subset is the training set, used for computing the gradient and updating the network weights and biases. The second subset is the validation set, which is used to monitor the error during the training process that normally decreases during the initial phase of training, as does the training set error. The third subset or test set is used to compare different models, using the test set error during the training process to evaluate the accuracy of the NN model.

There are four built-in functions available in MATLAB for dividing the data set into training, validation and test sets, namely, *Dividerand*, *Divideblock, Divideint*, and *Divideind*; the best function for the considered data set, is typically chosen by multiple test runs with each function.

2.5.2 Mathematical Functions of NN Model

In order to obtain the mathematical function of the output from the trained NN, the output from each hidden layer neuron H_1 to H_n, is determined first. The incoming inputs with appropriate weights w_i are summed up at each hidden layer neuron. Also, each hidden layer neuron has an additional input, the bias β_1 to β_n, which is used in the NN to generalize the solution and to avoid a zero value of the output, even when an input is zero. This summed signal is passed through an activation function (*tansig*) associated with each hidden layer neuron, which transforms the net weighted sum of all incoming signals into an output signal from the hidden layer neuron. Accordingly,

$$H_1 = tansig\ (w_{1,1} X_1 + w_{1,2} X_2 + w_{1,3} X_3 + w_{1,4} X_4 + \beta_1) \quad (2.12)$$

to

$$H_n = tansig\ (w_{n,1} X_n + w_{n,2} X_n + w_{n,3} X_n + w_{n,4} X_n + \beta_n) \quad (2.13)$$

Finally, the output function is obtained from the trained NN as follows:

$$\text{Output} = purelin\ (H_1 W_{1,1} + H_2 W_{1,2} + H_3 W_{1,3} + \ldots H_n W_{1,n} + £) \quad (2.14)$$

where *purelin* is a linear transfer function available in MATLAB.

2.6 Summary

This chapter presented a review of the background relevant to the research presented in the next chapters. A brief background on the basic characteristics of PEVs based on categories of environmentally friendly vehicles, SOC of PEVs, and BCB, and the three different charging levels for PEVs is presented. This is followed by a discussion on distribution system operation and OPF in distribution system. Then an introduction to queuing theory, to estimate the PEV 24-hour charging demand at a PEV charging station, is presented. Finally, a brief discussion on NN models is presented.

Chapter 3
Queuing Analysis Based PEV Load Modeling Considering Battery Charging Behavior and Their Impact on Distribution System Operation[1]

3.1 Introduction

This chapter presents a queuing analysis based method for modeling the 24-hour charging load profile of a PEV charging station. The queuing model considers the arrival of PEVs as a non-homogeneous Poisson process with different arrival rates over the day. The first PEV charging load profile assumes customer convenience as the factor that influences the hourly arrival rate of vehicles at the station, while the second profile is developed assuming that customers would respond to PEV charging prices and arrival rates are accordingly affected. One of the main contributions of this chapter is to model the PEV service time considering different factors such as the SOC of the vehicle battery as well as the effect of the BCB. The impact of PEV load models on distribution systems is studied for a deterministic case, and the impact of uncertainties is examined and compared using the stochastic optimal power flow and the MPC approaches.

The rest of this chapter is organized as follows. The nomenclature used in this chapter is presented in Section 3.2. In Section 3.3, the proposed mathematical model including the objective function and constraints are presented. The case study information is presented in Section 3.4.

---

[1] Parts of this chapter has been accepted for publication in:

- O. Hafez, and K. Bhattacharya, "Queuing analysis based PEV load modeling considering battery charging behavior and their impact on distribution system operation," IEEE Transactions on Smart Grid (in print).

Earlier versions of the work have been published in:

- O. Hafez, and K. Bhattacharya, "Modeling of PEV charging load using queuing analysis and its impact on distribution system operation,", in Proc. IEEE Power and Energy Society General Meeting, Denver, CO, USA, July 2015.
- O. Hafez, and K. Bhattacharya, "Queuing analysis based siting of PEV charging stations considering on distribution system impact,", in Proc. IEEE Power and Energy Society General Meeting, Boston, MA, USA, July 2016.

In Section 3.5 results and discussions are presented. Finally, concluding remarks are presented in Section 3.6.

3.2 Nomenclature

3.2.1 Sets and Indices

i, j	Index for buses
k	Index for time
l	Set of SOC intervals $l \in \{1, 2, 3,4\}$
N	Total number of buses in the system
n	Set of all possible options of simultaneous charging of PEVs, for a given N_0 $n \in \{0, 1, 2, 3, \ldots, N_0\}$
s	Index for stochastic scenario
sb	Index for substation bus
y	Index for PEV class

3.2.2 Parameters

C_{Bat}	Total PEV battery capacity, kWh
DD	Daily driven miles by PEV, mile
DD_{Max}	Maximum driving distance until PEV battery is fully discharged, mile
E_C	Daily recharge energy, kWh
E_M	Energy consumption of PEV battery per mile driven, kWh/mile
$E[Pch_{i,k}]$	Total expected PEV charging demand at time *k*
G	Conductance of feeder, p.u.
I	Charging current, A

I_{Max}	Charging current level, A
ITR_{Max}	Total number of iterations used for queuing model simulation
$M_1/M_2/N_0$	Queuing model, M_1 denotes PEV arrival rate (minute) / M_2 denotes PEV charging time (minute) / N_0 is the number of PEVs being charged simultaneously at a given hour
N_{Cap}	Maximum number of PEVs that can be charged simultaneously at the station
P(n)	Probability of *n*
Pch	Active power demand from charging PEVs, p.u.
PD, QD	Active, reactive power demand at a bus, p.u.
PS^{Max}	Maximum active power limit on substation transformer, p.u.
QS^{Max}	Maximum reactive power limit on substation transformer, p.u.
SOC	Battery state of charge
T	Charging time for a PEV, minute
μ	Mean service time, minute
V	Charging voltage level, p.u.
V^{Min}, V^{Max}	Minimum, maximum limit on bus voltages, p.u.
$Y_{i,j}$	Magnitude of admittance matrix element, p.u.
λ	Mean of inter-arrival time, minute
ρ	Occupation rate of PEV at charging station
θ	Angle of complex Y-bus matrix element, rad

3.2.3 Variables

$PG_{i,k}$, $QG_{i,k}$	Active, and reactive power generation at bus *i*, hour *k*, p.u.

$PG_{i,k,s}$, $QG_{i,k,s}$ Stochastic active, and reactive power generation at bus *i*, hour *k*, scenario *s*, p.u.

P_{Loss} Total system losses, p.u.

$E[P_{Loss}]$ Expected total system losses, p.u.

$PS_{i,k}$, $QS_{i,k}$ Active, and reactive power supplied through substation transformer at hour *k*, p.u.

$PS_{i,k,s}$, $QS_{i,k,s}$ Stochastic active, and reactive power supplied through substation transformer at hour *k*, scenario *s*, p.u.

$V_{i,k}$ Voltage magnitude at bus *i*, hour *k*, p.u.

$V_{i,k,s}$ Stochastic voltage magnitude at bus *i*, hour *k*, scenario *s*, p.u.

$\delta_{i,k}$ Voltage angle at bus *i*, hour *k*, rad

$\delta_{i,k,s}$ Stochastic voltage angle at bus *i*, hour *k*, scenario *s*, rad

3.3 Mathematical Modeling

3.3.1 PEV Queuing Model

Queuing analysis is applied to estimate the total charging power of PEVs. The PEV customers are considered to be served using $M_1/M_2/N_0$ queue model at a PEV charging station, where M_1 denotes the arrival rate which varies from hour to hour of the day and is modeled as a non-homogeneous Poisson process, the service time denoted by M_2 includes the waiting time and the charging time. The service time is modeled in this chapter considering the PEV BCB.

Poisson process is a continuous-time stochastic process that counts the number of arrivals in a given time interval where the time between each pair of consecutive arrivals has an exponential distribution with (mean of inter-arrival time) λ and each of these inter-arrival times are assumed to be independent of other inter-arrival times. It is useful for modeling arrival that occurs independently from each other [73]. Since the arrival of PEVs at the

charging station is a continuous-time stochastic process, Poisson process has been considered in this work.

In accordance to $M_1/M_2/N_0$ queuing analysis [68], the probability of the number of PEVs charging simultaneously at an hour is modeled as a discrete distribution, as follows:

$$p_k(n) = \frac{(N_0\rho)^n}{n!} p_k(0) \qquad n = 1,2,3,...., N_0 \tag{3.1}$$

where,

$$p_k(0) = \left[\sum_{m=0}^{N_0 - 1} \frac{(N_0\rho)^m}{m!} + \frac{(N_0\rho)^{N_0}}{N_0!} \frac{1}{(1-\rho)} \right]^{-1} \tag{3.2}$$

and ρ is the occupation rate of the PEV charging station and is calculated as follows:

$$\rho = \frac{1/\lambda_k}{N_0 \frac{1}{\mu_k}} \tag{3.3}$$

3.3.2 PEV Battery Charging Behavior (BCB) Model

The charging service time is affected by different factors, such as the charging level, battery capacity, battery SOC, and PEV BCB. One of the main objectives of PEV customers is to have fast charging at a charging station *i.e.*, minimum service time. In order to achieve this, the BCB of each class of PEVs are considered; for example, the battery of a typical Compact PEV during fast charging attains an SOC of 50% in 10 minutes, 75% in 15 minutes, beyond which there is a drop in charging rate, as shown in Figure 3.1 [33]. Considering a maximum required SOC for the PEVs to be 85%, it can be noted from Figure 3.1 that this is attained in 22 minutes, for Compact PEVs, and therefore, the service time depends on the BCB of the PEV class.

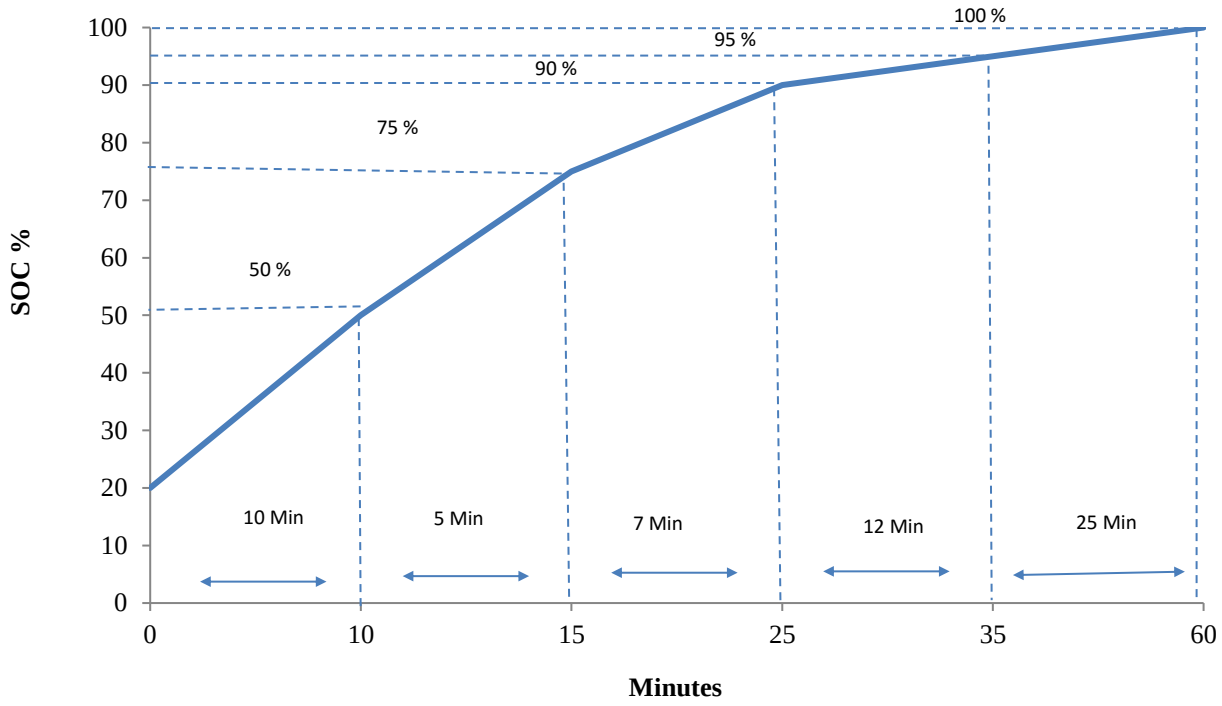

Figure 3.1: Typical BCB of a Compact PEV during fast charging [33].

The SOC of the battery can be obtained as follows:

$$SOC_y = 1 - \frac{E_{Cy}}{C_{Bat\,y}} \quad \forall\, y \tag{3.4}$$

In (3.4), E_{Cy} is the daily recharge energy of a PEV, and is obtained as follows:

$$E_{C_y} = \begin{cases} C_{Bat\,y} & if \quad DD_y \geq DD_{Max} \\ E_{My}\, DD_y & if \quad DD_y < DD_{Max} \end{cases} \tag{3.5}$$

where E_{My} is the energy consumption by a PEV of class y, per mile, and the following conditions are imposed, from the above BCB of the PEV (Figure 3.1):

$$SOC_y = \begin{cases} 0.2 \quad if \quad SOC_y \le 0.2 \\ SOC_y \quad if \quad 0.2 < SOC_y \le 0.85 \\ 0.85 \quad if \quad SOC_y > 0.85 \end{cases} \tag{3.6}$$

Once the SOC of a PEV is known, the required charging (or service) time of a PEV, given by *T*, is obtained from the BCB (Figure 3.1) using the piece-wise linear relationship:

$$T = \frac{SOC_{l\,y} - b_l}{a_l} \quad \forall \quad l \in \{1,2,3,4\}, \forall\ y \tag{3.7}$$

where a_l and b_l are the slope and intercept of the linear equation obtained from the BCB and depend on the SOC of interval *l*.

The charging current drawn by a PEV over the charging period *T*, at time *k* for PEV class *y* is given as follows:

$$I_{k,y} = \min\left(\frac{E_{C\,y}}{VT_k}, I_{Max}\right) \tag{3.8}$$

where I_{Max}, and *V* are dependent on the charging level and hence fixed. The maximum driving distance of a PEV, $DD_{Max\,y}$ is calculated as follows:

$$DD_{Max_y} = \frac{C_{Bat_y}}{E_{M\,y}} \tag{3.9}$$

Therefore, the total charging power for N_0 number of PEVs being charged simultaneously at time *k* is given as follows:

$$Pch_{i,k} = \sum_{m=1}^{N_0} I_{m,k,y} V \tag{3.10}$$

The total expected PEV charging demand at time k for all possible values of N_0 (where $N_0 \in 1$ to N_{cap}) is given as follows:

$$E[Pch_{i,k}] = \sum_{N_0}^{N_{cap}} P_k(N_0) Pch_{i,k} \tag{3.11}$$

The total PEV charging demand obtained from (3.11) is used in the OPF model discussed next, to examine the impact of PEV charging on the distribution system performance.

3.3.3 OPF Model for System Operation Including PEV Load

Once the PEV charging load is estimated using the queuing model, the impact on system operation is examined by formulating the following OPF model. Since the main objective of the distribution system operators is to meet the system demand while ensuring a good voltage profile for customers, the objective of minimization of feeder losses is considered, as given below:

$$P_{Loss} = \frac{1}{2} \sum_{k=1}^{24} \left[\sum_{i=1}^{N} \sum_{j=1}^{N} G_{i,j} \left(V_{i,k}^2 + V_{j,k}^2 - 2V_{i,k} V_{j,k} \cos\left(\delta_{j,k} - \delta_{i,k} \right) \right) \right] \tag{3.12}$$

The PEV charging load ($Pch_{i,k}$) is included in the active power balance at bus i where the charging station is located. The demand-supply balance for both active and reactive power is given by the load flow equations as follows.

$$PG_{i,k} - PD_{i,k} - Pch_{i,k} = \sum_{j=1}^{N} V_{i,k} V_{j,k} Y_{i,j} \cos\left(\theta_{i,j} + \delta_{j,k} - \delta_{i,k} \right) \tag{3.13}$$

$$QG_{i,k} - QD_{i,k} = -\sum_{j=1}^{N} V_{i,k} V_{j,k} Y_{i,j} \sin\left(\theta_{i,j} + \delta_{j,k} - \delta_{i,k}\right) \qquad (3.14)$$

The voltage magnitudes at each bus at hour *k* are constrained by their respective upper and lower limits which are assumed to vary up and down by 10%.

$$V_i^{Min} \le V_{i,k} \le V_i^{Max} \quad \forall \; i \; \in Load\ buses \qquad (3.15)$$

The slack bus voltage magnitude and voltage angle, which is the substation bus, are fixed, as follows.

$$V_{sb,k} = 1\, p.u., \qquad \delta_{sb,k} = 0$$

The substation capacity limit determines the maximum and minimum active and reactive power transfer capacity over the substation transformer.

$$0 \le PS_{i,k} \le PS_i^{Max} \quad i = sb \qquad (3.16)$$

$$0 \le QS_{i,k} \le QS_i^{Max} \quad i = sb \qquad (3.17)$$

The above NLP model is solved using the MINOS5.1 solver in the GAMS environment [74].

At each time step, the total charging load is estimated using the proposed queuing model, and then applied to the OPF. The flowchart describing the queuing process is shown in Figure 3.2. A large number of queuing simulation runs are needed; for every simulation run ITR_1 ($\in 1, \ldots, ITR_{Max}$), the hourly arrival rate is input, and N_0 is randomly selected in the range [1, N_{Cap}].

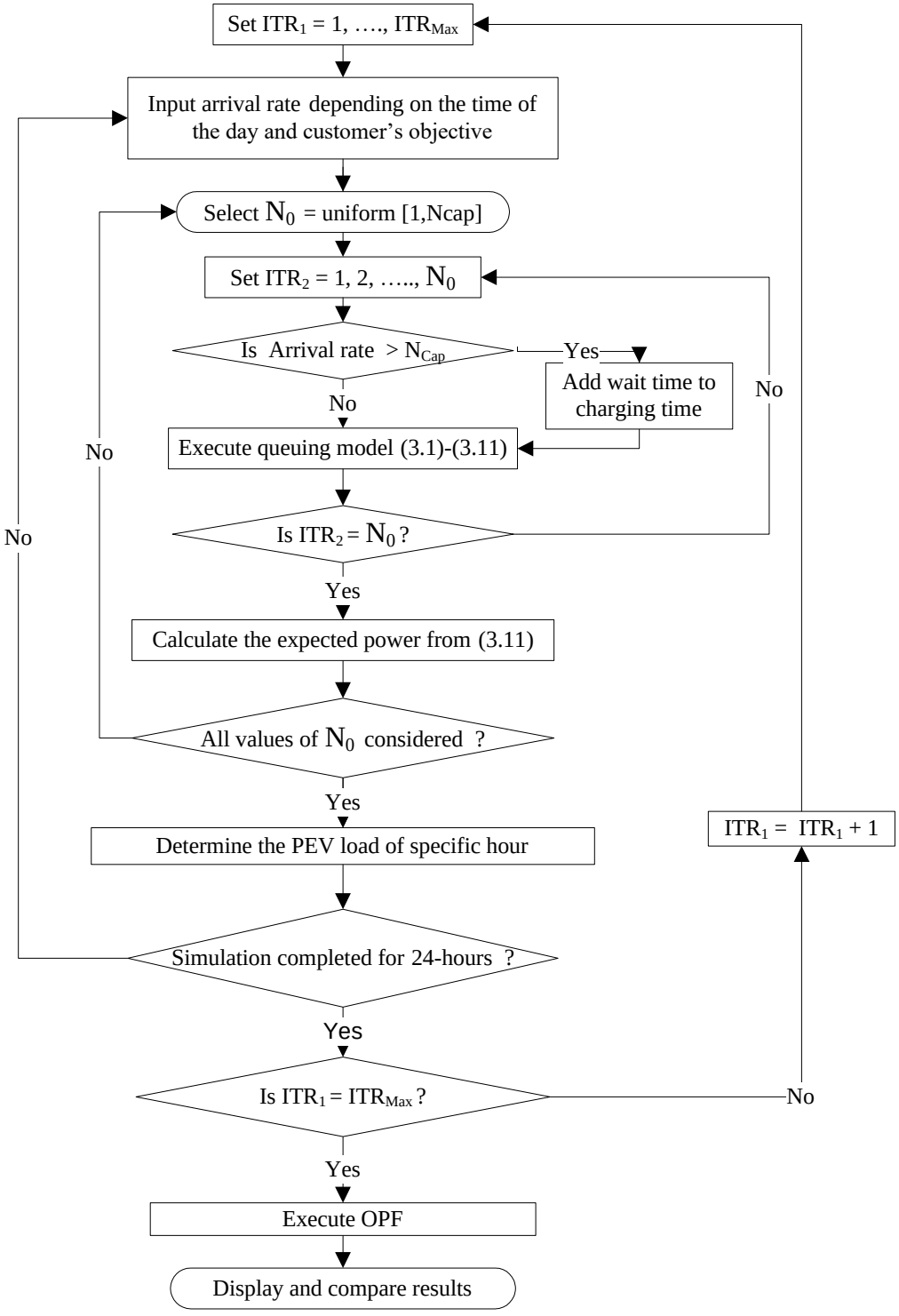

Figure 3.2: The flowchart of the queuing simulation process.

3.3.4 Stochastic OPF Including PEV Load

In the stochastic OPF the output of the queuing model is used to examine the impact of PEV charging loads on distribution system operation, with the objective of minimization of expected feeder losses as mentioned above, considering the scenarios of different queuing models, as given below:

$$E[P_{Loss}] = \frac{1}{2}\sum_{S=1}^{17} P_k(s)\left[\sum_{k=1}^{24}\left[\sum_{i=1}^{N}\sum_{j=1}^{N} G_{i,j}\left(V_{i,k,s}^2 + V_{j,k,s}^2\right) - 2V_{i,k,s}V_{j,k,s}\cos\left(\delta_{j,k,s} - \delta_{i,k,s}\right)\right]\right] \quad (3.18)$$

Where *s* represents the scenario, which in this chapter, represents N_0, *i.e.*, the number of PEVs charging simultaneously. The PEV charging load for each scenario ($Pch_{i,k,s}$) is included in the active power balance at bus *i* where the charging station is located. The demand-supply balance for both active and reactive power is given by the load flow equations as follows.

$$PG_{i,k,s} - PD_{i,k} - Pch_{i,k,s} = \sum_{j=1}^{N} V_{i,k,s}V_{j,k,s}Y_{i,j}\cos\left(\theta_{i,j} + \delta_{j,k,s} - \delta_{i,k,s}\right) \quad (3.19)$$

$$QG_{i,k,s} - QD_{i,k} = -\sum_{j=1}^{N} V_{i,k,s}V_{j,k,s}Y_{i,j}\sin\left(\theta_{i,j} + \delta_{j,k,s} - \delta_{i,k,s}\right) \quad (3.20)$$

The power flow equations (3.19)-(3.20) shows that fluctuations in PEV charging load in each scenario ($Pch_{i,k,s}$) leads to variations in the system bus voltages ($V_{i,k,s}$) and angles ($\delta_{i,k,s}$) across the network. The following constraint is enforced on the expected voltage at every bus *i* and time interval *k:*

$$V_i^{Min} \le \sum_{s=1}^{17} P_k(s) V_{i,k,s} \le V_i^{Max} \quad \forall \ i \ \in N \tag{3.21}$$

The voltage magnitude and angle at the slack bus, which is the substation bus, are fixed for all scenarios, as follows:

$$V_{sb,k,s} = 1\,p.u., \qquad \delta_{sb,k,s} = 0$$

The substation capacity limit determines the maximum and minimum active and reactive power transfer capacity over the substation transformer for all scenarios.

$$0 \le PS_{i,k,s} \le PS_i^{Max} \quad i = sb \tag{3.22}$$

$$0 \le QS_{i,k,s} \le QS_i^{Max} \quad i = sb \tag{3.23}$$

The above NLP model is solved using the SNOPT solver in the GAMS environment. There are several extensive research works on stochastic OPF with comprehensive detail on the solution of such problems [75].

3.3.5 Model Predictive Control (MPC)

The MPC approach is applied in this chapter to examine the impact of PEV charging loads on LDC's operation in the presence of uncertainties. The MPC approach determines a series of optimal operations over a finite horizon, wherein the decision for the next time step is obtained by solving the problem using the current state of the system as the initial state [30], [31], [76]. The MPC approach works on an iterative, finite-horizon optimization time-frame [*k:k+t*] where at the current time step *k* the OPF is solved using (3.12) - (3.17). This provides the optimal set of decisions at the current point of time, for the next 24 hours, based on the estimated PEV charging demand. Only the first sample from the set of optimal decisions is implemented. In the next iteration, the new state of the system is considered, the optimization horizon is shifted forward and the OPF is solved again; MPC repeats until the last time step [*k+t*] is reached.

3.4 Case Study

3.4.1 Summary of Cases Considered

The proposed model of PEV charging load is examined in this chapter considering different cases and scenarios in order to study the impact of the proposed model on distribution system operations considering deterministic and stochastic models. The different cases and scenarios considered are presented in Figure 3.3.

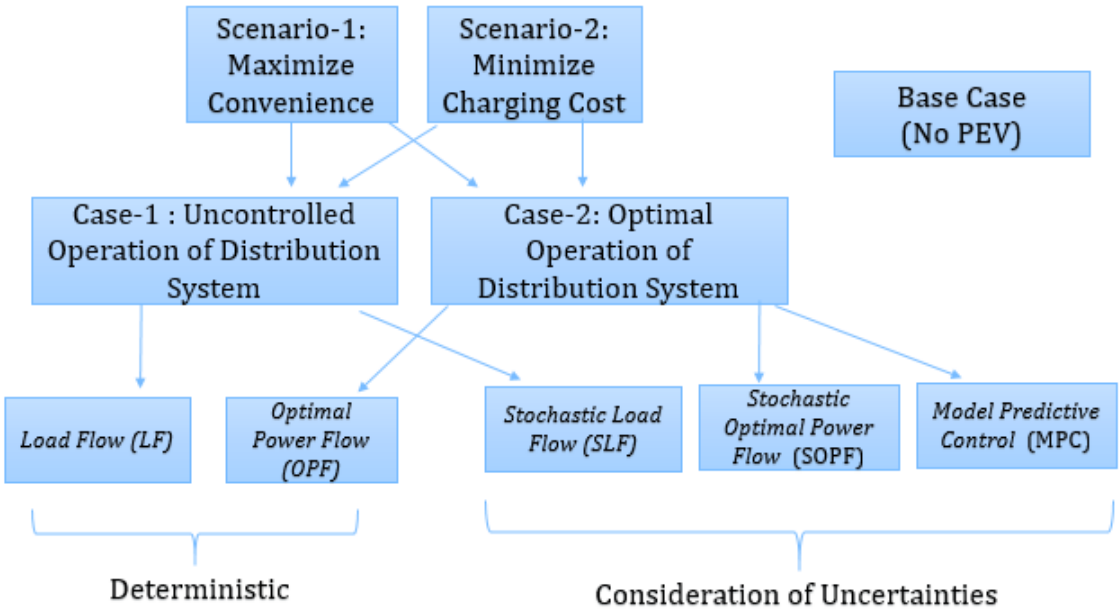

Figure 3.3: Summary of cases considered.

3.4.2 Distribution System and Mobility Data

The analysis reported in this chapter is carried out considering the IEEE 69-bus radial distribution system, whose single line-diagram is given in Figure 3.4 [77] with MVA_{Base} = 10 MVA. The distribution system is supplied through the substation at bus-1. It is assumed that a PEV charging station is arbitrarily located at bus-59, however if the charging station is located at remote buses for example at bus-65 or bus-27, the impact on the distribution

system operation could be even more significant. In this chapter, Level-3 charging is considered since high power level charging is preferred at PEV charging stations, and thus I_{Max} = 63 amps and V = 400 volts.

Distribution systems can be balanced by using various load balancing schemes, and hence can be represented by single phase equivalents [66]. The unbalanced nature of distribution system is more prevalent at the end-user level (residential customer level) but since this work considers a PEV charging station load model, it is assumed to be connected at 12.66 kV feeder level; and at this voltage level, the loads are assumed to be balanced three-phase, and all line segments are three-phase, and perfectly transposed [66].

With these assumptions, a single line-to-neutral equivalent circuit for the feeder has been used, and a three phase distribution system is represented by a single-phase equivalent.

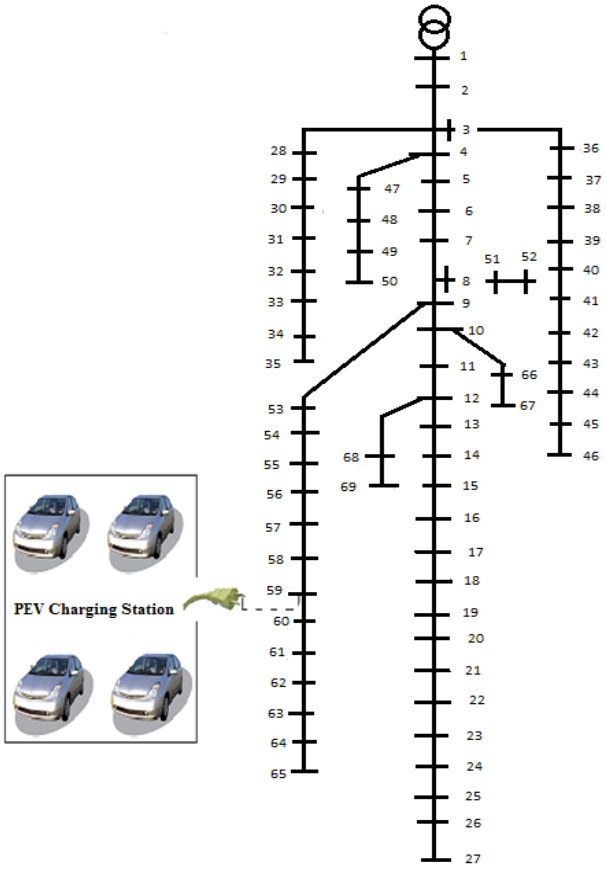

Figure 3.4: 69-Bus radial distribution system [77].

Waterloo Region TTS data and Ontario, Canada, TOU winter tariff rates are used in order to obtain realistic results. The Waterloo Region TTS is a comprehensive travel survey conducted every five years in the region wherein 5% samples of households are reached by telephone. In this work, the 2011 TTS for Waterloo Region is used which considers 43,165 unique trips. Figure 3.5 presents the winter TOU rates of Ontario over a day. The distribution of vehicles on the road over a 24 hour period is calculated using the same TTS data and shown in Figure 3.5.

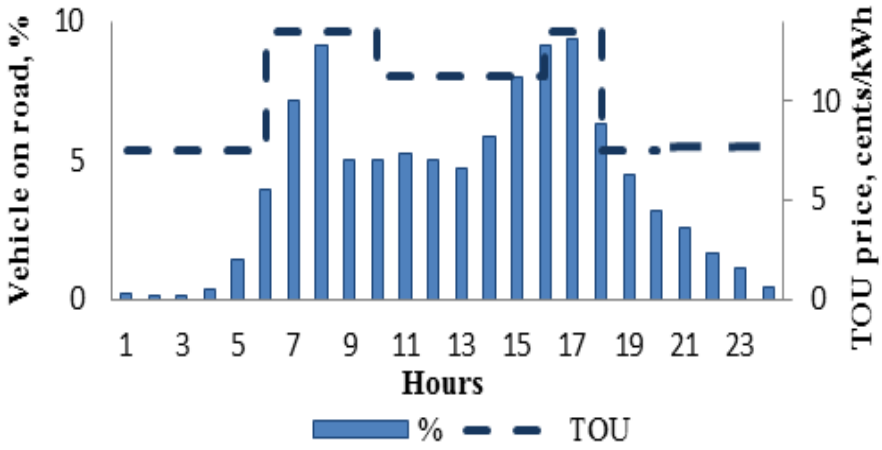

Figure 3.5: Distribution of vehicles on the road and Ontario winter TOU.

3.4.3 Modeling of Daily Driven Miles and PEV Arrival Rate, M_1

Figure 3.6 shows the distribution of daily miles driven on all vehicle driving days based on the TTS data. It is noted that the best fit for the TTS data (using EasyFit software [78]) is obtained with a lognormal distribution as evident from Figure 3.7. So, the daily driven miles by the PEVs, DD, is modeled as a lognormal distribution in this work, and is given by:

$$DD_y = e^{(\mu_M + \sigma_M f)} \tag{3.24}$$

where μ_M and σ_M are the mean and the variance of the lognormal distribution, respectively.

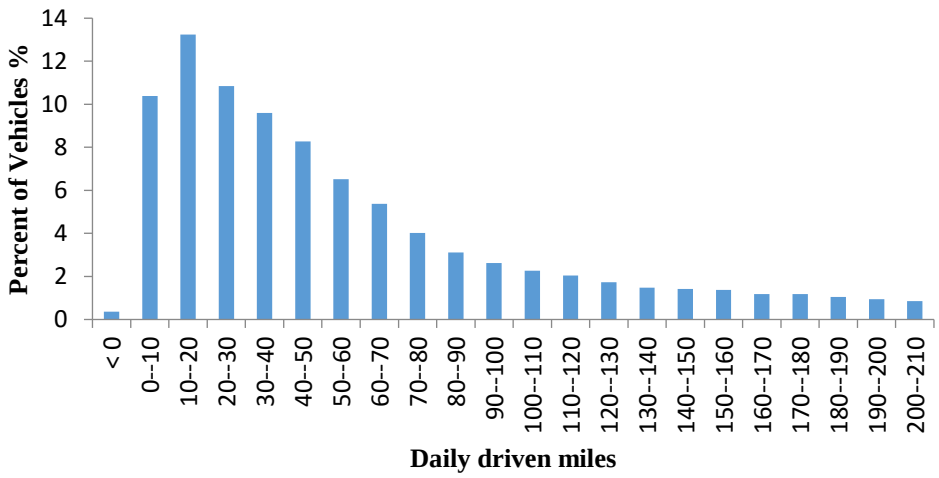

Figure 3.6: Distribution of daily driven distance per vehicle as per TTS.

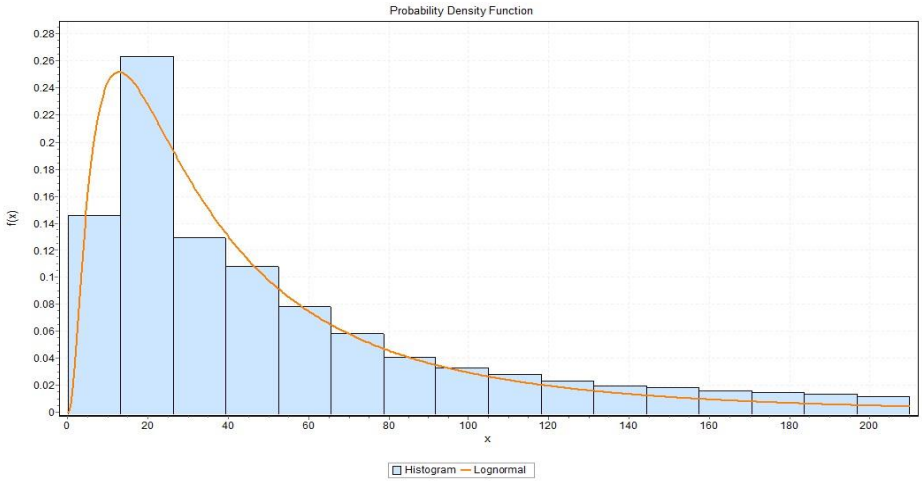

Figure 3.7: Distribution of daily driven distance per vehicle using EasyFit [78].

In this chapter, four classes of PEVs are considered- *Compact*, *Economy*, *Mid-Size*, and *Light Truck/SUV*, to present a realistic picture of the PEV charging station load. The queuing algorithm is initiated by randomly generating N_0. The PEV arrival rate M_1 depends on the hour of the day and customer's behavior pattern. Under a rational behavior assumption, two M_1 profiles are modeled as follows:

- Scenario-1: considers that the PEV arrival rate depends on customer convenience, *i.e.*, the number of vehicles on the road. When the number of vehicles on the road is high the arrival rate is high, irrespective of the price or LDC's operational constraints. In this chapter, using TTS data, a relationship between vehicles on the road and PEV arrival rate at the charging station is assumed. As shown in Figure 3.8, if the percent of vehicles on the road is up to 4%, at any hour, a uniformly distributed PEV arrival in the range of 1 to 4 PEVs/hour is assumed, and similarly 5 to 11 PEVs are assumed to arrive if 4-7% of vehicles are on the road, and so on. For example, at hour 7, about 7% of the vehicles are on the road (see Figure 3.5) and consequently, 5 to 11 PEVs may arrive for charging (as per Figure 3.8), on the other hand, at hour 17, 9.3% of the vehicles are on the road, and it is assumed that 12 to 17 PEVs may arrive for charging.

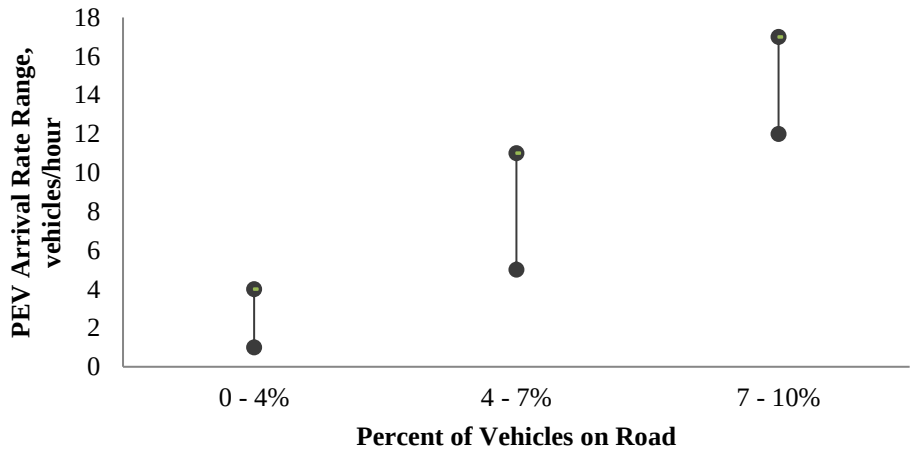

Figure 3.8: Relationship between vehicles on road and arrival rate of PEVs.

- Scenario-2: considers that the PEV arrival rate depends on the charging price, *i.e.*, more PEVs will charge when the price is low, and *vice versa*. In this scenario a relationship between Ontario's winter TOU price and PEV arrival rate at the charging station is assumed. As shown in Figure 3.9, if the charging price ranges between 7.5 and 11.2 cents, at any hour, a uniformly distributed PEV arrival in the range of 5 to 11 PEVs/hour is assumed, and similarly 12 to 17 PEVs are assumed to arrive if the charging price is in

the range of 1 to 7.5 cents. For example, at hour 7, the charging price is 13.5 cents (*see* Figure *3.5*) and consequently, only 1 to 4 PEVs may arrive for charging (*as per* Figure *3.9*).

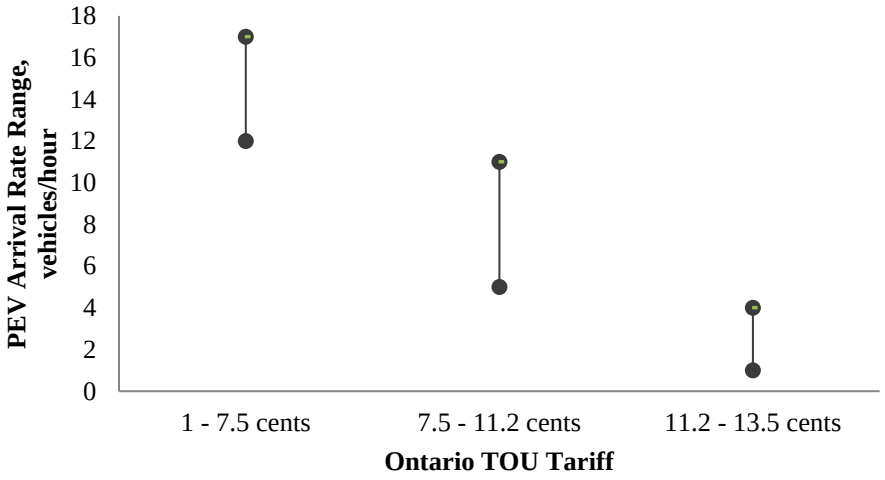

Figure 3.9: Relationship between TOU tariff and arrival rate of PEVs.

It is important to point out that, the arrival rates modeled in this chapter are based on some assumptions pertaining to vehicles on the road, charging price and how PEVs arrive for charging at the charging station. Such assumptions are necessary in order to understand the impact of PEV charging on the distribution grid but need be validated with realistic data from ground level surveys.

Moreover, as per Scenario-2, the arrival rate would be high at night since the PEV charging price is low at these hours. However, considering that the probability of charging during night is low, because of customer inconvenience, the arrival rate is modified appropriately, as shown in Figure 3.10, where the removed arrival data of early hours are indicated. Also to be noted that since home charging has been ignored in this work, there will be no effect on the early morning arrival rates. The two arrival rate profiles, as discussed

above, are modeled as non-homogeneous Poisson processes with mean λ_k which is the time dependent number of expected car arrivals at a charging station throughout the day.

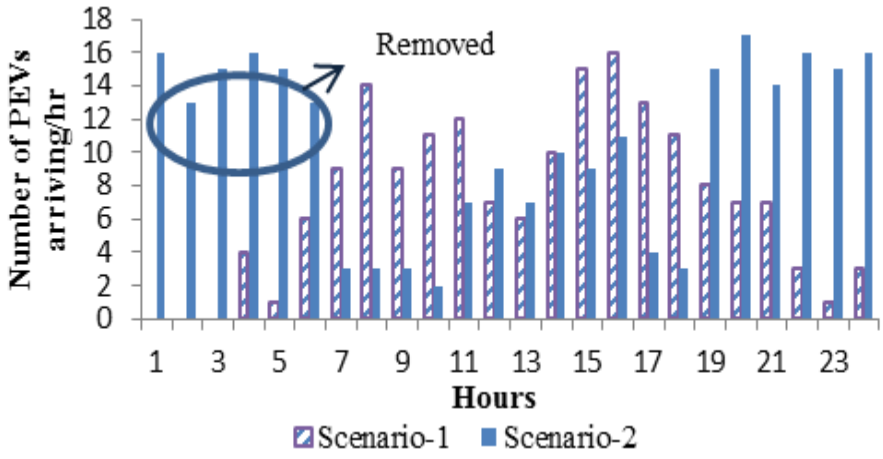

Figure 3.10: Number of PEVs arriving per hour at the charging station (Arrival rate).

3.4.4 Simulation of the Queuing Process

Once the arrival rate scenario is selected, for every value of N_0, the following steps are repeated:

- Assume the PEV classes to be uniformly distributed over the sample set N_0, randomly select a PEV class from amongst the four different classes.
- The battery capacity for each PEV class is uniformly distributed between their upper and lower limits.
- Calculate battery SOC for each PEV from its daily recharge energy (3.4), (3.6), which depends on different factors such as the daily driven miles, and battery capacity.
- Determine the time required for charging for each PEV, using the BCB given in (3.7).
- Determine the total charging power arising at the charging station, for the total N_0 PEVs using (3.8) - (3.11).

Following are the parameters used in this chapter to simulate the queuing process of PEVs charging at a charging station [28]:

TABLE 3.1

PARAMETERS FOR SIMULATION OF QUEUING MODEL [28]

ITR_{Max}		2000			
N_{Cap}		17			
λ_k		Non-homogeneous Poisson Process (Figure 3.8 & 3.10)			
μ_k		Non-homogeneous Poisson Process, includes BCB and SOC (Figure 3.9 & 3.10)			
PEV	Class	Compact	Economy	Mid-size	Light Truck / SUV
	C_{Bat}, kWh	8 – 12	10 - 14	14 – 18	19 - 23
	E_M, kWh/mile	0.2- 0.3	0.25-0.35	0.35-0.45	0.48-0.58
	DD, miles	Lognormal Distribution (Figure 3.6 & 3.7) μ_M = 40 miles, σ_M = 20 miles			

3.5 Results and Discussions

3.5.1 PEV Charging Load Using Queuing Analysis

In this section the effect of PEV charging on the distribution system performance is examined. Queuing analysis is used to model the 24-hour PEV charging demand at the charging station. The objective is to determine the optimal distribution system operation considering PEV charging demand while minimizing the system losses using the OPF model. The probability distribution of N_0 is obtained from (3.1) and shown in Figure 3.11 which is used as an input to the $M_1/M_2/N_0$ queuing model [79]. Different N_{Cap} values are examined within the proposed queuing model and it is noted that when N_{Cap} is high, the probability of simultaneously charging of N_{Cap} number of PEVs, *i.e.*, $P(N_{Cap})$ is very low, as seen from Figure 3.11. Because of this low probability, there is insignificant impact on the total expected charging demand for high values of N_{Cap}. By various trial runs it is noted that

beyond N_{Cap} *=17*, the effect on expected charging demand does not change significantly and hence, N_{Cap} *=17* was chosen.

It is noted from Figure 3.12 that the expected PEV charging demand is low, for low arrival rates (M_1 *= 40, i.e., a PEV arriving every 40 minutes*), and the discrete distribution pattern of the demand as a function of N_0 is skewed normal with a low mean value of N_0. As the arrival rate increases, *i.e.*, M_1 *= 25 (a PEV arriving every 25 minutes)*, and then for M_1 *= 10*, the expected PEV charging demand increases and the distribution pattern becomes a standard normal distribution with a high mean value of N_0.

Using the chronological arrival rate profiles for each scenario (Figure 3.10) and the probability distribution associated with a specific arrival rate, the expected PEV charging demand at a specific hour can be obtained, as shown in Figures 3.13 - 3.15. It is seen that when the arrival rate is high, the expected load is high, and the discrete distribution pattern of the PEV charging demand as a function of N_0 is normally distributed.

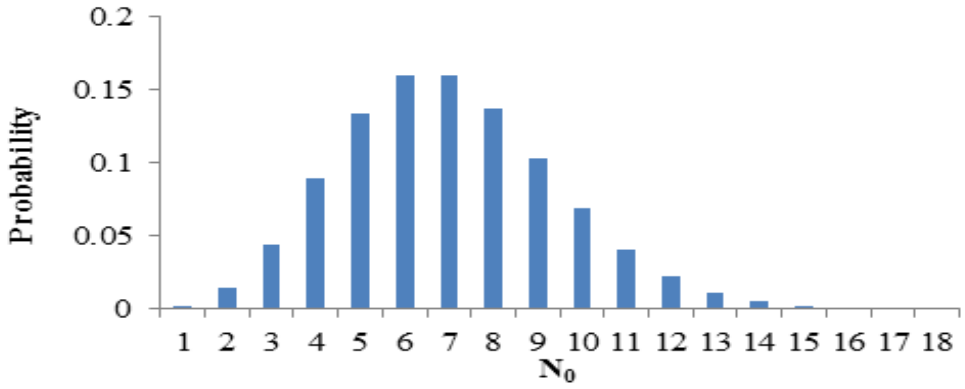

Figure 3.11: Probability distribution of N_0 as input to $M_1/M_2/N_0$ queuing model.

For example, at hour-8 the PEV arrival rate is high for Scenario-1 (Figure 3.13) while at hour-22 it is high for Scenario-2 (Figure 3.14), and the discrete distribution patterns are accordingly normally distributed at these hours, for the respective scenarios. When PEV charging takes place at hour 10 (Figure 3.15), which is not the most convenient hour and

neither the cheapest hour for customers to charge their vehicles, both scenarios have almost similar distributions.

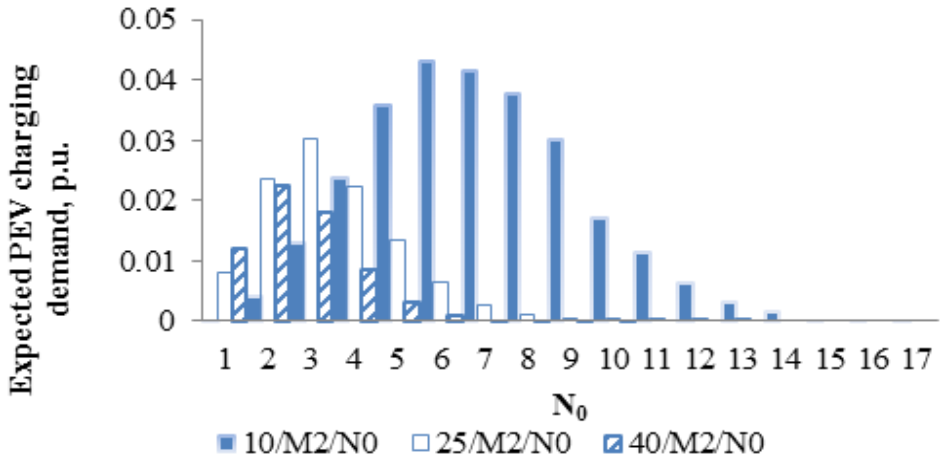

Figure 3.12: Expected PEV charging demand for some typical arrival rates.

The overall expected PEV charging demand obtained from (3.11) for both Scenarios, presented in Figure 3.16, shows that the PEV charging demand increases in both scenarios as compared to the Base Case. In Scenario-1 the charging demand appears during the peak price hours since these hours are more convenient for customers, while in Scenario-2 the increase is significant during off-peak price hours. It is also noted that as N_0 increases, the expected charging demand will gradually merge with the Base Case load profile as the probability of a large N_0 is low.

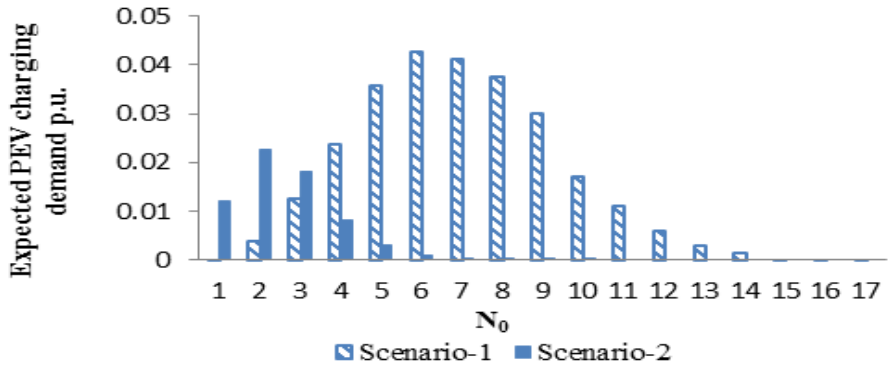

Figure 3.13: Expected PEV charging demand at hour-08 for different N_0.

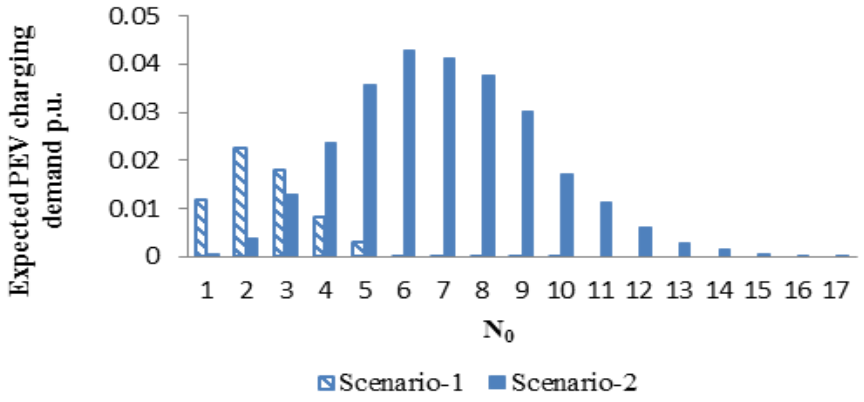

Figure 3.14: Expected PEV charging demand at hour-22 for different N_0.

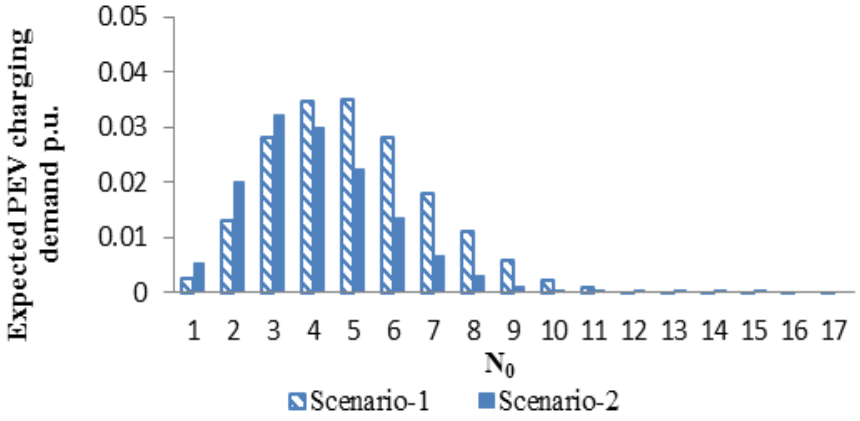

Figure 3.15: Expected PEV charging demand at hour-10 for different N_0.

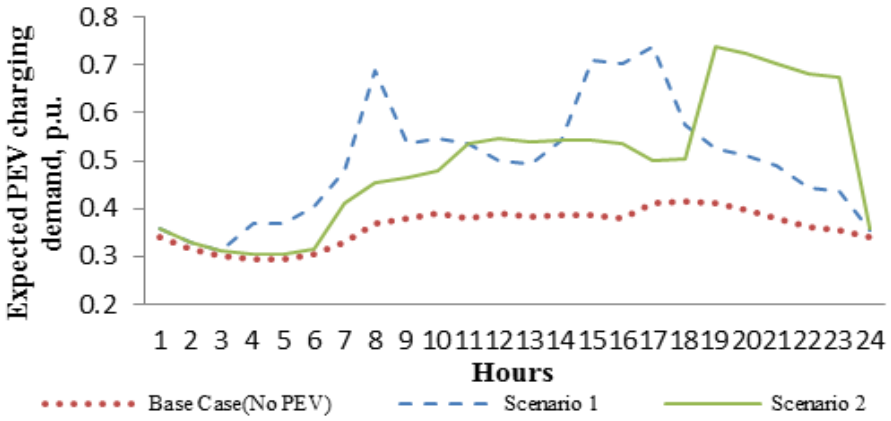

Figure 3.16: Total PEV expected charging demand for all queuing model.

3.5.2 Impact of BCB on Service Time and Charging Load

In classical queuing analysis based approaches [26-28], charging time is typically modeled using an exponential distribution with upper and lower limits randomly assigned to each PEV. In this work the BCB is considered so as to represent the PEV service time more precisely, as a function of the SOC. It is seen from Figure 3.17 that when BCB is considered, all the PEVs are served within the hour they arrive at the station, there is no overflow across the hour, and there is no waiting time.

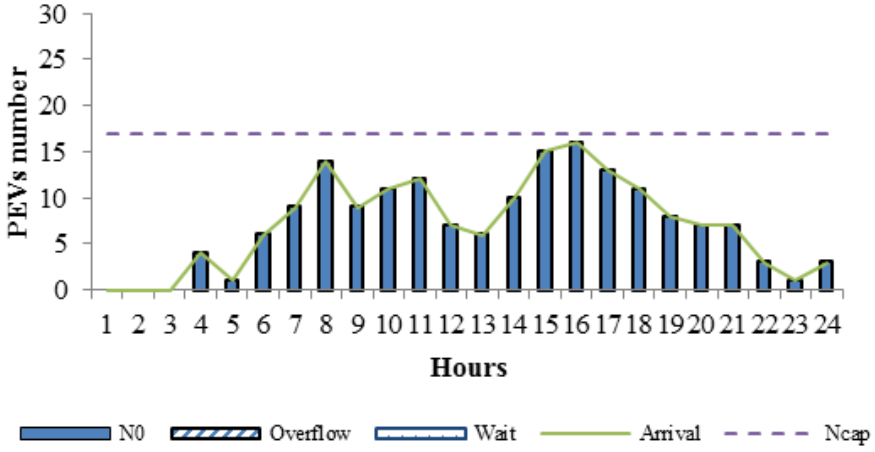

Figure 3.17: PEVs charging, overflow, waiting: considering BCB.

On the other hand, when BCB is not considered, and the charging time is selected randomly as in classical queuing analysis based approaches [26-28], where charging time is typically modeled using exponential distributions with upper and lower limits randomly assigned to each PEV, there will be service overflows if the selected charging time is more than 60 minutes. These service overflows will be transferred to the next hour, which may lead to waiting times if the total number of PEVs to be served, exceeds N_{Cap} (Figure 3.18). The effect of considering the BCB on the PEV demand profile is quite noticeable (Figure 3.19), when the BCB model is not considered the charging demand is higher at certain hours because of the service overflow and shifting of demand taking place, as discussed earlier.

In order to introduce a service overflow and waiting time for PEVs when considering BCB of the PEVs, it is now assumed that the arrival rate is greater than the station capacity, *i.e.*, $\lambda > N_{Cap}$. As can be seen from Figures 3.20 and 3.21, the service overflow and PEVs waiting are significantly increased when BCB is not considered. It is also noted that the average waiting time is significantly reduced when BCB is considered as compared to the case without BCB (Figure 3.22) which is in line with the preferences of customers for fast charging. Finally, Figure 3.23 shows the effect of BCB on total charging demand when the arrival rate exceeds the station capacity. Comparing this profile with Figure 3.19, it is noted that the charging demand is significantly affected by the BCB, and also when $\lambda > N_{Cap}$.

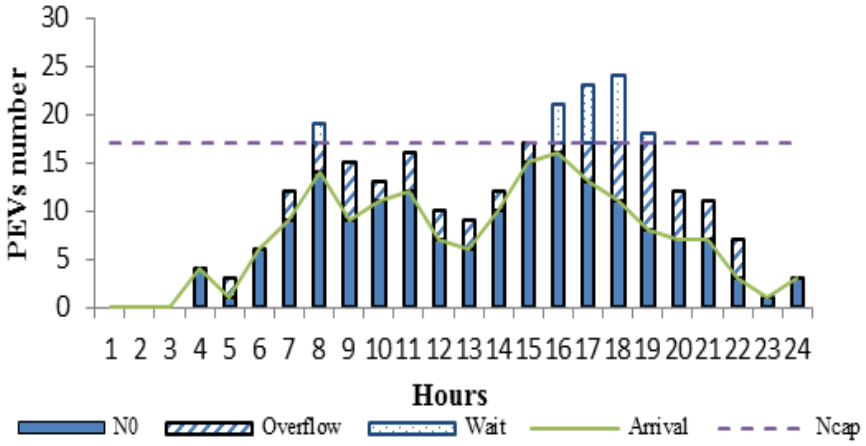

Figure 3.18: PEVs charging, overflow, waiting: not considering BCB.

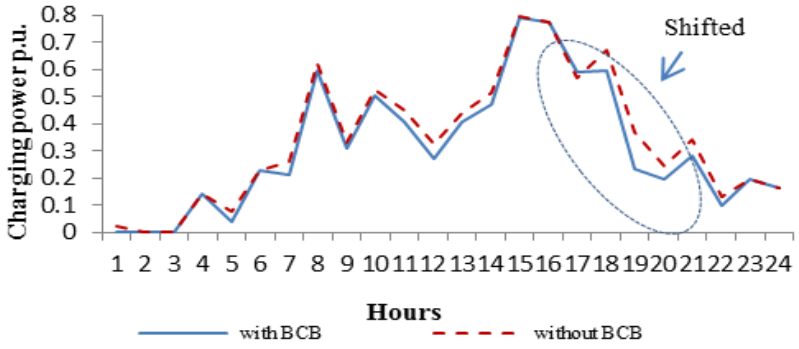

Figure 3.19: Effect of BCB on total charging demand.

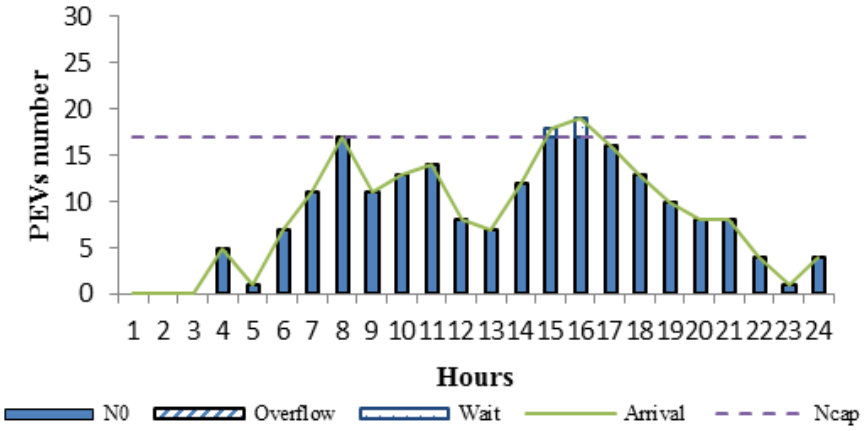

Figure 3.20: PEVs charging, overflow, waiting: considering BCB, $\lambda > N_{Cap}$.

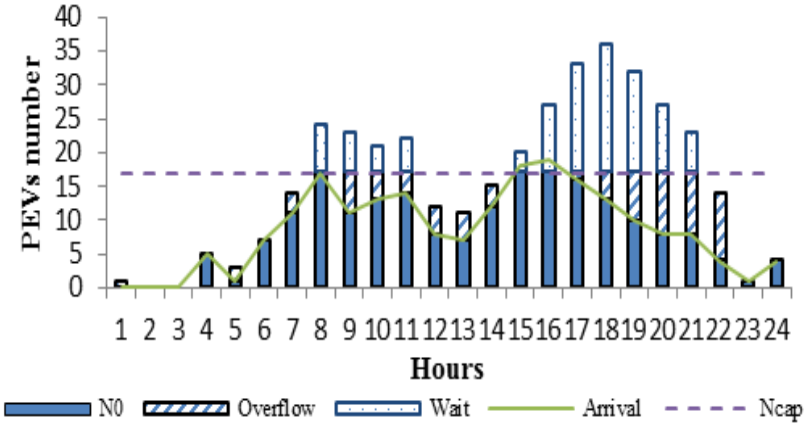

Figure 3.21: PEVs charging, overflow, waiting: not considering BCB, $\lambda > N_{Cap}$.

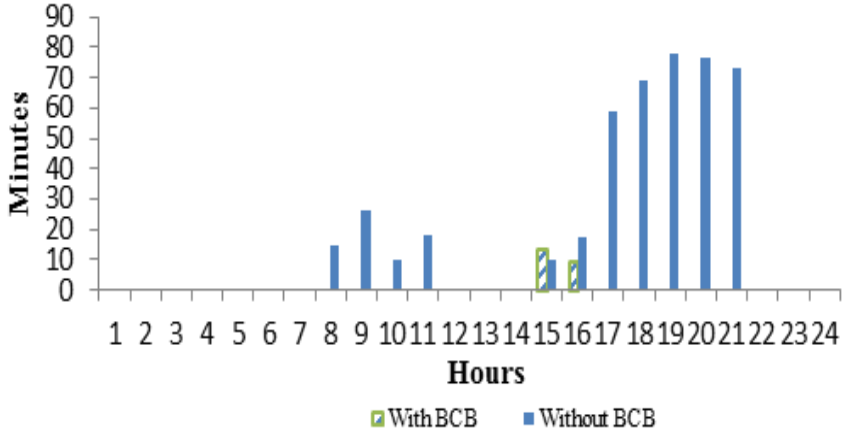

Figure 3.22: Effect of BCB on average waiting time, $\lambda > N_{Cap}$.

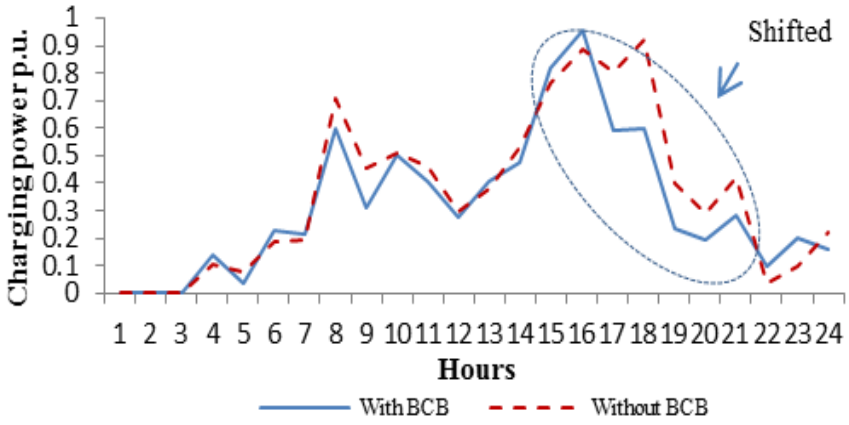

Figure 3.23: Effect of BCB on total charging demand, $\lambda > N_{Cap}$.

3.5.3 Impact of PEV Charging on Distribution System Operation

The Base Case is the case when no PEVs are present in the system. Analyses are then carried out to examine the impact of PEV charging loads considering:

3.5.3.1 Uncontrolled operation of distribution system

In this case power flow analysis is carried out to examine the impact of PEV charging loads appearing on the distribution feeder while the LDC takes no operational or control actions to manage the system voltages.

3.5.3.2 Optimal operation of distribution system

This case considers the OPF model and examines the impact of LDC's optimal operation actions and how the system voltages are controlled to ensure system security.

It is noted from Figure 3.24 that the expected system losses for the two scenarios of PEV charging with optimal operation of the distribution system are significantly higher than the Base Case, with no PEVs. It is noted that the expected loss is maximum for $N_0 = 3$, *i.e.*, when three PEVs are charging simultaneously, because $M_1/M_2/3$ results in the highest expected system load. It is also noted from Figure 3.24 that for $N_0 \geq 9$, *i.e.*, for nine or more

PEVs charging simultaneously, the expected system loss in both scenarios are almost the same as that in the Base Case.

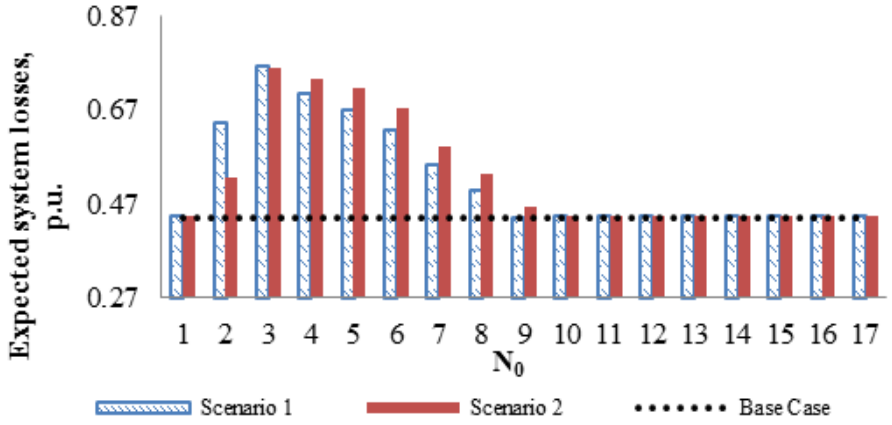

Figure 3.24: Impact of PEV charging on losses during optimal operation of system.

The expected bus voltage profiles are also affected by PEV charging. For example, at Bus-65, which is a remote bus and located close to the PEV charging station, significant drop in the expected voltage profile takes place at various hours, depending on the scenario considered (Figure 3.25 - Figure 3.28). Figures 3.25 and 3.26 presents the expected voltage profiles at bus-65 considering uncontrolled operation and optimal operation of the distribution system, respectively; the voltage drop is significant in uncontrolled operation (Figure 3.25), while much improved with optimal operation (Figure 3.26) because of the imposition of voltage constraints by the LDC. Figure 3.26 demonstrates that the LDC can indeed accommodate PEV charging loads by appropriate control and operational decisions to maintain the system voltages within limits.

In order to capture the uncertainties, stochastic power flow studies are presented with p.d.f. of the PEV charging load and compared with stochastic OPF, to examine the LDC's operational impacts. As expected, the stochastic OPF (Figure 3.28) ensures that the bus voltage at bus-65 is within the specified limit at all hours, while the stochastic power flow (Figure 3.27) gives an idea of the expected worsening of the bus voltage due to PEV charging.

It is noted from Figures 3.25 – 3.28 that the voltage drops coincide with the appearance of PEV charging loads; for example, the voltage drop is significant during peak hours in Scenario-1, because customers charge their PEVs as per their convenience; while in Scenario-2 customers opt to charge during low price hours and the voltage drop is most significant during the off-peak hours.

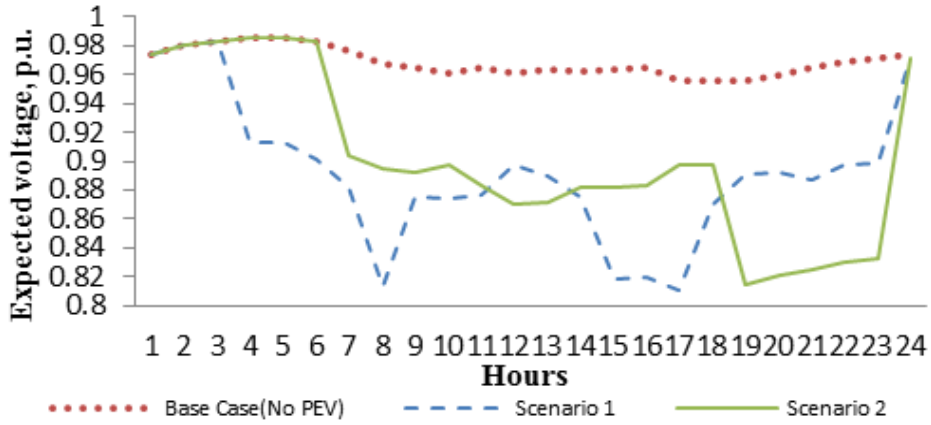

Figure 3.25: Expected voltage profile at Bus 65 for uncontrolled operation.

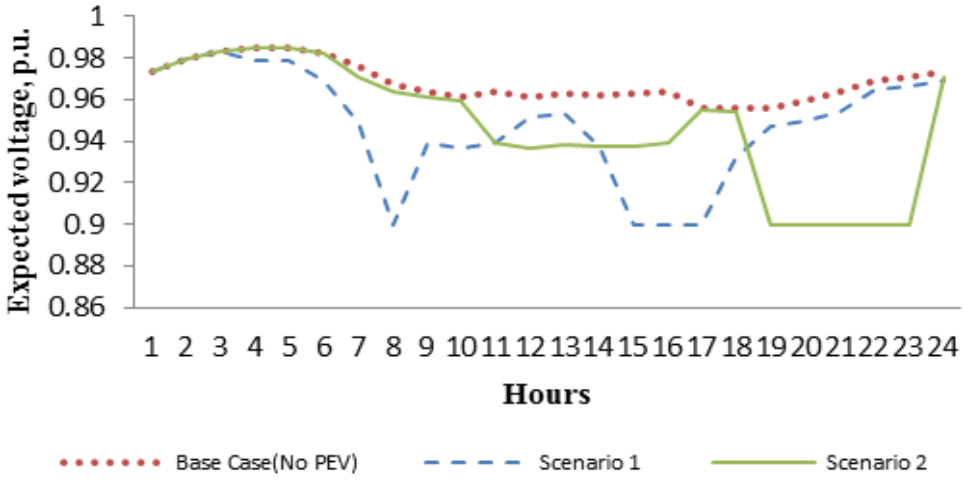

Figure 3.26: Expected voltage profile at Bus 65 for optimal operation.

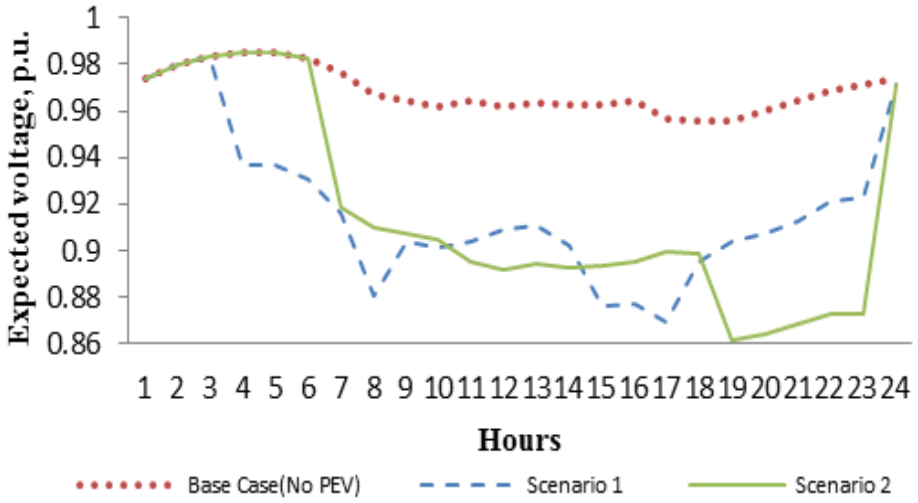

Figure 3.27: Expected voltage profile at Bus 65, stochastic uncontrolled operation.

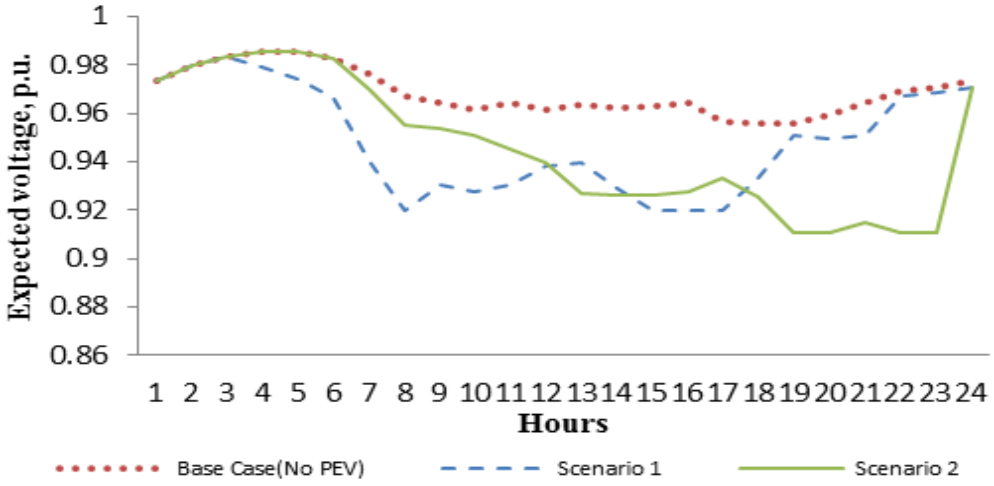

Figure 3.28: Expected voltage profile at Bus 65, stochastic optimal operation.

The profiles of expected active power transfer from the external grid over the substation transformer are also affected by PEV charging (Figures 3.29 – 3.32). When the optimal operation of the distribution system, is considered (Figures 3.30 and 3.32), the expected active power transfer is reduced as compared to the uncontrolled operation (Figures 3.29 and 3.31).

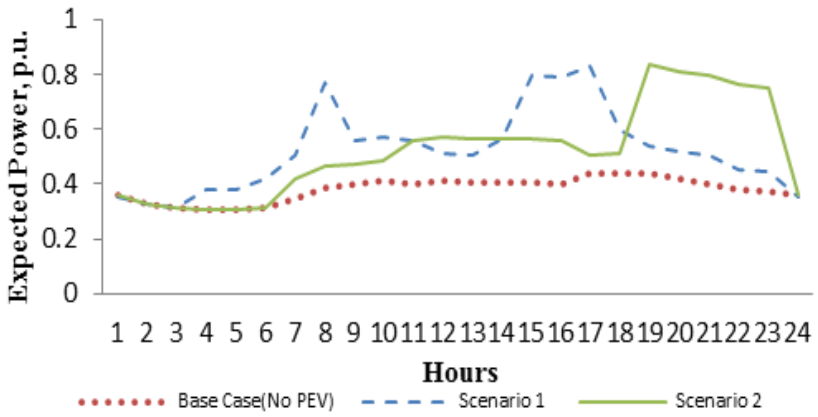

Figure 3.29: Expected active power transfer, uncontrolled operation.

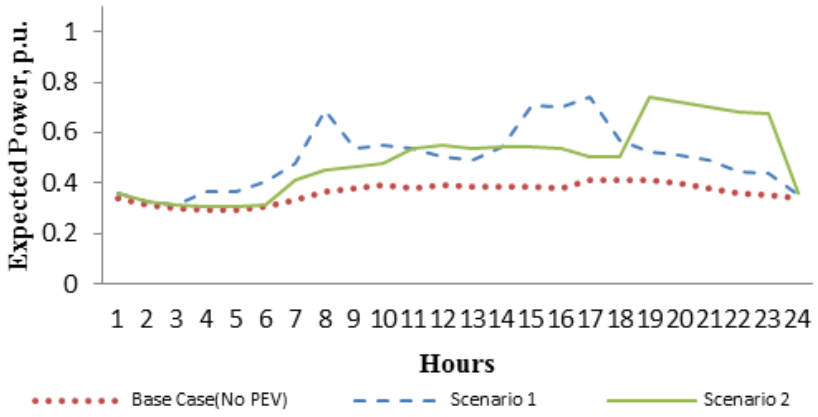

Figure 3.30: Expected active power transfer, optimal operation.

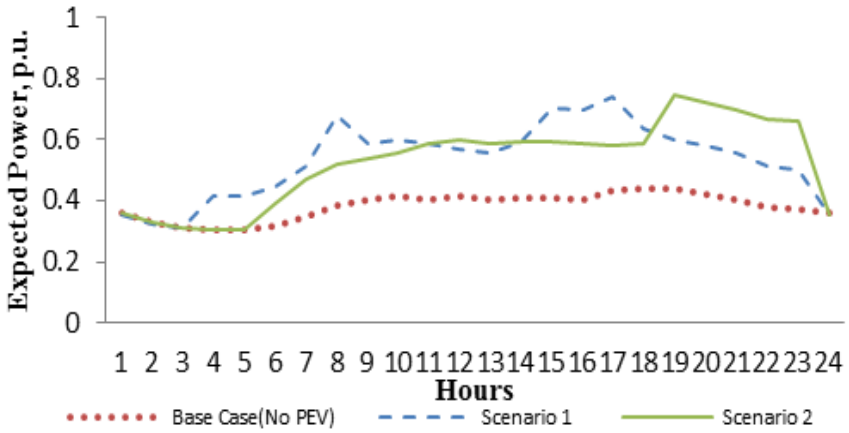

Figure 3.31: Expected active power transfer, stochastic uncontrolled operation.

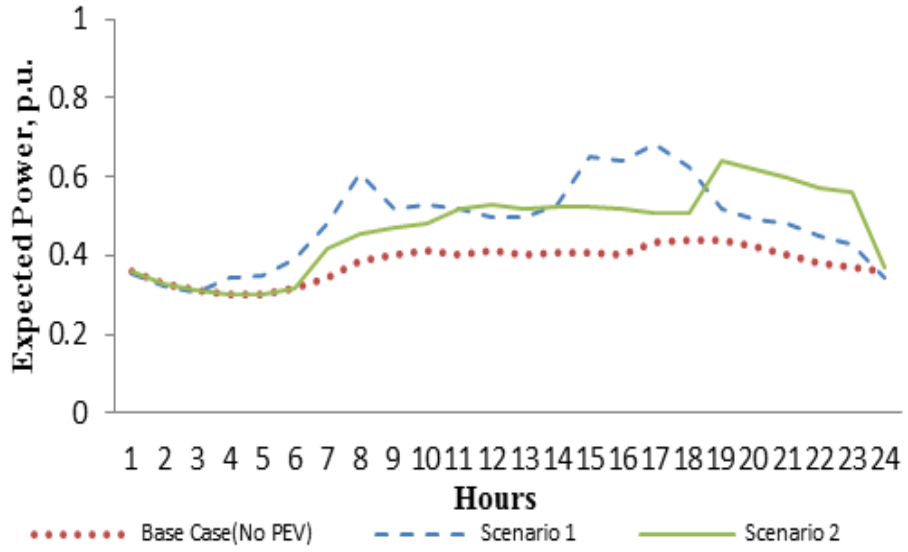

Figure 3.32: Expected active power transfer, stochastic optimal operation.

As discussed earlier, the MPC approach is considered in this chapter to examine the impact of the PEV charging load on the LDC's operations in the presence of uncertainties, and these are compared with the optimal operation of the distribution system. The expected voltage profiles at bus-65 for these cases and the two scenarios are presented in Figures 3.33 and 3.34, respectively. The profiles of expected active power transfer from the external grid are presented in Figures 3.35 and 3.36, respectively. It is noted that when MPC is considered, the expected voltage profile is improved and the active power transfer is reduced as compared to the corresponding optimal operations profiles (Figures 3.33 - 3.36).

Figures 3.37 and 3.38 present the hourly expected system losses considering the MPC and the OPF models for both scenarios. It is noted that the system losses are reduced by 17.95% and 16.08% in Scenario-1 and 2, respectively with the MPC based approach as compared to the OPF. Therefore, the overall operational performance of the distribution system considering the uncertainty of PEV charging demand, is improved when the MPC based approach is considered for LDC operations.

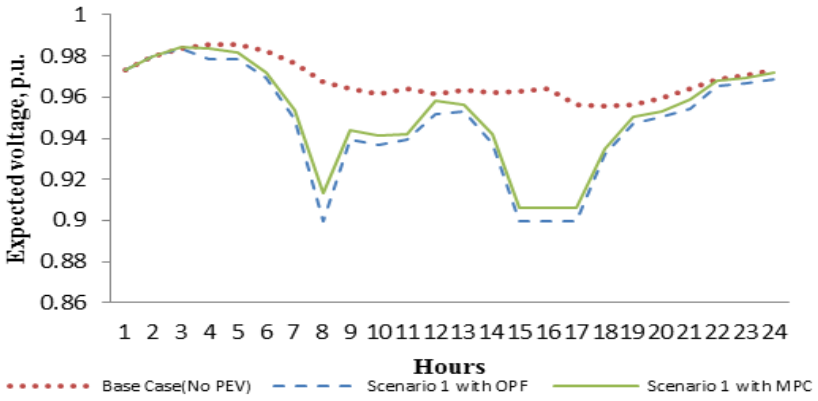

Figure 3.33: Comparison of optimal operation versus MPC for Scenario-1.

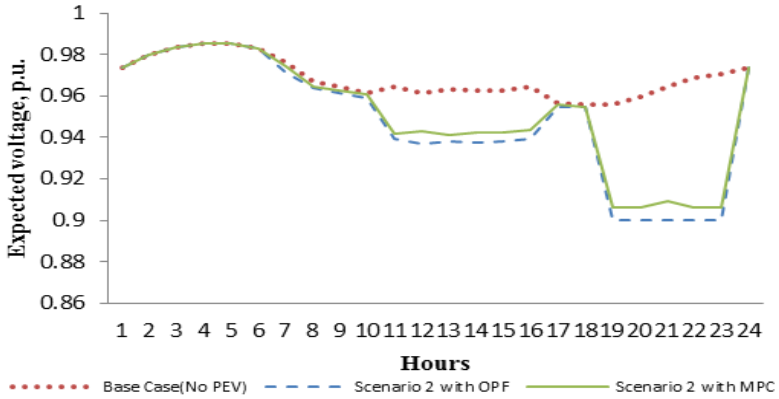

Figure 3.34: Comparison of optimal operation versus MPC for Scenario-2.

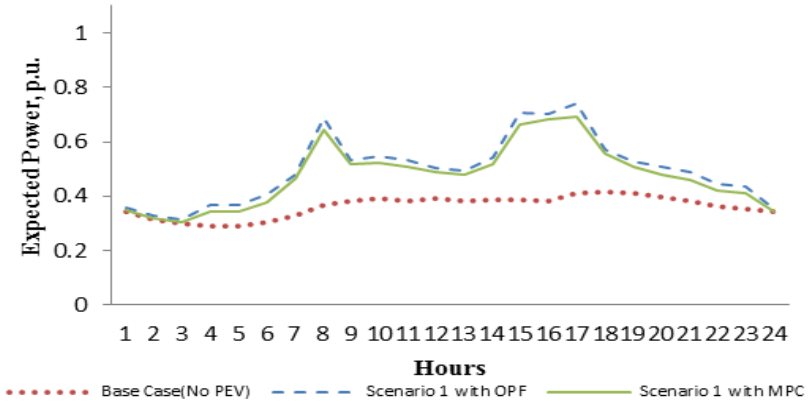

Figure 3.35: Comparison of optimal operation versus MPC for Scenario-1.

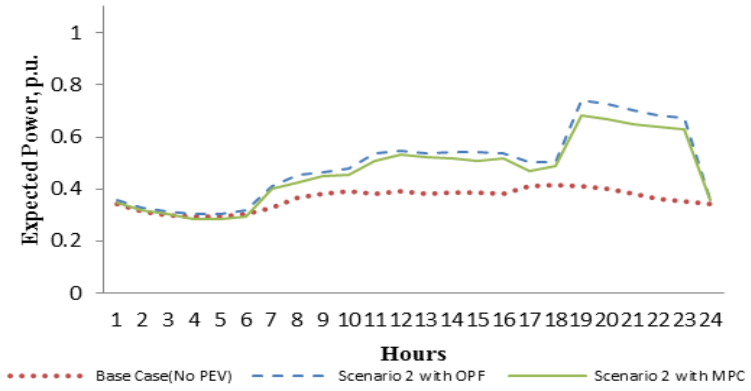

Figure 3.36: Comparison of optimal operation versus MPC for Scenario-2.

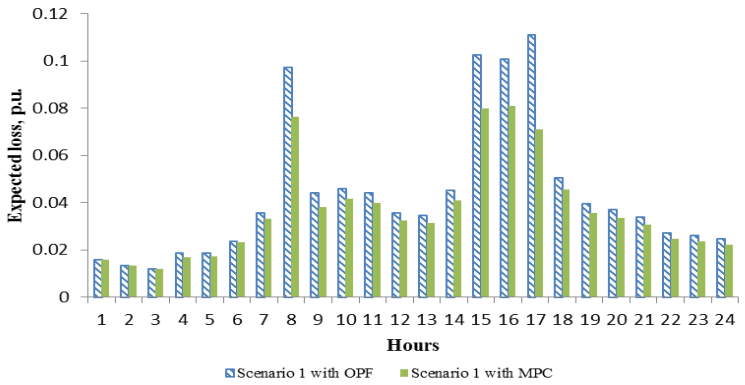

Figure 3.37: Comparison of optimal operation versus MPC for Scenario-1.

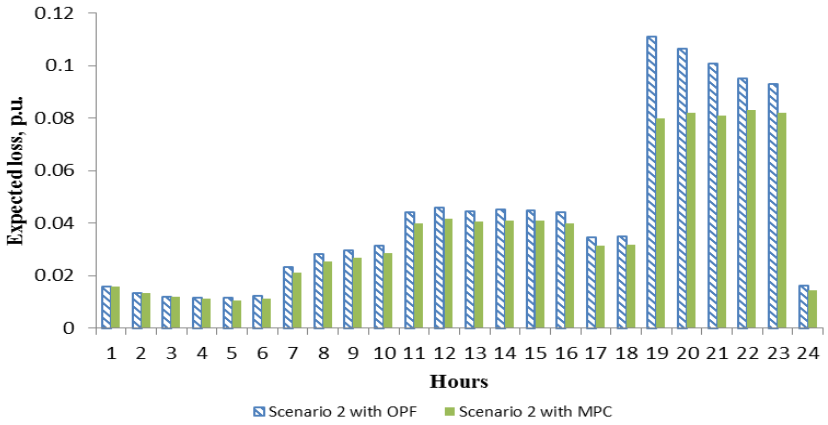

Figure 3.38: Comparison of optimal operation versus MPC for Scenario-2.

3.6 Summary

In this chapter, a queuing analysis based methodology for modeling the 24-hour charging demand of PEVs at a charging station was presented. Four different PEV classes with their appropriate parameters that determined the charging behavior were taken into consideration. The proposed queuing model considered the arrival of PEVs as a non-homogeneous Poisson process with different arrival rates at different times of the day and the PEV BCB was also considered. Different arrival rate patterns were considered for different groups of customers- one based on customer convenience and the other based on PEV charging price which were estimated from Waterloo Region TTS data and Ontario TOU rates respectively. A novel feature of the proposed PEV charging load model was that a piece-wise linear function of the SOC was used to represent the BCB of PEVs, and hence determine the charging time which then integrated with the $M_1/M_2/N_0$ queuing model. The developed load model of PEVs was then incorporated in deterministic and stochastic analysis frameworks of the distribution system, through power flow and OPF models as well as MPC based method, to study their impact on the distribution system, and examine how the LDC can accommodate PEV charging loads while maintaining the system constraints.

Chapter 4

Integrating Electric Vehicle Charging Stations as Smart Loads for Demand Response Provisions in Distribution Systems[2]

4.1 Introduction

This chapter presents a mathematical model for representing the total charging load at an EVCS in terms of controllable parameters; the load model developed using a queuing model followed by a NN. The queuing model constructs a data set of PEV charging parameters which are input to the NN to determine the controllable EVCS load model. The queuing model considers arrival of PEVs as a non-homogeneous Poisson process, while the service time is modeled considering detailed characteristics of the battery. The smart EVCS load is a function of number of PEVs charging simultaneously, total charging current, arrival rate, and time; and various class of PEVs. The EVCS load is integrated within a distribution operations framework to determine the optimal operation and smart charging schedules of the EVCS. Objective functions from the perspective of the LDC and EVCS owner are considered for studies. A 69-bus distribution system with an EVCS at a specific bus, and smart load model is considered for the studies. The performance of the smart EVCS vis-à-vis an uncontrolled EVCS is examined to emphasize the DR contributions of a smart EVCS and its integration into distribution operations.

The rest of this chapter is organized as follows. Section 4.2 presents the nomenclature pertaining to the mathematical model presented in this chapter. The proposed novel framework and mathematical models for developing the EVCS smart load model and its integration in the distribution operations model are presented in Section 4.3. In Section 4.4, the system description pertaining to the case study carried-out, is presented. The results and discussions are presented in Section 4.5 and the concluding remarks in Section 4.6.

---

[2] Some parts of this chapter has been accepted for publication in:

- O. Hafez, and K. Bhattacharya, "Integrating electric vehicle charging stations as smart loads for demand response provisions in distribution systems," IEEE Transactions on Smart Grid (in print).

4.2 Nomenclature

4.2.1 Sets and Indices

cs	Index for charging station
i, y	Index for buses
k	Index for time
N_B	Total number of bus in the system
j	Index for PEV class *j* = {automobile car, van (mini, cargo, passenger), sports utility vehicle, and pickup truck}
s	Index for input layer neurons
ss	Index for substation bus
r	Index for hidden layer neurons
t	Index for output layer neurons

4.2.2 Parameters

B^{Cap}	Total PEV battery capacity, kWh
DD	Daily driven miles by PEV, mile
E_C	Energy consumption of PEV battery per mile driven, kWh/mile
$G_{i,y}$ `	Conductance of feeder section *i-y*, p.u.
$H_{j,k,r}$	Hidden layer neuron
$I_{j,k}$	Charging current drawn by PEVs of class *j* at hour *k* , A
$M_1/M_2/N$	Queuing model, M_1: PEV arrival time-lag (minutes) / M_2: PEV charging time (minutes) / N: Number of PEVs charging simultaneously at a given hour *k*
N^{Max}	Maximum number of PEVs that can be charged simultaneously at the EVCS
N_j^{Max}	Maximum number of PEVs of class j that can be charged simultaneously at the EVCS
N_I, N_H, N_O	Number of input layer, hidden layer and output layer neurons
$N\lambda_k$	Number of PEV arrived at charging station
$PD_{i,k}$, $QD_{i,k}$	Active, reactive power demand at a bus at hour *k*, p.u.
$\underline{TPD}, \overline{TPD}$	Lower and upper limit on system demand, p.u.

PS^{Max}	Maximum active power transfer limit on substation transformer, p.u.
QS^{Max}	Maximum reactive power transfer limit on substation transformer, p.u.
V^{Min}, V^{Max}	Minimum, maximum limit on bus voltage, p.u.
$w_{j,s,r}$	Weights on hidden layer of the NN
$W_{t,r}$	Weights on output layer of the NN
W^{Max}	Maximum number of PEVs that can wait for service at the EVCS
$Y_{i,y}$	Magnitude of admittance matrix element, p.u.
λ_k	Arrival rate of PEVs at the EVCS at hour *k*, minute
β_r, Γ	Input bias, output bias of NN
$\theta_{i,y}$	Angle of complex Y-bus matrix element, rad

4.2.3 Variables

J_1, J_2	Objective functions
$N_{j,k}$	Number of PEVs charged simultaneously, of class *j* at hour *k*
$Pch_{j,k}$	Active power PEV charging demand, of class *j* at hour *k*, p.u.
$PD_{EVCS,k}$	Total EVCS charging demand, at hour *k*, p.u.
$PG_{i,k}$, $QG_{i,k}$	Active, reactive power generation at hour *k*, p.u.
$PS_{i,k}$, $QS_{i,k}$	Active and reactive power injected through substation transformer at hour *k*, p.u.
R_k	Number of PEVs rejected from charging, at hour *k*
TN_k	Total number of PEVs charged simultaneously from all classes, at hour *k*
$TPch_k$	Total active power PEV charging demand from all class of vehicles, at hour *k*, p.u.
V_i	Bus voltage, p.u.
W_k	Number of PEVs waiting for service at hour *k*
δ	Voltage angle at a bus, rad.

4.3 Proposed Framework and Mathematical Models

This chapter proposes a smart distribution system operations framework including the DR contributions from a smart EVCS. The proposed framework is depicted in Figure 4.1, where the queuing model receives inputs from the NHTS dataset [12] in terms of PEV class, battery capacity, SOC, etc., to construct the output profiles for the number of PEVs charged, total charging current, arrival rate, and time. The queuing model considers the arrival of PEVs as a non-homogeneous Poisson process and the novel piece-wise linear representation of the SOC presented in Chapter-3, is used to represent the BCB within the charging time in the $M_1/M_2/N$ queuing model. The output profile from the queuing model serves as the training and validation data sets for the NN, to express the charging power for each class of PEV as a function of these parameters. The output of the CSCLE, developed using the supervised NN learning is integrated within the novel distribution operations model that considers PEV smart charging constraints, and EVCS related constraints to determine the smart operational decisions of the EVCS while considering various distribution operations constraints. As shown in Figure 4.1, the LDC sends a peak demand cap signal to the EVCS and which induces a DR service from the latter, whereby the PEVs are accordingly scheduled for charging.

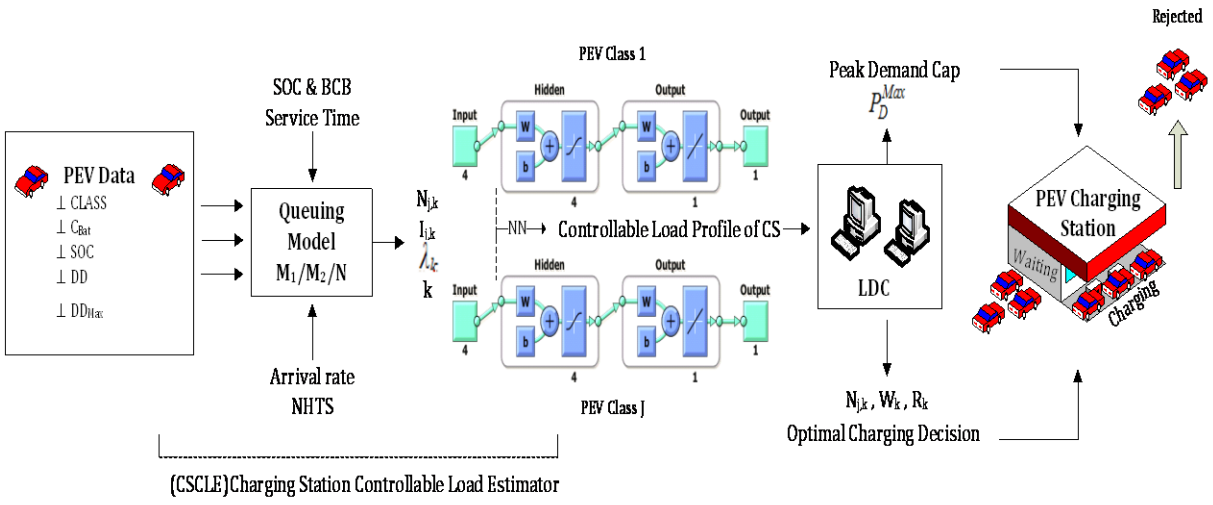

Figure 4.1: Interaction between LDC and EVCS.

4.3.1 Charging Station Controllable Load Estimator (CSCLE)

The EVCS smart load model is arrived at in two steps, as mentioned earlier. In the $M_1/M_2/N$ queuing model, M_1 denotes the arrival rate, modeled as non-homogeneous Poisson process based on NHTS dataset [12], M_2 denotes the service time of a PEV customer modeled using the SOC of the PEV considering the BCB, while N is the number of customers being served simultaneously. These data sets of PEV charging parameters obtained from the queuing model are then used in the second step, the NN model, as training and validation datasets to express the EVCS load as a function of different parameters.

The EVCS smart charging load profile considering all PEVs belonging to class j, is denoted by $Pch_{j,k}$ and can be expressed mathematically as a function of the number of PEVs being charged simultaneously ($N_{j,k}$), total charging current ($I_{j,k}$), arrival rate of PEVs at the EVCS (λ_k), and time (k), as follows:

$$Pch_{j,k} = f(N_{j,k}, I_{j,k}, \lambda_k, k). \tag{4.1}$$

As mentioned earlier, since k is an independent parameter, λ is independent process, and $I_{j,k}$ depends on the PEV class, the EVCS smart load in (4.1) can be represented as a function of $N_{j,k}$ only, as follows:

$$Pch_{j,k} = f(N_{j,k}). \tag{4.2}$$

From (4.2), it is evident that once the functional relationship between $N_{j,k}$ and $Pch_{j,k}$ is established using the NN, the EVCS smart load can be controlled by appropriate decisions on $N_{j,k}$.

The structure of the feed-forward NN used in this work is shown in Figure 4.2. The NN is trained in MATLAB using the Levenberg-Marquardt algorithm for back propagation. While training the NN, the entire dataset is divided into three subsets. The first subset is the training set, used for computing the gradient and updating the network weights and biases. The second subset is the validation set, which is used to monitor the error during the training process that normally decreases during the initial phase of training, as does the training set

error. The third subset or test set is used to compare different models, using the test set error during the training process to evaluate the accuracy of the NN model. During the training process N_H is varied to arrive at the best fit for the PEV charging load model.

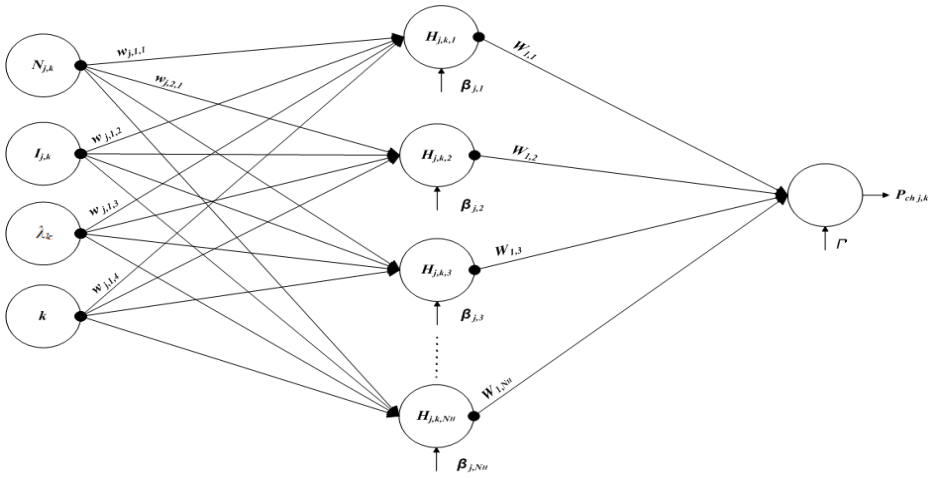

Figure 4.2: NN structure as part of CSCLE to determine smart EVCS load model.

In order to obtain a mathematical function of $Pch_{j,k}$ from the trained NN, the output from each hidden layer neuron $H_{j,k,1}$ to $H_{j,k,4}$ for different PEV classes are determined first. The incoming inputs with appropriate weights $w_{j,s,r}$ are summed up at each hidden layer neuron. Also, each hidden layer neuron has an additional input, the bias β_1 to β_4, which is used in the network to generalize the solution and to avoid a zero value of the output, even when an input is zero. This summed signal is passed through an activation function (*tansig*) associated with each hidden layer neuron, which transforms the net weighted sum of all incoming signals into an output signal from the hidden layer neuron. Accordingly,

$$H_{j,k,1} = \tan sig(w_{j,1,1}N_{j,k} + w_{j,1,2}I_{j,k} + w_{j,1,3}\lambda_k + w_{j,1,4}k + \beta_{j,1}) \quad (4.3)$$

$$H_{j,k,2} = \tan sig(w_{j,2,1}N_{j,k} + w_{j,2,2}I_{j,k} + w_{j,2,3}\lambda_k + w_{j,2,4}k + \beta_{j,2}) \quad (4.4)$$

$$H_{j,k,3} = \tan sig(w_{j,3,1}N_{j,k} + w_{j,3,2}I_{j,k} + w_{j,3,3}\lambda_k + w_{j,3,4}k + \beta_{j,3}) \quad (4.5)$$

$$H_{j,k,4} = \tan sig(w_{j,4,1}N_{j,k} + w_{j,4,2}I_{j,k} + w_{j,4,3}\lambda_k + w_{j,4,4}k + \beta_{j,4}) \quad (4.6)$$

In this work the NN is run for each PEV class individually. Finally, $Pch_{j,k}$ can be obtained from the output neuron of the trained NN as follows:

$$Pch_{j,k} = purelin(H_{j,k,1}W_{1,1} + H_{j,k,2}W_{1,2} + H_{j,k,3}W_{1,3} + H_{j,k,4}W_{1,4} + \Gamma) \quad (4.7)$$

where *purelin* is a linear transfer function available in MATLAB.

4.3.2 Distribution Operations Model with Controllable EVCS

After all weights are determined, the distribution operations model is formulated by including the EVCS smart load model developed from the CSCLE framework, discussed in the previous subsection. Some new constraints are necessary to capture the smart charging schedules and the smart EVCS operational aspects.

4.3.2.1 Objective Functions

Two different objective functions are considered, first is the minimization of feeder losses, which is the desired objective from the perspective of the LDC. Since the main objective of the distribution system operators is to meet the system demand while ensuring a good voltage profile for customers, the objective of minimization of feeder losses is considered, and is given as follows:

$$J_1 = \frac{1}{2}\sum_{k=1}^{24}\left[\sum_{i=1}^{N_B}\sum_{j=1}^{N_B} G_{i,j}\begin{pmatrix} V_{i,k}^2 + V_{j,k}^2 - 2V_{i,k}V_{j,k} \\ \cos\left(\delta_{j,k} - \delta_{i,k}\right) \end{pmatrix}\right] \quad (4.8)$$

The second is the maximization of the number of PEVs services or charged at the EVCS over a day, representing the perspective of the EVCS owner, and is given as follows:

$$J_2 = \sum_{k=1}^{24}\sum_{j=1}^{J} N_{j,k} \quad (4.9)$$

4.3.2.2 Demand Supply Balance

The demand supply balance for active and reactive power is given by the power flow equations, augmented by including the total EVCS smart load at the EVCS bus to the active power equation, as follows:

$$PG_{i,k} - PD_{i,k} = \sum_{j=1}^{N_B} f(V_{i,k}, \delta_{i,k}) \qquad \forall\ i,\ i \neq cs \qquad (4.10)$$

$$PG_{cs,k} - PD_{cs,k} - TPch_{cs,k}(N_k) = \sum_{j=1}^{N_B} f(V_{cs,k}, \delta_{cs,k}) \qquad (4.11)$$

$$QG_{i,k} - QD_{i,k} = -\sum_{j=1}^{N_B} f(V_{i,k}, \delta_{i,k}) \qquad \forall\ i \qquad (4.12)$$

Where

$$TPch_{cs,k}(N_k) = \sum_{j=1}^{J} Pch_{j,k}(N_{j,k}) \qquad (4.13)$$

In (4.13) the total charging power $TPch_{cs,k}$ at the EVCS at hour k is the sum of the charging powers of each class of PEVs and is included in (4.11) at the specific bus where the EVCS is located. It is to be noted that $TPch_{cs,k}$ is a decision variable, unlike most other works, and is optimally determined from the model solution, by optimally determining N_k. It is to be noted that the PEV charging load has been modeled in this work as real power demand only. The PEV battery systems are typically considered to be unity power factor loads as per the common practice [25], [26], [28]. In some recent works, researchers have examined how PEVs can provide reactive power support services to the grid through capacitor banks associated with PEV batteries and chargers [80], [81], which is however not considered in this work, in order to focus on the stated objectives.

4.3.3 Controlled Operation of EVCS

These constraints pertain to EVCS smart operation by effective control of the number of PEVs charging simultaneously, N_k, number of PEVs waiting for charging, W_k, and the number of PEVs rejected for charging, R_k. Accordingly, the total number of PEVs charging simultaneously at hour k, is given by:

$$TN_k = N\lambda_k - W_k - R_k \qquad (4.14)$$

where TN_k is the sum of the number of PEVs, across all classes, charging simultaneously at hour k, and is given by:

$$TN_k = \sum_{j=1}^{J} N_{j,k} \tag{4.15}$$

Also, in (4.14), R_k is given by:

$$R_k = N\lambda_{\mathrm{k}} - (TN_k + W^{Max}) \tag{4.16}$$

The total number of PEVs being charged simultaneously at hour k, is constrained by the EVCS capacity, as follows:

$$TN_k \leq N^{Max} \tag{4.17}$$

Furthermore, the EVCS may also impose limits on the maximum number of PEVs of a particular class that can be charged at a time. Hence, the following constraint is imposed:

$$N_{j,k} \leq N_j^{Max} \tag{4.18}$$

The maximum number of PEVs that can wait for charging at hour k, are constrained by the EVCS space availability and is given by:

$$W_k \leq W^{Max} \tag{4.19}$$

4.3.4 Limit on EVCS Peak Demand

In order to ensure that the EVCS charging demand does not create additional peaks in the LDC's load profile, the following constraint is added:

$$\underline{TPD} \leq PD_{EVCS,k} \leq \overline{TPD} \tag{4.20}$$

Where $PD_{EVCS,k}$ denotes the total charging demand of the EVCS at hour k, $\underline{TPD}$ represents the minimum charging load as defined in the agreement with the EVCS owner, as a DR provider, while, $\overline{TPD}$ specifies the maximum peak demand of the EVCS allowed by the LDC.

In addition to the above, the system operational constraints such as bus voltage limits and substation capacity limits are also imposed. The above NLP model is solved using the MINOS5.1 solver in GAMS environment.

4.4 Case Study System

4.4.1 Distribution System Topology

The analysis presented in this chapter is carried out considering the IEEE 69-bus radial distribution system, whose single line-diagram is given in Figure 4.3 [77] with MVA_{Base} = 10 MVA. The distribution system is supplied through the substation at bus-1. It is assumed that an EVCS is arbitrarily located at bus-59, without any loss of generality, however if the charging station is located at remote buses for example at bus-65 or bus-27, the impact on the distribution system operation could be even more significant.

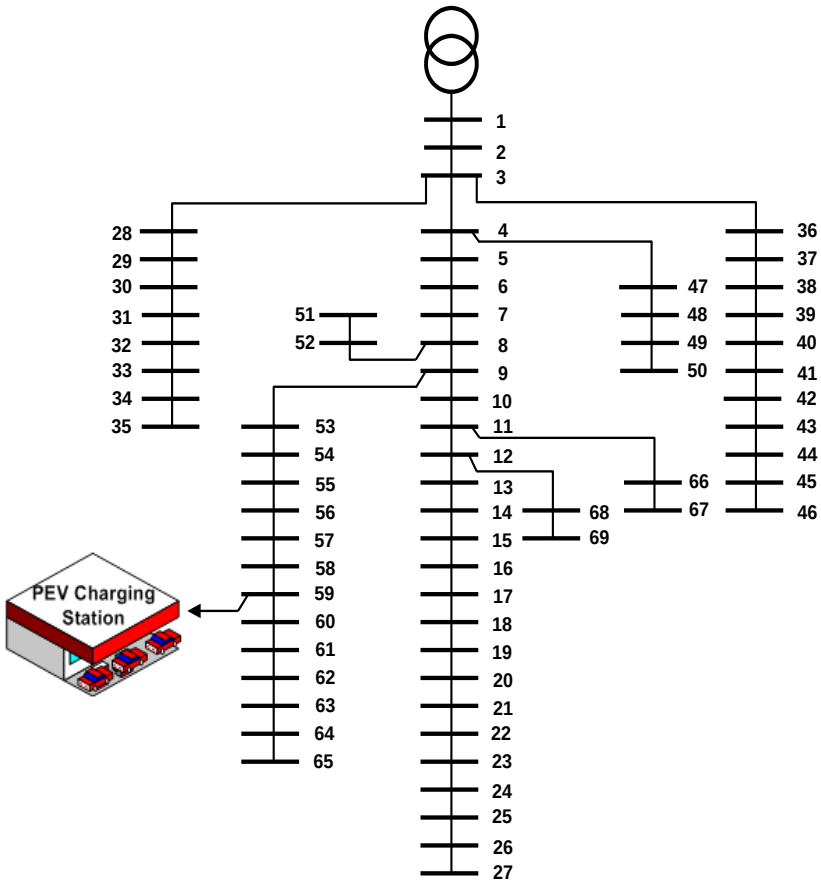

Figure 4.3: 69-Bus radial distribution system [77].

4.4.2 NHTS Data and Modeling PEV Arrival Rate

Since the availability of data pertaining to penetration of PEVs and PEV charging load recordings are still very limited, NHTS 2009 [12] data for light-duty vehicles is used in this work to model the PEV charging demand. The dataset comprises information on 12,469 vehicles, of four specific class of vehicles- automobile car, sports utility vehicle (SUV), van, and pickup truck; with the arrival destination being to buy gas at the gas-station, assuming that PEVs have the same pattern for arriving at the EVCS for charging their vehicles.

With this large dataset of information, the arrival rate of PEVs is realistically modelled for a large range of customer classes; the normalized hourly distribution of PEVs arriving for charging is presented in Figure 4.4. Furthermore, in order to draw the correspondence between fuel-driven vehicles and PEVs for the data processing work, in this chapter, four different PEV classes have been used with their appropriate battery sizes to match the NHTS classes, as given in Table 4.1. Nevertheless, the developed modeling framework is generic and demonstrates its effectiveness, and any appropriate realistic arrival rate data from an EVCS may be used to determine actual schedules and rejections.

TABLE 4.1
PEV PARAMETERS FOR CHARGING LOAD MODEL

NHTS Class [12]	Automobile Car	SUV	Van	Pickup Truck
PEV Class	Compact	Economy	Mid-size Van	Light Truck
B^{Cap}, kWh	8 – 12	10 – 14	14 – 18	19 – 23
E_C, kWh/mile	0.2- 0.3	0.25-0.35	0.35-0.45	0.48-0.58
DD, miles	Lognormal Distribution, μ_M = 40 miles, σ_M = 20 miles			

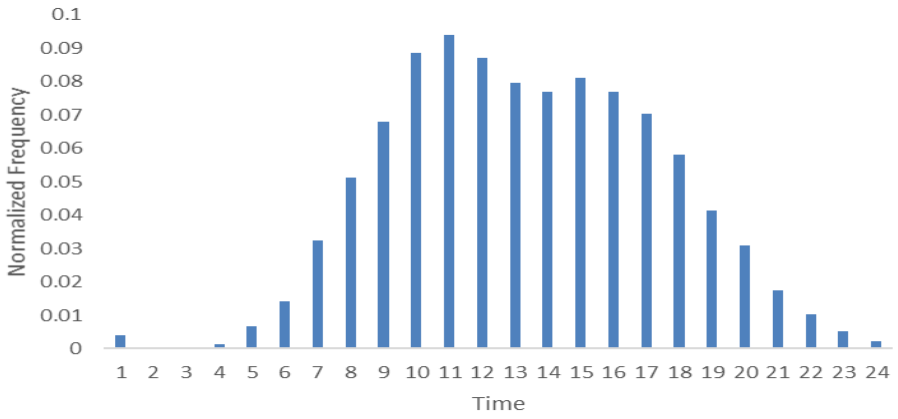

Figure 4.4: Arrival rate frequency distribution.

4.4.3 Neural Network

In this work, the vehicular data for 90 days is used considering 24, one-hour time intervals per day. There are four input layer neurons corresponding to the four inputs- *N*, *I*, λ, and *k*, and one output layer neuron corresponding to the output *Pch*. The NN has one hidden layer with N_H =4, *i.e.*, four hidden layer neurons; this was obtained by various trial simulations. An input matrix of dimension 4x2160 is created from the queuing model simulations, while the output vector is of dimension 1x2160. For this study, the data division ratios between the training, validation, and test sets are assumed to be 0.7, 0.15, and 0.15, respectively.

4.5 Results and Discussions

The NN is used to model the controllable EVCS load in terms of controllable variables and parameters from the perspective of the LDC and the EVCS owner. Four MATLAB functions for data division are used to train the NN, as discussed earlier, in order to identify the best function to divide the data sets into training, validation and testing subsets, and the corresponding values of R-squared are compared. The estimated total EVCS load, using the proposed NN, is compared with that from a PEV charging data set obtained from the queuing model and is observed to be very closely matching. It is also noted that the function *dividerand* best captures the EVCS charging demand estimate (Figure 4.5).

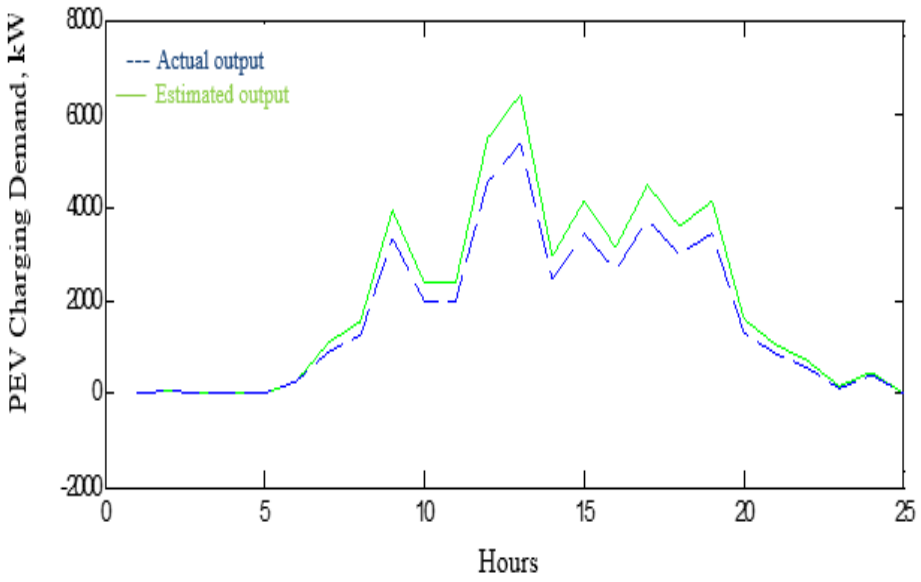

Figure 4.5: Estimated output using the *dividerand* function of the NN toolbox.

4.5.1 Controlled Operation of EVCS: LDC Perspective

This case assumes that the distribution system is operated from the LDC's perspective, and the EVCS smart operation is accordingly determined. The typical criterion for LDCs operation, as mentioned earlier, is minimization of losses, given by (4.8). Figure 4.6 presents the optimal number of PEVs to be charged, which remains the same with or without consideration of the class capacity constraint (4.18). It is to be noted that although the number of PEVs to be served are optimally distributed over the day, a significant number are rejected during hours 9-17 when the arrival rate is high, even though the EVCS capacity is not reached. This is because of the choice of the objective function, *i.e.*, the loss minimization perspective of the LDC. Further, when the class capacity constraint (4.18) is considered, although the total number of PEVs being charged does not change, it does bring about some changes in the number of PEVs of a given class being charged at an hour, as seen from Figure 4.7 and Figure 4.8.

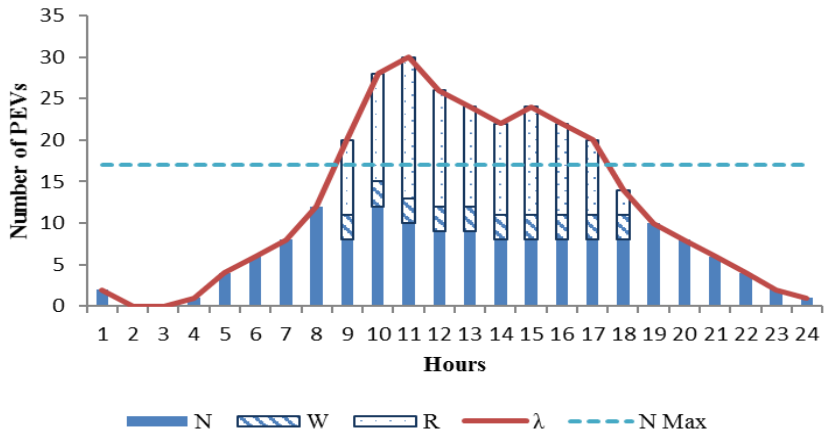

Figure 4.6: Optimal PEV schedule at EVCS, LDC Perspective.

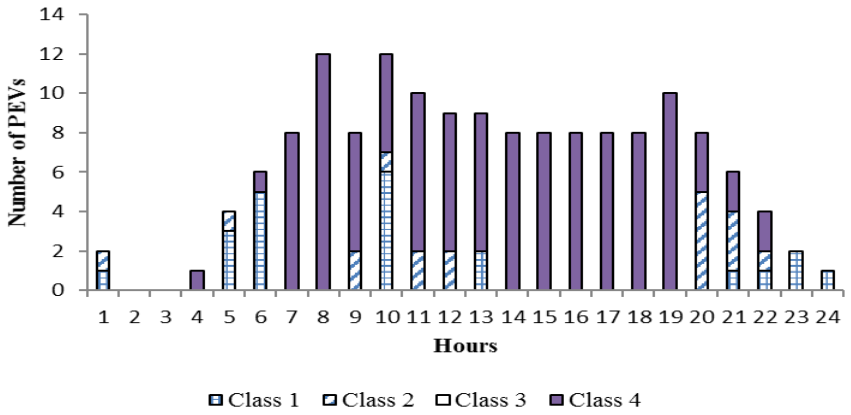

Figure 4.7: Optimal number of PEVs served without considering class constraints, LDC Perspective.

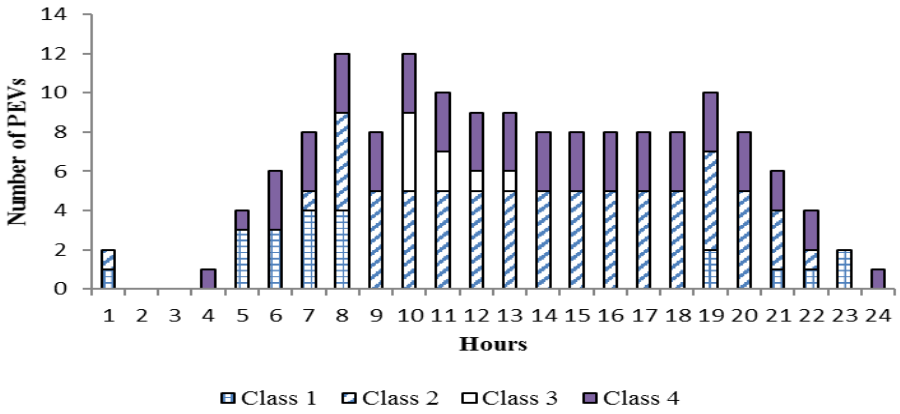

Figure 4.8: Optimal number of PEVs served considering class constraints, LDC Perspective.

Figures 4.9- 4.12 present the optimal number of PEVs to be charged, overall system demand, voltage profile at Bus-59, and PEV charging demand at Bus-59 respectively, considering limits on the EVCS peak demand (4.20). This represents a situation in smart grid environment, where the LDC sends a peak demand signal to the EVCS on an hour-to-hour basis, and the EVCS incorporates this control signal as an additional constraint in its charging schedule. Essentially the EVCS therefore provides a DR service to the LDC. Figures 4.9 - 4.12 demonstrate that the LDC can indeed improve system operation, reduce the peak load, and alleviate the need for network augmentation in the presence of PEV charging loads.

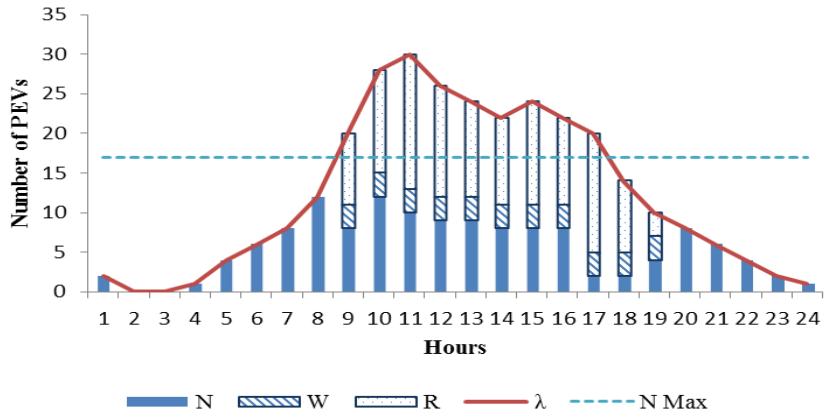

Figure 4.9: Optimal PEV schedule at EVCS considering P_{Max}, LDC Perspective.

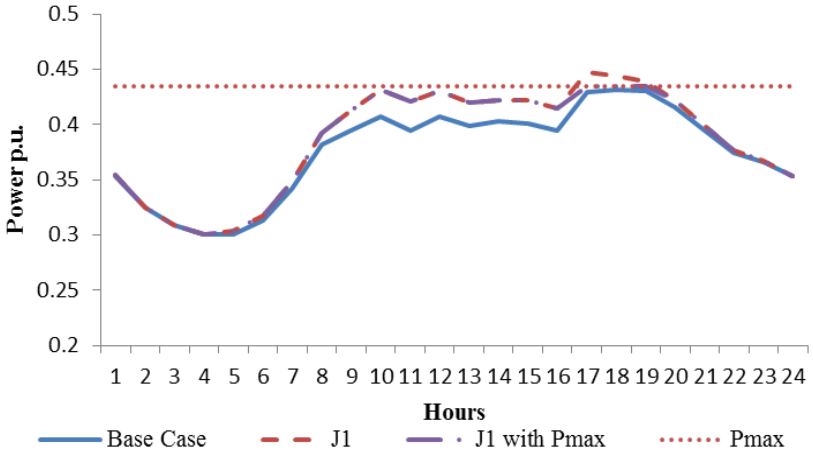

Figure 4.10: System demand without, with optimal EVCS demand, LDC Perspective.

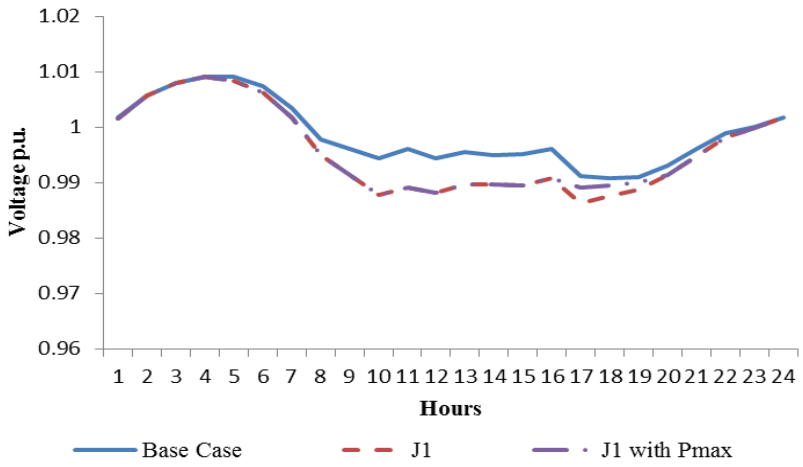

Figure 4.11: Voltage profile at Bus-59 for controlled EVCS, LDC Perspective.

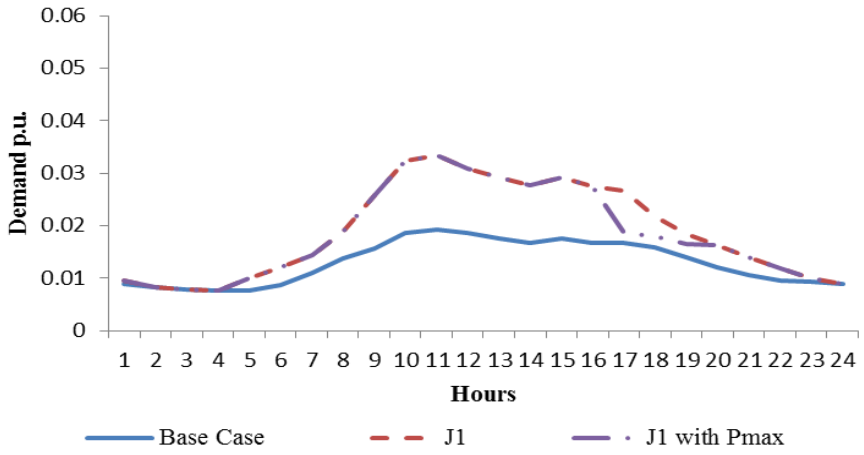

Figure 4.12: Total PEV charging demand at Bus-59, LDC Perspective.

4.5.2 Controlled Operation of EVCS: Owner's Perspective

This case assumes that the LDC operates the distribution system taking into account the interests of the EVCS owner, while adhering to system operational constraints. To this effect the objective is to maximize the number of PEVs being charged simultaneously, given by (4.9). Figure 4.13, presents the optimal number of PEVs to be charged, with and without the class capacity constraint (4.18). It is noted that N is optimally distributed over the day, and the number of PEVs to be served is significantly higher as compared to when the LDC operated to minimize system losses.

It is noted that the EVCS operates at full capacity, *i.e.*, $N = N^{Max}$, during hours 9-17 when the arrival rate is high (Figure 4.13) and the number of vehicles refused charging, is much less. The total number of PEVs being served at an hour, with or without the class constraint (4.18) is found to be the same, although the class-wise distribution of charging does vary when (4.18) is included, as seen from Figure 4.14 and 4.15.

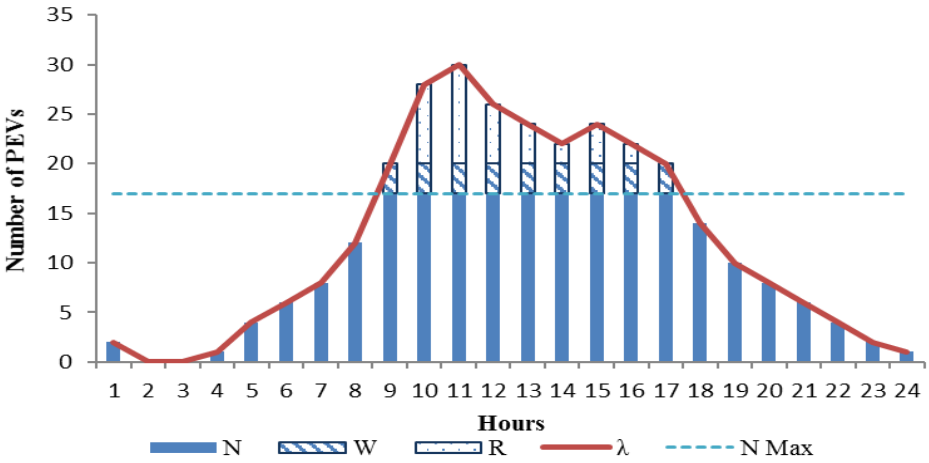

Figure 4.13: Optimal PEV schedule at EVCS, Owner's Perspective.

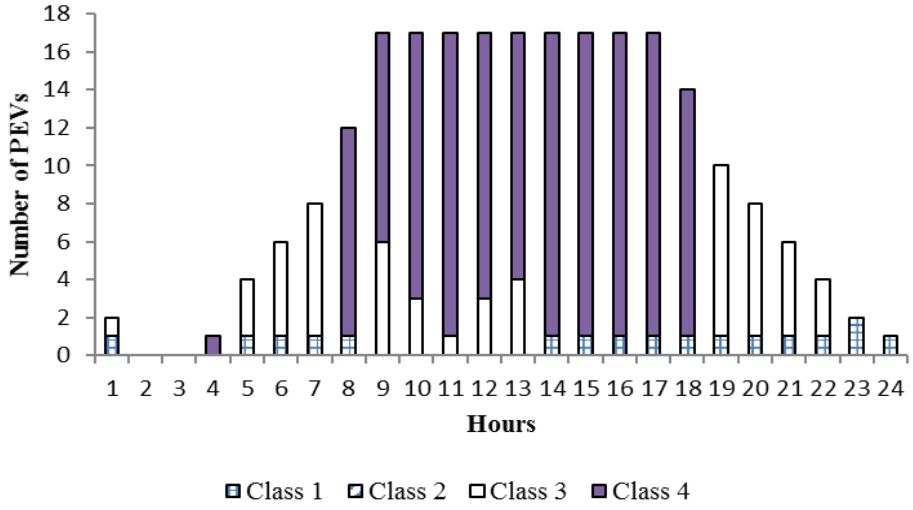

Figure 4.14: Optimal number of PEVs served without class constraints, Owner's Perspective.

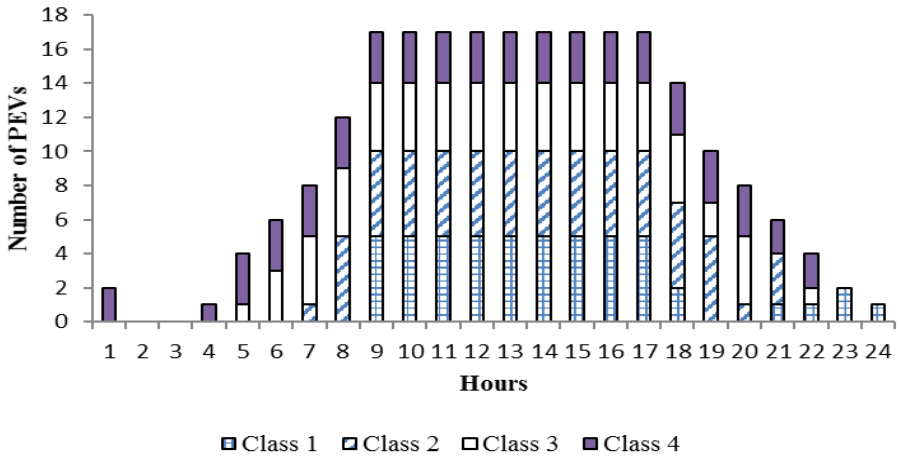

Figure 4.15: Optimal number of PEVs served considering class constraints, Owner's Perspective.

Figures 4.16 - 4.19 present the optimal number of PEVs to be charged, overall system demand, voltage profile at Bus-59, and PEV charging demand at Bus-59, respectively, considering the peak demand limit (4.20). Figures 16 demonstrates that the optimal number of PEVs charged is much lower when (4.20) is included, as compared to the case without (4.20), which results in less power drawn by the LDC from the external grid (Figure 4.17), and much improved voltage profiles (Figure 4.18), and the EVCS provides a DR service by reducing it charging demand as seen in Figure 4.19.

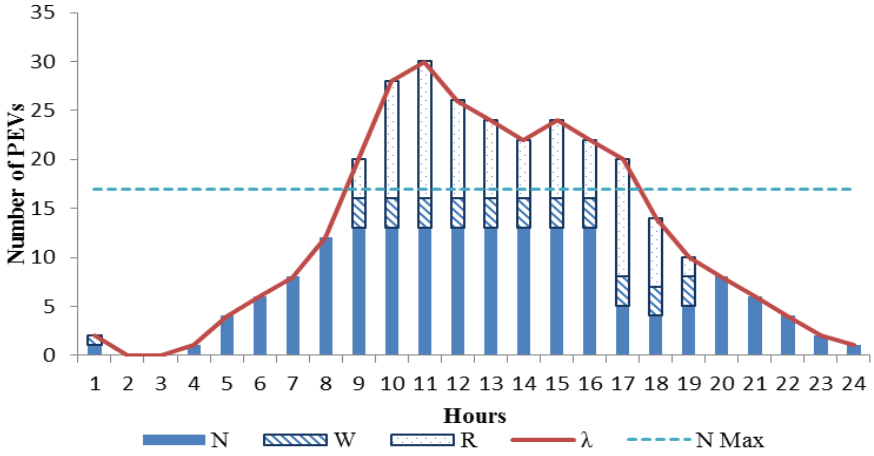

Figure 4.16: Optimal PEV schedule at EVCS considering PMax, Owner's Perspective.

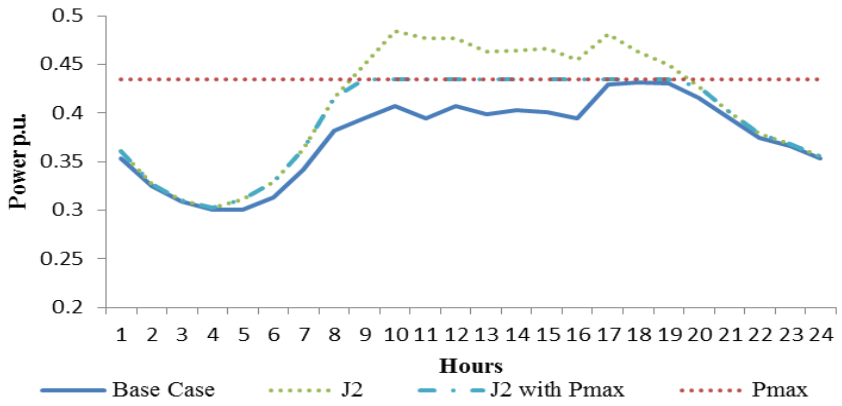

Figure 4.17: System demand without, with optimal EVCS demand: Owner's Perspective.

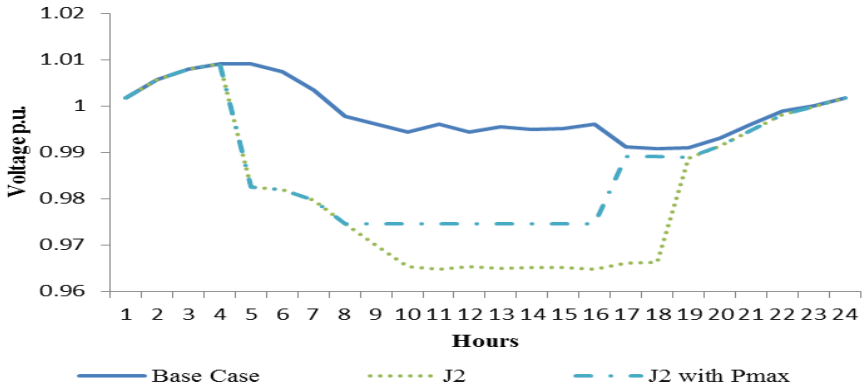

Figure 4.18: Voltage profile at Bus-59 for controlled EVCS, Owner's Perspective.

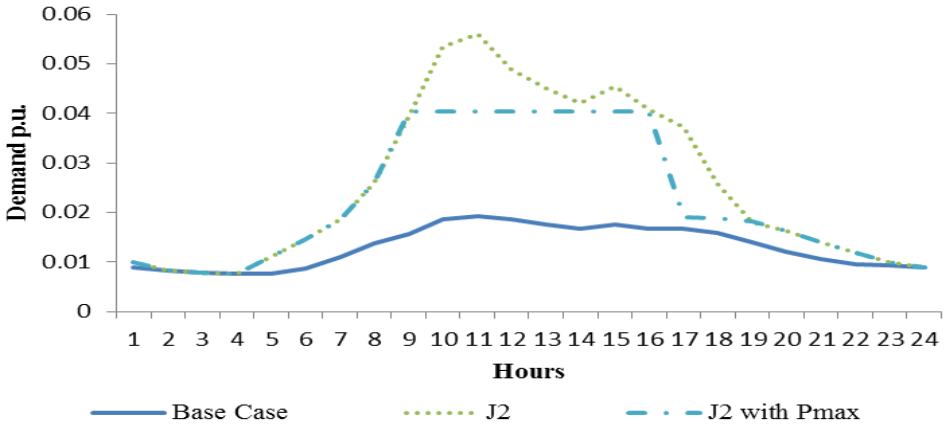

Figure 4.19: Total PEV charging demand at Bus-59, Owner's Perspective.

A comparison of uncontrolled EVCS versus controlled EVCS with different objective functions, without and with (4.20), is presented in Table 4.2. The revenue earnings for the EVCS (REV) are calculated considering winter Time-of-Use prices applicable in Ontario, Canada [59]. It is noted that uncontrolled operation of the EVCS accommodates more PEVs for charging and hence yields a high revenue (136.7 $/day) for the EVCS, but consequently requires much more power drawal from the external grid (13.11 p.u.), and results in high system losses (0.93 p.u.).

Controlled operation of the EVCS from the owner's perspective, *i.e.*, with the objective of maximizing N, results in a reduction in total number of PEVs charged/day (TN) to 231 PEVs, as compared to uncontrolled EVCS operation where 294 PEVs are charged. An increased number of vehicles are kept on waiting or are rejected. The EVCS revenue reduces to 99.6 $/day. When the peak demand constraint (4.20) is imposed, TN further reduces to 171 PEVs, the revenue of EVCS dips to 95.5 $/day.

Finally, the controlled operation of the EVCS from the LDC's perspective, *i.e.*, with the objective of minimizing losses, results in a further reduction in TN to 152 PEVs without (4.20) and 134 PEVs when (4.20) is imposed. The EVCS revenue reduces to 93.4 $/day.
It is therefore noted that the EVCS provides a DR service to the LDC after a peak demand signal is received, and the EVCS incorporates this as an additional constraint (4.20) in its charging schedule. It is noted that the LDC can indeed improve system operation, reduce the peak load, and alleviate the need for network augmentation in the presence of PEV charging loads compared without peak demand constraint scenario for both perspectives (Table 4.2).

TABLE 4.2

COMPARISON OF ALL CASES AND SUMMARY BENEFITS

	Controlled EVCS				Uncontrolled
	Objective: Min {Loss}		Objective: Max {N}		
	No P_{Max} constraint	With P_{Max} constraint	No P_{Max} constraint	With P_{Max} constraint	
TN	152	134	231	171	294
REV	93.8	93.4	99.6	95.5	136.7
TL	0.335	0.328	0.471	0.391	0.93
TP	9.27	9.24	9.78	9.44	13.11

TN: Total number of PEVs charged/day

REV: EVCS revenue, $/day

TL: Total system loss, p.u./day

TP: Total energy drawn from grid by EVCS, p.u./day

It is noted that controlled operation of the EVCS has some impact on the distribution system performance. Figure 4.20 shows that as expected, the total EVCS load is significantly increased when the EVCS owner's perspective (*maximizing* J_2) is considered as compared to the LDC's perspective (*minimizing* J_1). The bus voltage profiles are also affected by PEV charging (Figure 4.21). For example, at Bus-59, which is the EVCS bus, significant voltage drop takes place at various hours, depending on the operations perspective. In case of the EVCS owner's perspective the voltage profiles are significantly deteriorated, although they are within the operating limits of 0.95 p.u., while in the LDC's perspective the voltage profile is significantly better. A comparison of the controlled EVCS operation from both perspectives, at Bus-59, are presented in Figure 4.22; the increase in the demand due to EVCS charging is significant considering the owner's perspective as compared to the LDC's perspective.

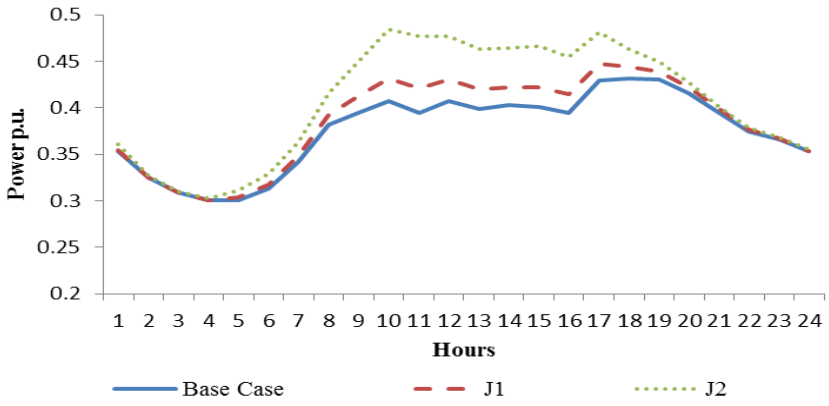

Figure 4.20: Comparison of system demand without and with optimal EVCS demand.

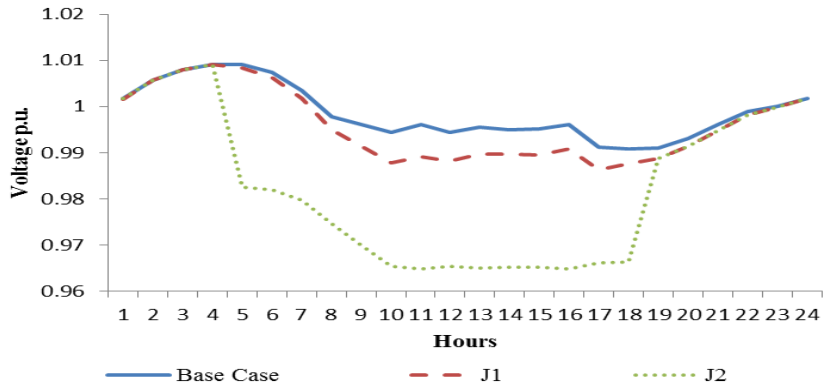

Figure 4.21: Comparison of voltage profile at Bus-59 for controlled EVCS demand.

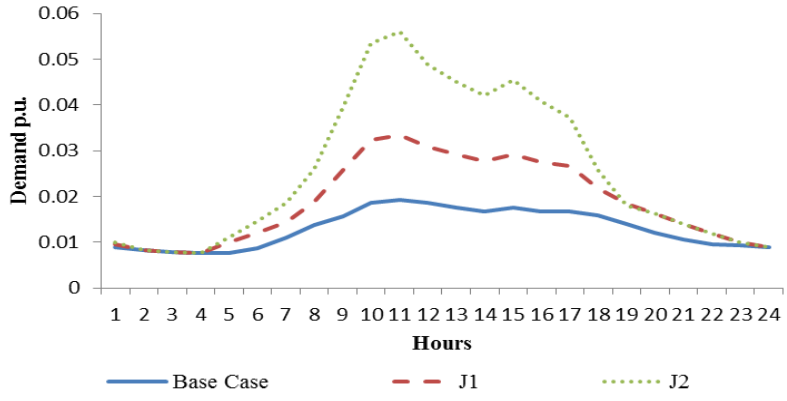

Figure 4.22: Total PEV charging demand at Bus-59 for both perspectives.

4.5.3 Uncontrolled Operation of Charging Station

This subsection captures the impact of controlled EVCS load (modeled as per the proposed approach) and compares that with uncontrolled EVCS operation, using the EVCS load estimated using the queuing model. Uncontrolled operation of the EVCS means, all PEVs arriving for charging, at any time, irrespective of the arrival rate, are right away provided a charging service. The expected uncontrolled EVCS load (Figure 4.23) is significantly increased depending on the arrival rate of PEVs, as compared to the case with no PEV.

The expected voltage profile at Bus-65 for uncontrolled operation of EVCS is given in Figure 4.24. As expected, the voltage profile drops significantly coinciding with the appearance of EVCS loads during hours 9–17. While, as noted earlier in the LDC controlled operation of EVCS, from either LDC's or EVCS owner's perspectives, the voltage profiles are significantly better (Figure 4.21). This demonstrates that the LDC can easily and smartly accommodate significant amount of PEV charging loads considering appropriate control strategies for the EVCS.

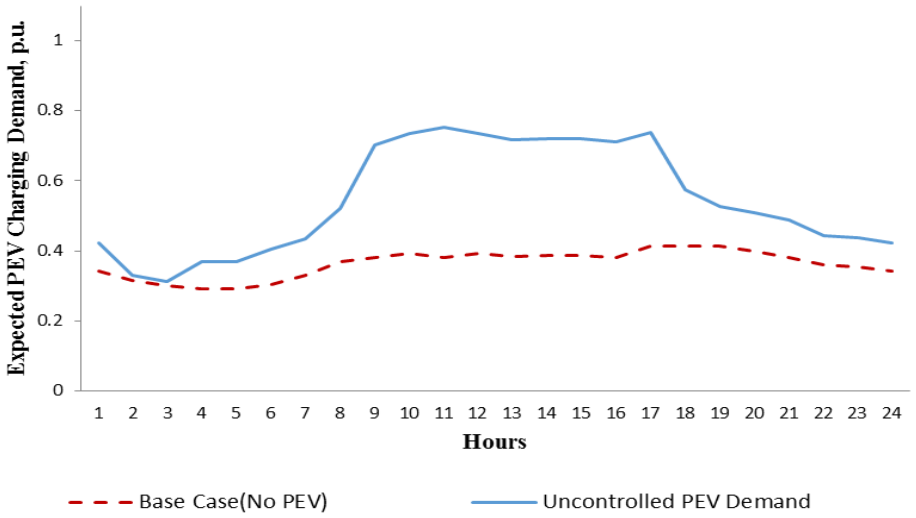

Figure 4.23: Expected uncontrolled charging demand.

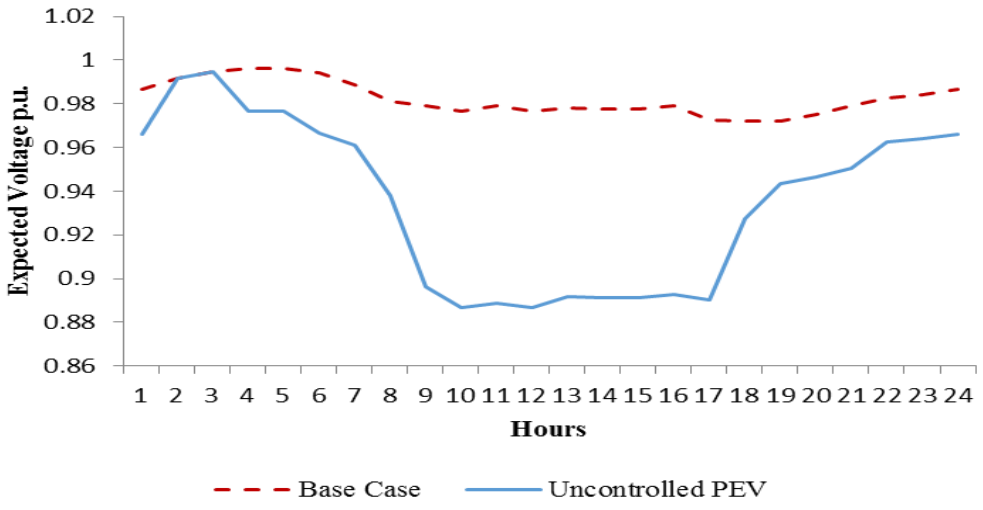

Figure 4.24: Expected voltage profile at Bus-65 for uncontrolled PEV charging.

4.6 Summary

This chapter presented the comprehensive modeling of EVCS load using controllable variables such as- the number of PEVs being charged simultaneously, total charging current, arrival rate, and time. The work further examined the contribution of such smart EVCS loads to DR and their integration in the distribution systems operations framework. The controllable load profile of EVCS was obtained using the novel framework for CSCLE. The CSCLE comprised a queuing model that considered several classes of vehicles, arriving at the EVCS as a non-homogeneous Poisson process, and determined the charging load for each. This dataset was used to train a NN and hence to determine the controllable charging load model of the EVCS.

The charging load model was integrated with a distribution optimal operations model to obtain the optimal charging decisions for the EVCS. Two different objective functions were considered, minimizing total feeder losses which represented the LDC's perspective; and maximizing the number of PEVs charged simultaneously, representing the EVCS owner's perspective. A 69-bus distribution system test case was presented to study the controlled operation of EVCS loading and its contribution to DR service.

It was noted from the studies that the EVCS owner's objective of maximizing the number of PEVs being charged simultaneously, can result in deterioration of bus voltages, and high feeder losses while accommodating more PEVs for charging, and rejecting only a few. On the other hand, the LDC's perspective of minimizing feeder losses resulted in significant rejections and wait times.

Chapter 5
Optimal Design of Electric Vehicle Charging Stations[3]

5.1 Introduction

In this chapter the optimal design of an EVCS with the goal of minimizing the lifecycle cost, while taking into account environmental emissions is presented. Different energy sources are considered, with realistic inputs on their physical, operating and economic characteristics. The charging demand of the EVCS is estimated considering real drive data. Analysis is also carried out to compare the economics of a grid-connected EVCS with an isolated EVCS and the optimal break-even distance for the grid connected EVCS to be a viable option, is determined. It is to be noted that this chapter does not considered the operational aspects of PEVs, charging station, or studies the system impacts from PEV charging. The well known energy modeling software for hybrid renewable energy systems, HOMER [82] is used in the studies reported in this chapter.

The rest of the chapter is organized as follows: Section 5.2 presents the nomenclature pertaining to the mathematical model presented, Section 5.3 presents the problem definition, Section 5.4 briefly discusses the system under consideration and different cases considered for optimal EVCS design. The system input data is presented in Section 5.5. In Section 5.6 the EVCS design results are presented and discussed. Finally, Section 5.7 presents the summary and conclusions of this chapter.

---

[3] Initial versions of the work appeared in:

- O. Hafez, and K. Bhattacharya, "Optimal planning and design of a renewable energy based supply system for microgrids," International Journal of Renewable Energy, Vol. 45, 2012, pp.7-15.
- O. Hafez, and K. Bhattacharya, "Optimal break-even distance for design of micro-grids,", in Proc. IEEE Electrical Power & Energy Conference (EPEC), London, ON, Canada, Oct 2012.

5.2 Nomenclature

x	Index for EVCS supply options and system components (solar PV, converter, diesel generator, battery energy storage system (BESS), grid connection)
N	EVCS project life, yr
N_x	EVCS component life, yr
i	Annual real interest rate (the discount rate), %
$PWF(i,N)$	Present worth factor
$TNPC$	Total net present cost, $
AC_x	Total annualized cost of component x, $/yr
AC_{Cx}	Annualized capital cost of component x, $/yr
C_{Cx}	Initial capital cost of component x, $
AC_{Rx}	Annualized replacement cost of component x, $/yr
C_{Rx}	Replacement cost of component x, $
$SFF(i,N)$	Sinking fund factor
S_x	Salvage value of component x at the end of the project life, $
N_{Rx}	Remaining life of component x at the end of the project life, yr
AC_{OMx}	Annual O&M cost of component x, $/yr
η_{Boiler}	Boiler efficiency
C_{Fuel}	Cost of fuel for boiler, $/kg
LHV_{Fuel}	Lower heating value of the boiler fuel, kWh/kg
C_{Boiler}	Cost of thermal energy from the boiler, $/kWh
E_{Grid}	Electricity sold to the grid by EVCS, kWh/yr
E_{EVCS}	Electrical energy demand of the EVCS, kWh/yr

$E_{Thermal}$	EVCS thermal energy demand, kWh/yr
NPC	Net present cost, $
COE	Levelized cost of energy, $/kWh

5.3 The Mathematical Model

The mathematical models used herein for the different system configurations are available in HOMER [82]. The model inputs are the EVCS load demand (both electric and thermal), the solar energy availability profile of the region, and the cost and size data of all system components considered. The software then considers different dispatch strategies that yield the minimum project cost for each EVCS configuration. The optimal EVCS design is determined by minimizing the total net present cost (NPC) comprising the capital cost, replacement cost, operation and maintenance (O&M) cost, fuel consumption cost, and cost of purchased power from the grid. Figure 5.1 presents the general architecture of EVCS design using HOMER.

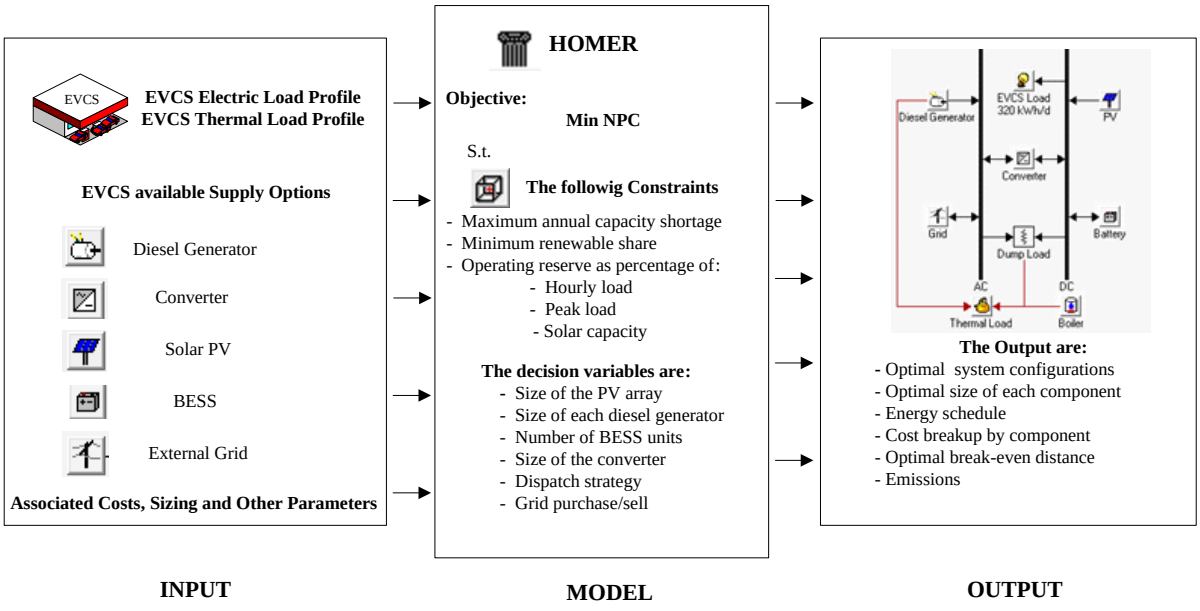

Figure 5.1: Architecture of EVCS design using HOMER [82].

It is noted from Figure 5.1 that the EVCS design using HOMER comprises the INPUT, MODEL, and OUTPUT modules. The INPUT module develops the information pertaining to all energy supply options, cost data, PEV related data to estimate the charging demand, etc. The MODEL module is a linear optimization to determine the least-cost design option, with significant degrees of flexibility in choosing and applying the constraints. The OUTPUT module provides the optimal EVCS design configuration with associated analytical results.

The objective of minimization of the total NPC is given as follows:

$$TNPC = \sum_{\in x} AC_x \times PWF(i, N) \tag{5.1}$$

where the total NPC of the EVCS is the total present value of all the component costs, and the present worth factor (*PWF*) is given as follows [83]:

$$PWF_{(i,N)} = \frac{(1+i)^N - 1}{i(1+i)^N} \tag{5.2}$$

and the total annualized cost of the EVCS is the sum of the annualized costs of each component *x*. The annualized cost of an EVCS component *x* comprises the O&M cost, capital, and replacement costs, annualized over the EVCS life, and is given as follows:

$$AC_x = AC_{Cx} + AC_{Rx} + AC_{OMx} \tag{5.3}$$

where the annualized capital cost of component *x* is given as follows:

$$AC_{Cx} = \frac{C_{Cx}}{PWF(i, N)} \tag{5.4}$$

In (5.3) the annualized replacement cost is calculated as follows:

$$AC_{Rx} = C_{Rx} \times SFF(i, N_x) - S \times SFF(i, N) \tag{5.5}$$

It is to be noted that the replacement cost of a component may be different from its initial capital cost. The sinking fund factor (SFF) is a ratio used to calculate a series of equal annual cash flows from its future value and is given as follows [83]:

$$SFF(i, N) = \frac{i}{(1+i)^N - 1} \tag{5.6}$$

Also, noted that the component life can be different from the project life, and the salvage value is the value remaining in a component at the end of the project life and is calculated as follows:

$$S = C_{Rx} \times \frac{N_{Rx}}{N_x} \tag{5.7}$$

Note that if the EVCS is connected to the grid, electricity purchase and sales need to be accounted for in the annual O&M cost. Finally, the levelized cost of energy (COE) is obtained as follows:

$$COE = \frac{\sum_{\in x} AC_x - C_{Boiler} E_{Thermal}}{E_{EVCS} + E_{Grid}} \tag{5.8}$$

In (5.8), the total annualized cost, net of the cost of serving the EVCS thermal load is divided by the total useful electric energy production which comprises the EVCS electrical energy demand and the amount of electricity sold to the grid by the EVCS. Also, in (5.8) C_{Boiler} is the cost of thermal energy from the boiler (applicable if the boiler is supplying EVCS thermal load) and is calculated as follows:

$$C_{Boiler} = \frac{C_{Fuel}}{\eta_{Boiler}\ LHV_{Fuel}} \tag{5.9}$$

The constraints that must be added to the system are the maximum annual capacity shortage, which is assumed to be 0%. The minimum renewables share is set to 0%. The operating reserve is set as the sum of three components comprising a percentage of the hourly load (10%), a percentage of the peak load (0%), and a percentage of solar power output (50%).

5.4 Case Studies

Renewable energy technology option, diesel generation, and the option of EVCS being connected to the grid are considered to determine the optimal design of EVCS. Two different cases based on the different supply options are examined, as follows:

5.4.1 Case-1: Isolated EVCS

This case helps address the "range anxiety", which is a common concern of EV owners regarding the distance the vehicle can travel, and EV owners can plan longer trips with more confidence if an EVCS is as readily available as a gas station [5]. Therefore, the design of an EVCS along highways as an isolated microgrid with different supply options such as, solar PV, diesel generation, and battery energy storage system (BESS) is studied and considered as Case-1. The system configuration of Case-1 is resented in Figure 5.2, and the EVCS design objective is to minimize the total capital, O&M, replacement and fuel costs, of each component of the system. The decision variables are the size of the diesel generator, solar PV array, battery bank, and converter. The EVCS thermal load is assumed to be served by the boiler, or the waste heat recovery system of the diesel generator, or excess energy from other sources; the optimal supply options is selected by the model.

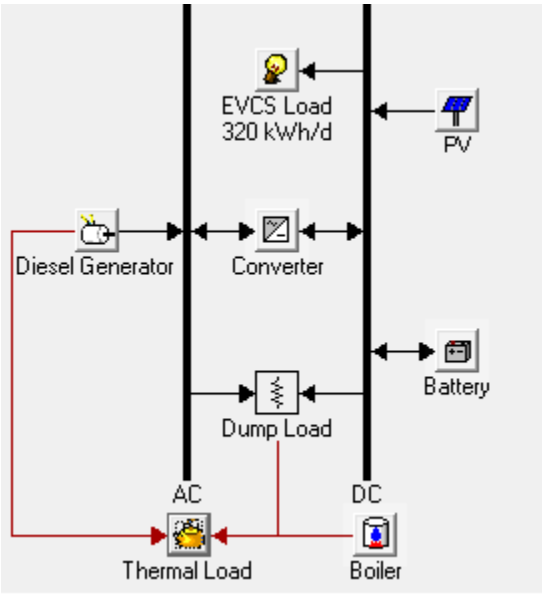

Figure 5.2: Available portfolio of energy supply options in Case-1.

5.4.2 Case-2: Grid Connected EVCS as a Smart Energy Hub

In this case, the EVCS is assumed to be connected to the grid as a smart energy hub with different supply options such as solar PV, diesel generation, BESS, and grid. Figure 5.3 presents the proposed system configuration. The smart EVCS design objective is to minimize

the total cost of capital, O&M, replacement, and fuel costs, associated with each component in the system. The decision variables are the size of the diesel generator, solar PV array, battery bank, and converter. Since the EVCS can purchase and sell power from and to the grid, the model is modified to consider the net costs (purchases minus sales) of the EVCS. The prices offered in the Feed-In-Tariff (FIT) program of Ontario, Canada, are considered for purchase and sell energy from and to external grid [84]. The optimal EVCS thermal load supply options are determined based on the system configurations assumed in this case. Table 5.1 presents a summary of all the cases considered in this chapter.

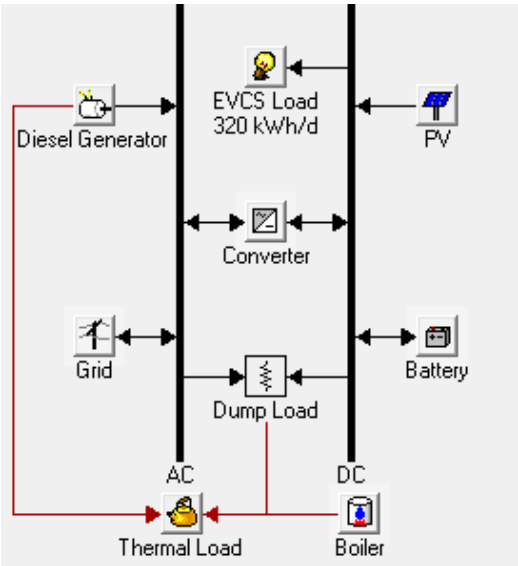

Figure 5.3: Available portfolio of energy supply options in Case-2.

Table 5.1

SUMMARY OF CASES

Case	Description of Case
1	Isolated EVCS (a) Diesel Based (b) Solar PV with BESS (c) Diesel-Solar PV-BESS Mix
2	Grid Connected EVCS as a Smart Energy Hub (a) Diesel Based (b) Solar PV with BESS (c) Diesel-Solar PV-BESS Mix

5.5 System Input Data

5.5.1 EVCS Load

The EVCS load profile is obtained from Drive-4-Data [85], which is a real-world dataset for PEVs maintained by the Waterloo Institute for Sustainable Energy (WISE) at the University of Waterloo. Participating Drive-4-Data drivers have a CrossChasm Technologies C5 Vehicle Datalogger attached to their vehicles, which collects, via wireless-cellular, a minimum of PEVs speed as a function of time, drive cycle and powertrain information, such as vehicle acceleration, and battery SOC. Furthermore, the Datalogger can also provide GPS data, enabling access to the vehicle's driving routes and location which is needed by researchers to determine optimal EVCS locations [85]. In this work the 2013 Chevrolet Volt drive cycles from May 2013 to May 2014 with 16 kWh battery capacity is used to generate the PEV charging demand profile. The total number of PEVs assumed to arrive for charging at the EVCS is 20.

Furthermore, NHTS 2009 [12] data for light-duty vehicles is used to distribute the PEV charging demand over the day; with the arrival destination being to buy gas at the gas-station, assuming that PEVs have the same pattern for arriving at the EVCS for charging their vehicles. The normalized hourly distribution of PEVs arriving for charging is presented in Figure 5.4.

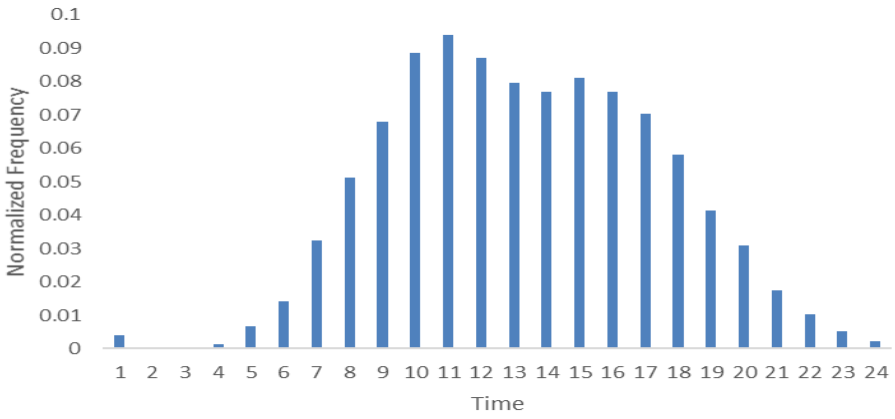

Figure 5.4: Arrival of PEVs at EVCS over the day.

5.5.2 Thermal Load

The total daily thermal energy demand of the EVCS is assumed to be only 10% of the EVCS electrical energy demand. A 24-hour Load Scale Factor (shown in Figure 5.5) is assumed for the thermal base load and the daily load profile is obtained. Thereafter, the EVCS thermal load profile for each day of the year is obtained by adding daily and hourly noise, by randomly drawing a daily perturbation factor from a normal distribution with a mean of zero and a standard deviation of 15%. In addition, it randomly draws the hourly perturbation factor from a normal distribution with a mean of zero and a standard deviation of 20% [82]. The scaled annual thermal energy demand average is 32 kWh/d with a load factor of 0.41. In this work the thermal load is assumed to be served by the boiler, or by the diesel generator from which waste heat can be recovered, as well as excess energy from other sources.

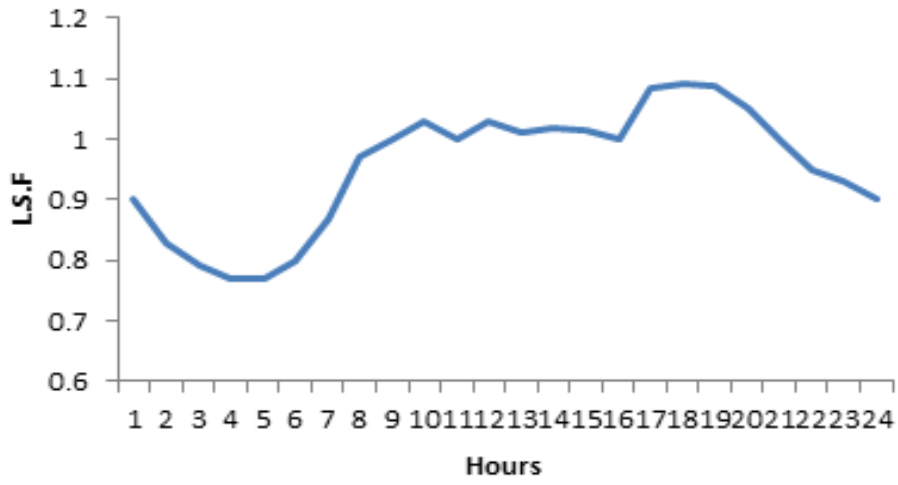

Figure 5.5: Load scale factor for hourly thermal load profile of EVCS.

5.5.3 Solar Resource

The solar radiation data of Waterloo, Ontario, (43° 39' N, 80° 32' W) is considered, which is obtained from the NASA Surface Meteorology and Solar Energy website [86]. The annual average solar radiation for this area is 3.64 kWh/m^2/day. Figure 5.6 shows the month-wise average solar radiation profile over a one-year period.

Capital and replacement costs of PV panel include shipping, tariffs, installation, and dealer mark-ups are considered. Some maintenance is typically required on the solar PV panels. A derating factor of 90% reduces the solar PV production by 10% to account for varying effects of temperature and dust on the panels.

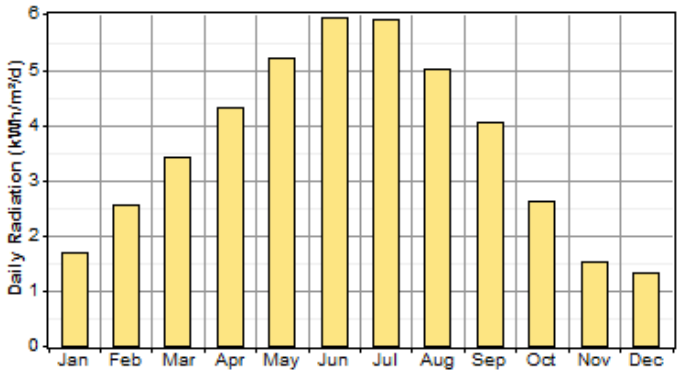

Figure 5.6: Solar radiation profile for Waterloo.

5.5.4 Input Data (Costs, Sizing and Other Parameters)

In Table 5.2 the capital cost, replacement cost and O&M cost of each supply option considered, are presented, while the different sizing options and other associated parameters are presented in Table 5.3.

Table 5.2

COST DATA OF ENERGY SUPPLY RESOURCES [87]

Options	Capital Cost	Replacement Cost	O&M Cost
Solar	$7.50/W	$7.50/W	$10/year
Battery	$75/ Battery	$75/ Battery	$2/Battery /year
Converter	$1,000/kW	$1,000/kW	$100/year
Grid Extension	$20,000/km	$20,000/km	$10/year/km
Diesel Generator (4.25 kW)	$2,550	$2,550	$0.15/h

Table 5.3
DATA ON SIZING AND OTHERS PARAMETERS OF ENERGY SUPPLY RESOURCES

Options	Options on Size and Unit Numbers	Life	Other Information
Solar	1, 10, 50, 100, 150, 200, 300, 500 kW	20 yrs	De-rating factor = 90%
Battery	10, 50, 100, 200, 500, 1,000, 1,500	845 kWh	Nominal capacity 225 Ah
Converter	0, 10, 50, 100, 200, and 500 kW	15 yrs	Can parallel with AC generator. Converter Efficiency = 90% Rectifier Efficiency = 85%
Grid Connection	10, 25, 50, 100, 500, 1,000 kW	-	Purchase = $0.12/kWh Sellback = $0.39/kWh [84]
Diesel Generator	0 to 500 kW	500,000 h	Minimum load ratio = 30% Heat recovery ratio = 10%
Diesel Fuel	-	-	Price = $0.70/L Density of 820 kg/m^3 Carbon Content 88% Sulfur Content 0.33%

5.5.5 Economics

The annual real interest rate is considered to be 6%. The real interest rate is equal to the nominal interest rate minus the inflation rate. The project life is 25 years.

5.6 Results and Discussions

In this section the different designs of EVCS are examined from the standpoint of economics, emissions, and operational performance. Two cases are considered as mentioned earlier, the isolated EVCS, and a grid-connected EVCS as a smart energy hub. The objective is to determine the optimal design of EVCS while minimizing the lifecycle cost, taking into account environmental emissions and considering various energy supply options.

In Case-1 the EVCS is assumed to be an isolated microgrid fed by diesel generators. Although this may seem to be as unrealistic scenario in a common situation, there are several countries where reliance on diesel as primary energy source is very significant, *i.e.*, Saudi Arabia. In such circumstances, diesel option is a relevant example. However, diesel generator

units are very expensive because of their high cost of maintenance, fuel supply, and fuel transportation. In addition, the diesel generators are emission intensive. Therefore, supplying the EVCS with solar PV and BESS sources is also examined; Accordingly, the EVCS is assumed to be supplied by a mixed configuration comprising both diesel and solar PV sources. In Case-2 it is assumed that the EVCS is grid-connected and has the option of drawing/selling-back energy from/to the external grid, while also having its own resources.

5.6.1 Optimal Plan Configurations

The optimal EVCS design for each case is obtained from HOMER simulations, using the parameters described in the previous section, and the optimal configurations are shown in Figures 5.7, and 5.8. The corresponding details of the optimal EVCS plans for the two cases are presented in Table 5.4.

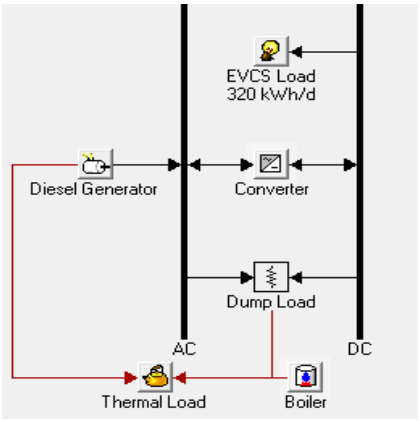

(a) Diesel Based

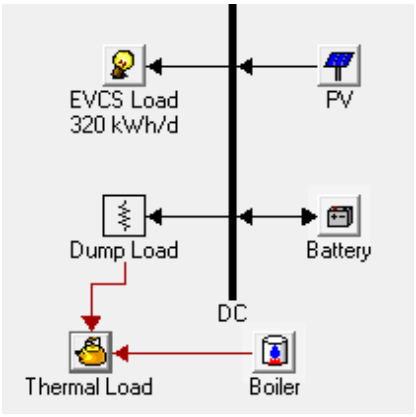

(b) Solar PV with BESS

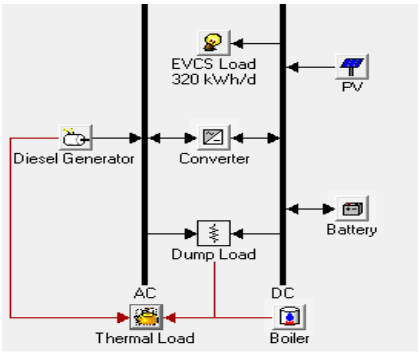

(c)Diesel-Solar PV-BESS mix

Figure 5.7: Optimal EVCS configurations in Case-1: Isolated EVCS.

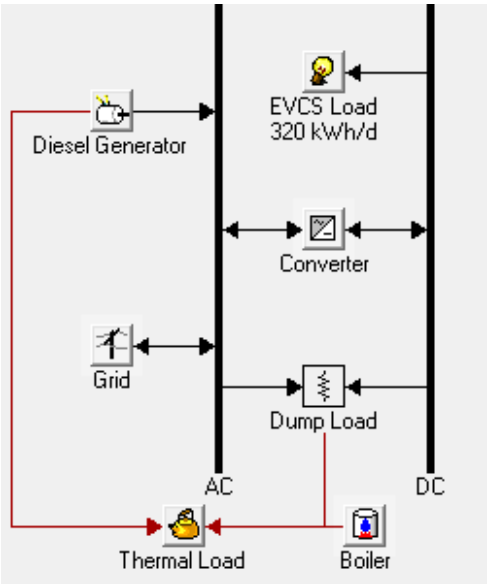

(a) Diesel Based

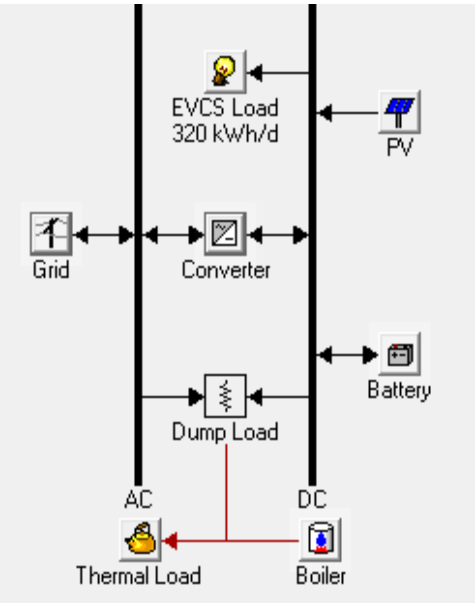

(b) Solar PV with BESS

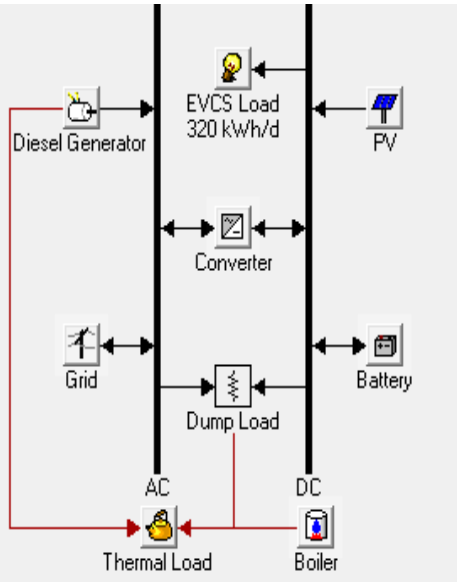

(c) Diesel-Solar PV-BESS mix

Figure 5.8: Optimal EVCS configurations in Case-2: Grid connected EVCS.

Table 5.4

OPTIMAL EVCS DESIGN

Component	Case-1			Case-2		
	(a)	(b)	(c)	(a)	(b)	(c)
Diesel, kW	100	0	50	100	0	100
Solar PV, kW	0	300	50	0	250	10
Converter, kW	50	0	50	50	50	50
Battery, numbers	0	1000	500	0	1000	1000
Purchase from Grid, kW	0	0	0	50	50	50
Sell to Grid, kW	0	0	0	10	10	10

As can be seen from the optimal configurations and design plans, in Case-1, while the diesel dependent EVCS Case-1(a) selects diesel generation to meet its demand, the renewable based EVCS Case-1(b) relies on solar PV, and BESS only. The diesel-solar PV-BESS mix EVCS Case-1(c) opts for a reduced diesel generation capacity and some solar PV capacity.

Case-2(a), the diesel dependent EVCS case selects diesel generation to meet its demand, with ability to drawing/selling energy from/to the external grid, as a smart energy hub. In addition to the grid-connected option the EVCS relies on solar PV, and BESS in Case-2(b). The diesel-solar PV-BESS mix EVCS Case-2(c) opts for a reduced solar PV capacity and drawing/selling energy from/to the external grid.

Table 5.5 shows the NPC, levelized COE, and the O&M costs for the different cases. It is noted that the NPC and the levelized COE are significantly low in Case-1(c) and 2(c) as compared with Case-1(a) and (b), and 2(a) and (b), and hence are the most favorable designs for isolated and grid-connected EVCS. When the EVCS is based on solar and BESS only, it is noted that the levelized COE is significantly high in both isolated and grid-connected EVCS Case-1(b) and 2(b) because of the large capital cost component. Although in the diesel dependent EVCS the levelized COE is reduced, to 1.075 $/kWh in Case-1(a) and to 0.675 $/kWh in Case-2(a), and it is higher than the diesel-solar PV-BESS mix because of the significantly high cost of fuel in diesel based EVCS, as shown in Figurer 5.9(a) and (c) and 5.10(a), and (c). It is also to be noted that in Case-2 there is a negative O&M cost, which pertains to the revenue earned by the EVCS from selling power to external grid.

Table 5.5

COMPARISON OF COST COMPONENTS

Component	Case-1			Case-2		
	(a)	(b)	(c)	(a)	(b)	(c)
Net Present Cost, M$	1.617	2.724	0.945	1.020	2.138	0.835
Levelized COE energy, $/kWh	1.075	1.816	0.625	0.675	1.476	0.551
O&M Cost, M$/year	0.118	0.031	0.035	0.071	0.011	0.045

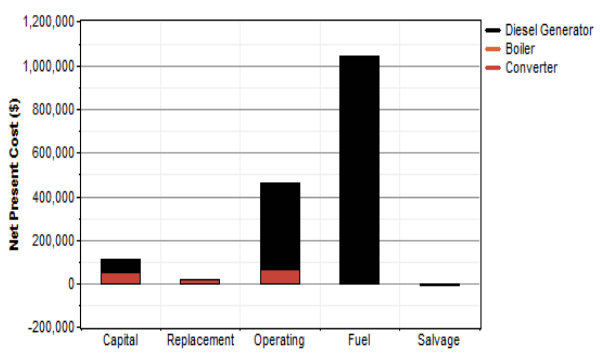

(a) Diesel Based

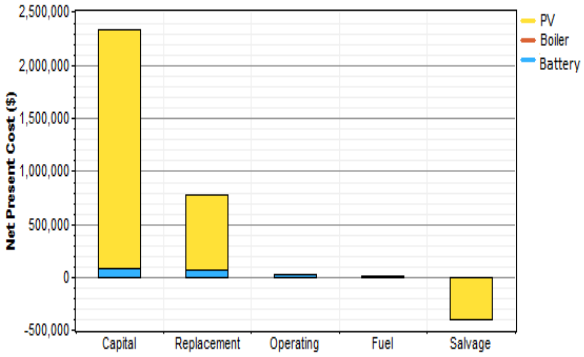

(b) Solar PV with BESS

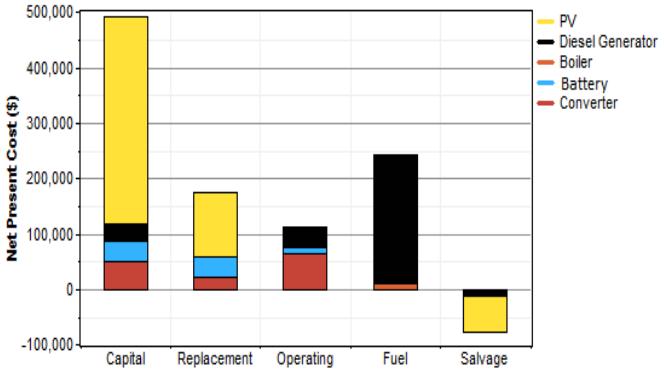

(c) Diesel-Solar PV-BESS mix

Figure 5.9: Optimal cost components for Case-1: Isolated EVCS.

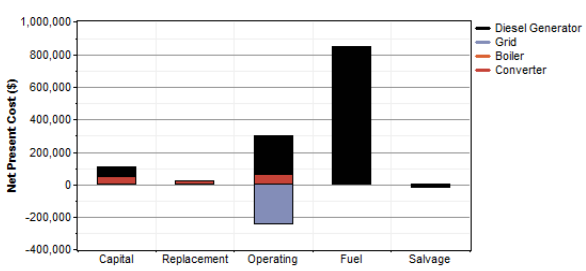

(a) Diesel Based

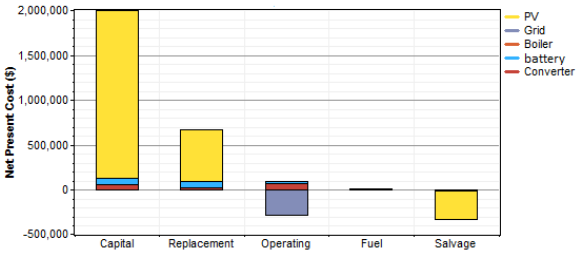

(b) Solar PV with BESS

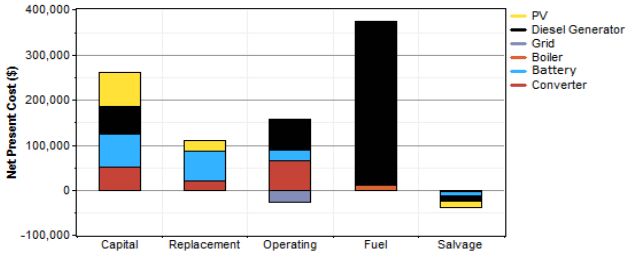

(c) Diesel-Solar PV-BESS mix

Figure 5.10: Optimal cost components for Case-2: Grid connected EVCS.

Figure 5.11, and 5.12 presents the annual cash flows for the two cases, respectively. It is seen that in the diesel based EVCS (Case-1(a)) Figure 5.11, the diesel generator and converter incur a capital cost at the beginning of the project, and converter incurs a replacement cost at year 15, while the system incurs a regular stream of fuel and O&M cost. However, in Case-1(b), the solar PV with BESS based EVCS only incurs an initial investment cost while the replacement cost is sporadically distributed over its lifetime (Figure 5.11(b)) and the other costs are negligible. In Figure 5.11(c), the cash flow pattern is similar to (b) with an additional regular stream accounting for cost of fuel and O&M arising because of the presence of diesel generator.

The annual cash flow of Case-2 is similar to Case-1, however because of the sellback power to the grid and associated revenue earnings by the EVCS, the O&M cost is significantly reduced (Figure 5.12(a)). Also, the system incurs a regular high stream of fuel

and O&M cost as compared to Case-1(c), because of the significant increase in diesel generation capacity (Figure 5.12(c)).

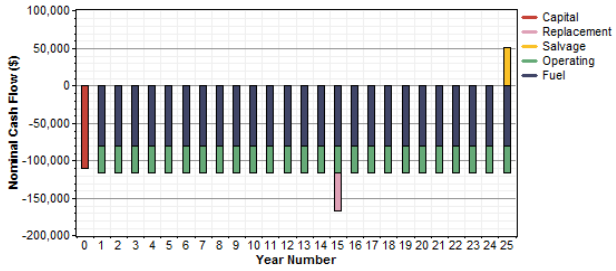

(a) Diesel Basesd

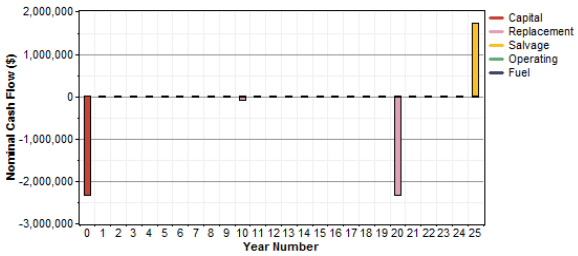

(b) Solar with BESS

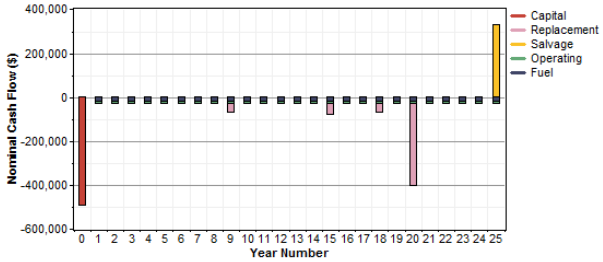

(c) Diesel-Solar PV-BESS mix

Figure 5.11: Cash flow for Case-1: Isolated EVCS.

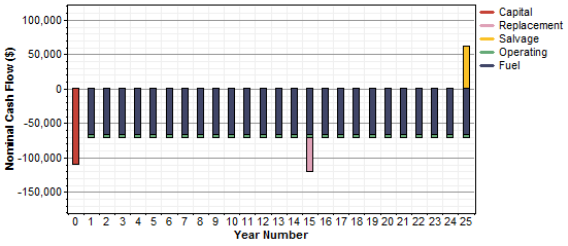

(a) Diesel Based

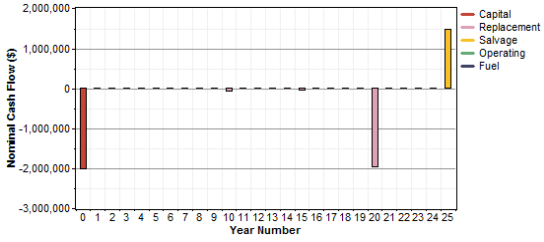

(b) Solar with BESS

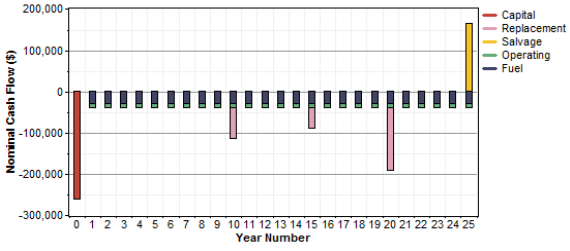

(c) Diesel-Solar PV-BESS mix

Figure 5.12: Cash flow for Case-2: Grid connected EVCS.

5.6.2 Optimal Production and Consumption Profiles in Various EVCS Configurations

Comparisons of electrical energy production and consumption for various cases are presented in Figures 5.13, and 5.14, and Table 5.6. As shown in Table 5.6, in the solar PV with BESS based EVCS (Case-1(b) and 2(b)), the total energy produced is much higher than other cases, and the EVCS has to transfer a substantial portion of the energy (excess energy) to resistive heating which can be used to serve a thermal load. This is because, solar PV energy is intermittent and non-dispatchable and the EVCS being fully reliant on these sources, is exposed to these risks. The diesel based EVCS (Case-1(a) and Case-2(a)) relies only on diesel which results in no excess energy, while Case-2(a) has the option of drawing/selling additional energy from/to external grid. In Case-2(c), the solar PV production is significantly reduced as compared with Case-1(c) and its energy contribution is only 8%, and the energy supply in this case mostly depends on diesel and external grid (Figure 5.14(c)).

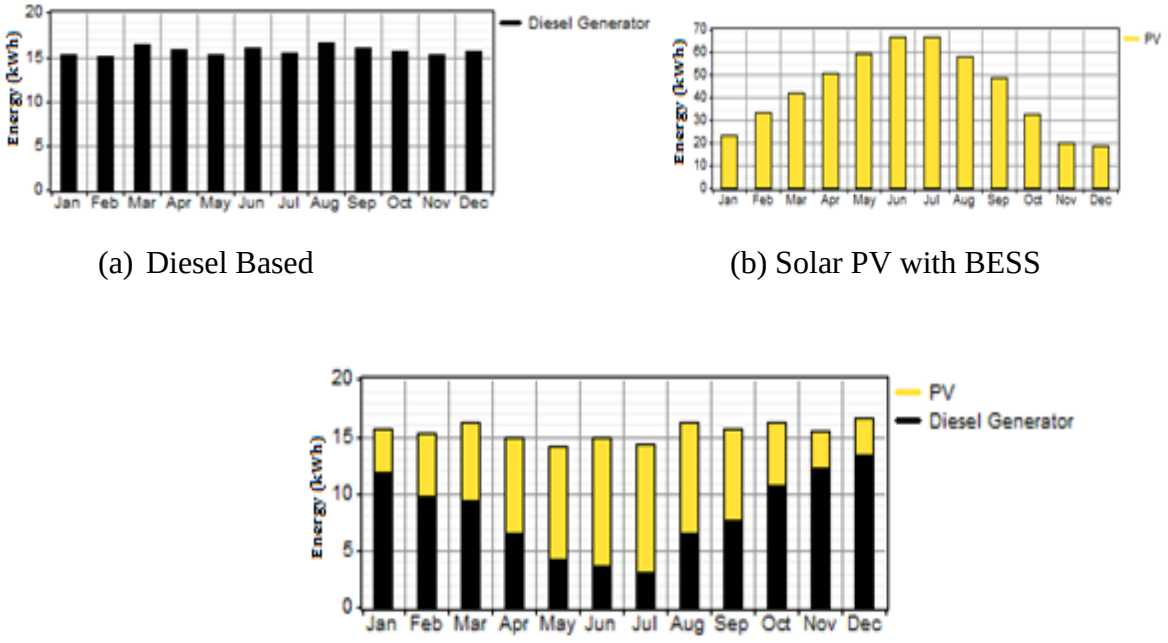

(a) Diesel Based

(b) Solar PV with BESS

(c) Diesel-Solar PV-BESS mix

Figure 5.13: Power production for Case-1: Isolated EVCS.

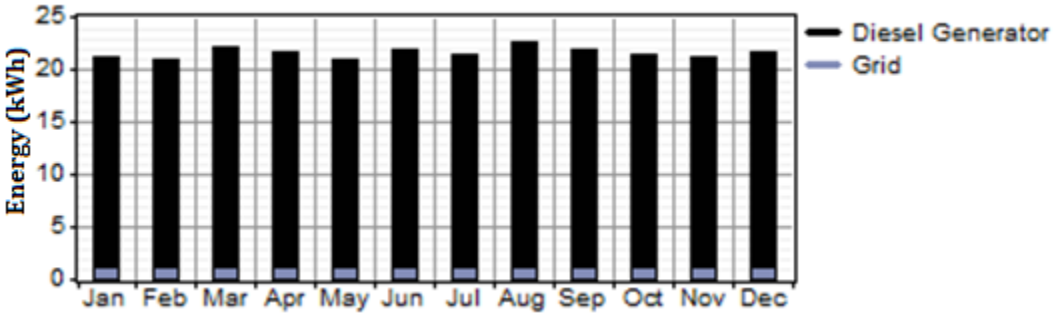

(a) Diesel Based

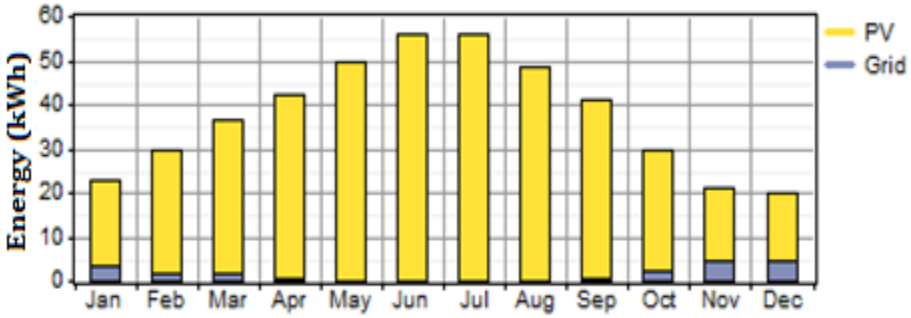

(b) Solar PV with BESS

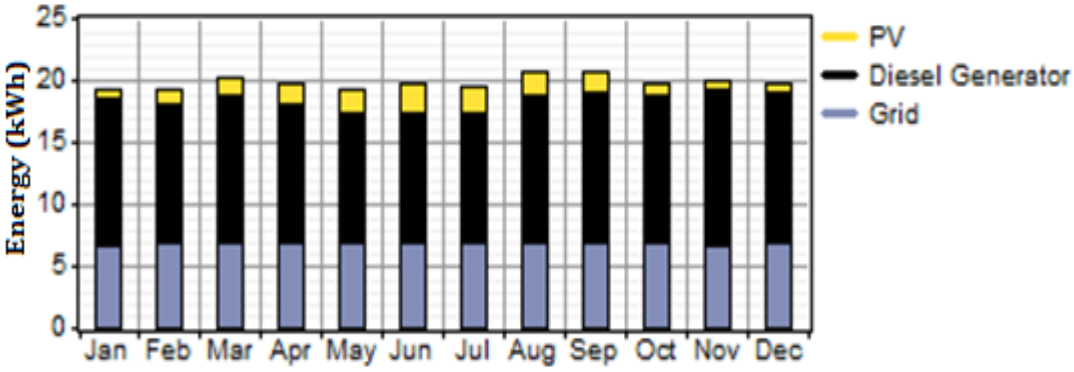

(c) Diesel-Solar PV-BESS mix

Figure 5.14: Power production for Case-2: Grid connected EVCS.

Table 5.6

COMPARISON OF ENERGY PRODUCTION AND CONSUMPTION

	Case-1			**Case-2**		
	(a)	(b)	(c)	(a)	(b)	(c)
Component	**Production, MWh/yr**					
Diesel Generator	137.387 (100%)	0	71.769 (53%)	178.689 (95%)	0	101.121 (58%)
Solar PV	0	153.386 (100%)	63.326 (47%)	0	216.732 (96%)	12.669 (8%)
Drawn Energy from External Grid	0	0	0	10.399 (5%)	14.207 (4%)	59.924 (34%)
Renewable Energy Contribution	0%	100%	47%	0%	96%	8%
Total	137.387	153.386	135.095	189.088	230.939	173.714
	Consumption, MWh/yr					
EVCS Electrical Load Energy Served	116.779	116.779	116.779	116.779	116.779	116.779
EVCS Thermal Load Energy Served	11.680	11.680	11.680	11.680	11.680	11.680
Energy Sell Back to Grid	0	0	0	51.700	63.033	23.898
Excess Energy (as resistive heating)	0	32.442	0	0	20.551	0
Losses	20.608	4.165	18.316	20.609	30.576	33.037

Table 5.7 presents the optimal operation of battery and converter for the two cases. The difference between the energy charge and discharge of battery, and in and out of converter in each case; is the losses and is reported in Table 5.6. For example, the BESS charging energy is 30,655 kWh/yr in Case-1(b) and the discharged energy is 26,490 kWh/yr, which implies a total loss of 4.165 MWh/yr. In Case-1(a) and 2(a) the optimal energy transferred from the diesel generator to EVCS through rectifier is presented.

Table 5.7

OPTIMAL OPERATION OF BATTERY AND CONVERTER OF EVCS

Component (kWh/yr)	**Case-1**			**Case-2**		
	(a)	(b)	(c)	(a)	(b)	(c)
Battery Energy, charge	-	30,655	52,988	-	76,807	66,509
Battery Energy, discharge	-	26,490	45,438	-	66,161	57,244
Inverter Energy, in	-	-	-	-	70,032	13,607
Inverter Energy, out	-	-	-	-	63,033	12,246
Rectifier Energy, in	137,387	-	71,769	137,388	14,207	149,413
Rectifier Energy, out	116,779	-	61,003	116,779	12,076	127,002

5.6.3 Optimal Energy Supply Options of EVCS Thermal Load

The EVCS thermal load is assumed to be supplied from different supply options which are boiler, waste heat recovery system of diesel generator, and excess energy from other sources. Figures 5.15, and 5.16 and Table 5.8 presents the supply options used and the percentage of each to meet the EVCS thermal load in each case. It is noted that the EVCS thermal load is fed through the waste heat energy of diesel generator in Case-1(a) and 2(a); while the excess energy and boiler are the supply options in Case-1(b) and 2(b). In Case-1(c) and 2(c), waste heat energy of diesel generator and boiler mix is used to supply the EVCS thermal load.

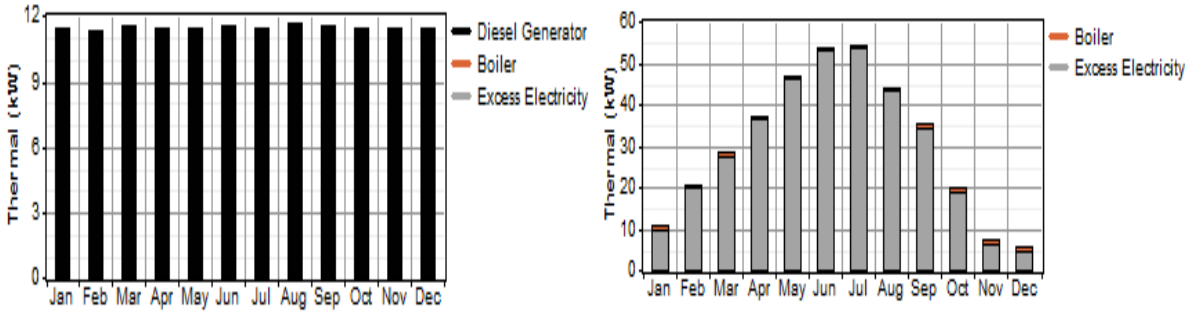

(a) Diesel Based (b) Solar PV with BESS

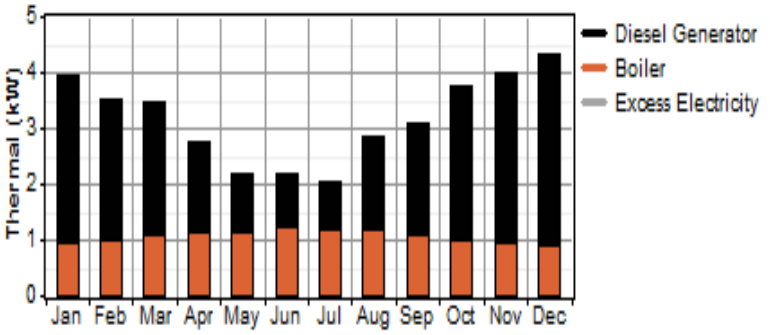

(c) Diesel-Solar PV-BESS mix

Figure 5.15: Optimal supply options of EVCS thermal load for Case-1:Isolated EVCS.

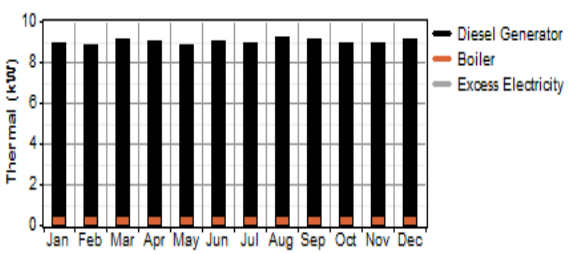

(a) Diesel Based

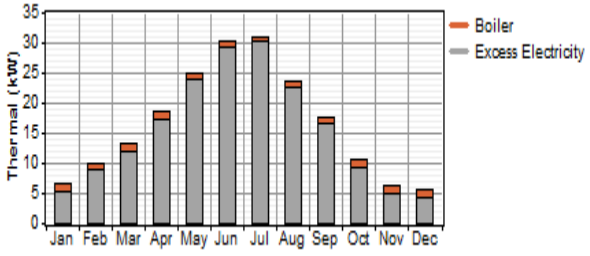

(b) Solar PV with BESS

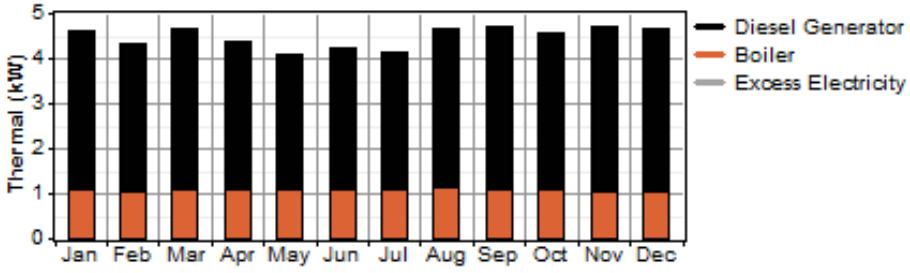

(c) Diesel-Solar PV-BESS mix

Figure 5.16: Optimal supply options of EVCS thermal load for Case-2: Grid connected EVCS.

Table 5.8

OPTIMAL EVCS THERMAL LOAD SOURCES

Source	Case-1			Case-2		
	(a)	(b)	(c)	(a)	(b)	(c)
Boiler	0	3%	34%	5%	7%	24%
Generator Waste Heat Energy	100%	0	66%	95%	0	76%
Excess Energy from other Sources	0	97%	0	0	93%	0

5.6.4 Effect of Distance from Grid and the Optimal Breakeven Distance

In this analysis, the distance of the proposed EVCS site is taken into consideration and the optimal plans with all different supply options of the isolated EVCS (Case-1) are determined assuming that the EVCS can draw power from the external grid. Figure 5.17 shows that the NPC of diesel based EVCS in Case-1(a), with grid connectivity option, is significantly less when the EVCS is very close to the external grid point of connection (say, zero kilometers). As the grid connectivity distance increases, the NPC increases, but remains lower than the one without external grid option for up to 69.9 kms. Beyond that, it is no longer economical for the Case-1(a) to connect to the external grid. However, in Case-1(b), the break-even distance is significantly increased and is beyond 125 kms, when it is no longer economical to connect to the external grid (Figure 5.18). On the other hand, in Case-1(c), the break-even distance is only 36.6 kms (Figure 5.19).

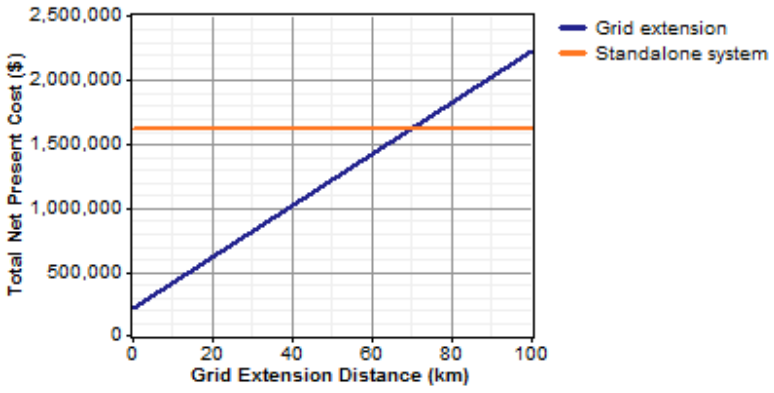

Figure 5.17: Variation of NPC with grid connectivity distance for Case-1(a).

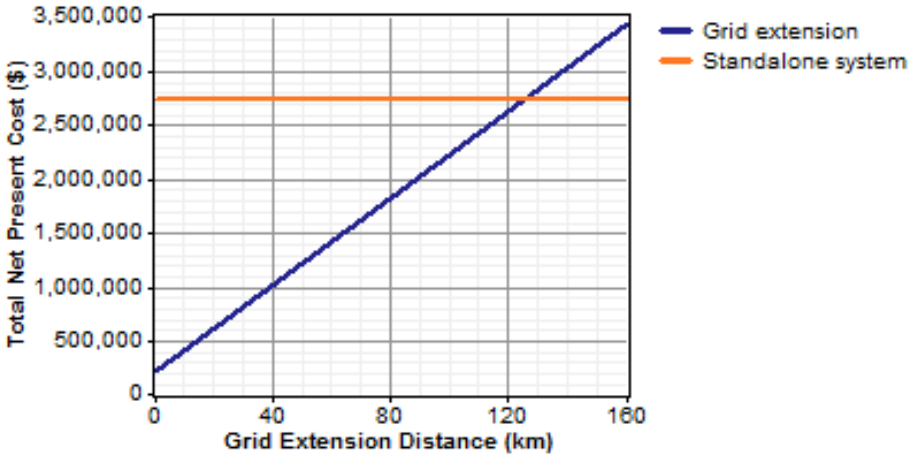

Figure 5.18: Variation of NPC with grid connectivity distance for Case-1(b).

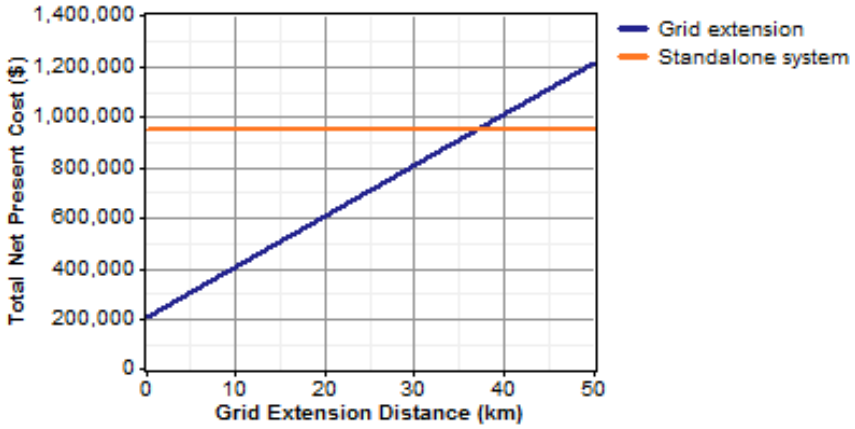

Figure 5.19: Variation of NPC with grid connectivity distance for Case-1(c).

5.6.5 Comparison of Environmental Emissions from Various EVCS Configurations

As mentioned before, one of the main objectives of this work is to reduce emissions by using green energy sources. The results presented in Table 5.9 show that the solar PV with BESS based EVCS in both cases significantly reduces the total system emissions (Case-1(b) and 2(b)) as compared to all others cases. However, although diesel- solar PV-BESS mix emits more than the solar PV with BESS based, it is still quite environmentally friendly when compared to the only diesel based option.

Table 5.9

CASE-WISE COMPARISON OF EMISSIONS

Emissions, kg/yr						
Pollutant	**Case-1**			**Case-2**		
	(a)	(b)	(c)	(a)	(b)	(c)
Carbon dioxide	305,589	2,417	71,594	223,488	9,815	132,613
Carbon monoxide	754	0	169	613	0	264
Unburned hydrocarbons	83.6	0	18.8	67.9	0	29.2
Particulate matter	56.9	0	12.8	46.2	0	19.9
Sulfur dioxide	614	4.94	144	388	12.8	319
Nitrogen oxides	6,731	0	1,511	5,412	25.4	2,401

5.7 Summary

This chapter presents the optimal design and comparative studies for an isolated EVCS, and a grid connected EVCS as a smart energy hub configuration. Various supply options are included in this study such as diesel based, solar PV with BESS based and diesel-solar PV-BESS mix. Studies are carried out using the HOMER software which provides a very efficient tool for case studies and policy analysis.

Analysis reveals that if the EVCS is located within city range and can be operated as a smart energy hub with diesel- solar PV-BESS mix supply options, it is the most economically favorable option. However, in order to allow the EV customers to travel for long distances with contentment the isolated EVCS along highways is studied in this work and from the analysis it is noted that the diesel-solar PV-BESS mix EVCS has the lowest NPC and a fairly small carbon footprint, when compared to a diesel-based EVCS. Although a

fully renewable-based EVCS, which has no carbon footprint, is the most preferred, the NPC is higher.

Grid connected EVCS as a smart energy hub is considered to give an idea of EVCS located within city range in a high density area, and hence the EVCS can't only rely on the external grid and has to have its own resources. As can be stated from analysis of Case-2, also the diesel-solar PV-BESS mix EVCS is the most economically favorable option and a fairly small carbon footprint, when compared to a diesel-based EVCS. Although a solar PV with BESS-based EVCS, which has no carbon footprint, the NPC is higher.

Finally, analysis is also carried out to determine the break-even grid extension distance from the isolated EVCS location. It is noted that the solar PV with BESS based isolated EVCS can benefit the most by grid connectivity, followed by the diesel-based isolated EVCS, because of their high costs.

Chapter 6
Conclusions

6.1 Summary

The research presented in this thesis concentrated on the smart PEV charging station operation and design considering distribution system impact. The motivations for this research, and review of associated literature, which laid out the main research objectives, were presented in Chapter 1.

In Chapter 2, the relevant background topics pertaining to the research were discussed. The basic categories and characteristics of PEVs, their SOC and BCB, and charging levels were discussed. The chapter further discussed power system structures with different voltage levels, the primary distribution feeder configurations, the general power flow equations, and OPF formulation. An introduction to queuing theory including its general definition, important characteristics, examples of common queuing systems and applications were discussed briefly. Finally, NN based simulations, NN structure, and mathematical functions of NN models were discussed.

Chapter 3 presented a queuing analysis based methodology for modeling the 24-hour charging demand profile of a PEV charging station. The arrival rates were considered to depend on customer behavior and their response to PEV charging price. Model of the PEV service time considering the SOC of the vehicle battery and the effect of the BCB was presented. The impact of PEV load models on distribution systems was studied for a deterministic case, and the impact of uncertainties was examined and compared using the stochastic OPF and the MPC approaches.

In Chapter 4, the total charging load at an EVCS was modeled in terms of controllable parameters; the load model developed using a queuing model followed by a neural network. The queuing model constructed a data set of PEV charging parameters which were input to the NN to determine the controllable EVCS load model. The smart EVCS load was a function of number of PEVs charging simultaneously, total charging current, arrival rate, and time; and various classes of PEVs. The EVCS load was integrated within a

distribution operations framework to determine the optimal operation and smart charging schedules of the EVCS. The performance of a smart EVCS vis-à-vis an uncontrolled EVCS was examined to emphasize the DR contributions of a smart EVCS and its integration into distribution operations.

Chapter 5 presented the optimal design of a hybrid, renewable energy based EVCS with the goal of minimizing the lifecycle cost, while taking into account environmental emissions. Different EVCS configurations such as- isolated EVCS, and grid connected EVCS as a smart energy hub were designed and compared to evaluate their economics, operational performance and environmental emissions. Analysis was also carried out to determine the break-even distance for connection of the smart EVCS with the main grid. The well-known energy modeling software for hybrid renewable energy systems, HOMER, was used in the studies reported in this chapter.

6.2 Contributions

The main contributions of the research presented in this thesis are as follows:

- A novel queuing model based representation of the PEV charging demand of a charging station was proposed considering two different arrival rates; the arrival rates being modeled as continuous and random, non-homogeneous Poisson processes. For the first time, a detailed representation of the BCB of PEVs and the SOC, and the time taken to charge PEVs, including a finite waiting time was considered in the queuing model.
- The developed PEV load model was integrated within a distribution operation model for analysis of impacts considering both deterministic and stochastic conditions.
- A novel approach to model the EVCS load as smart load was presented by proposing a Charging Station Controllable Load Estimator (CSCLE) which comprised a queuing model, used to construct the PEV charging data set as an input to a NN; and a NN model, to estimate the smart charging demand profile of the EVCS as a function of different parameters.

Thereafter, the proposed smart load model of the EVCS was integrated within a novel distribution operations framework that considered PEV smart charging constraints, and EVCS related constraints. The smart operational decisions at the EVCS were determined from the perspectives of both the LDC and the EVCS owner.

- The EVCS smart charging framework was envisaged to receive peak demand signals from the LDC and accordingly adjust its charging schedules to provide a DR service to the LDC. The contribution of such smart EVCS loads to DR and their integration in the distribution systems operation framework was examined.
- A novel configuration of an EVCS was proposed wherein the EVCS operated as a smart energy hub. The optimal design of such a smart EVCS considering various energy supply options and with realistic inputs on their physical, operating and economic characteristics was determined.

6.3 Future Work

Based on the research presented in this thesis, some further research ideas and directions can be identified, as follows:

- The queuing model based PEV charging load models were developed for the charging stations only. These models could be extended to account for different charging facilities such as, parking lots, offices, and shopping centers with different charging levels.
- Since a distribution system may include unbalanced configurations, detailed three-phase models need be developed to examine the impact of PEV charging loads. Moreover, an optimization model could be developed to determine the optimal capacity required of the distribution feeders to accommodate PEVs so that the existing plans could be modified based on the optimal sizing of EVCS for the existing distribution system.

- A rational driver will always select the EVCS considering traffic factors, such as its location and distance and hence the optimal siting and sizing of EVCS need also be studied. Also, in large scale distribution systems and in densely populated areas, there may be a need for multiple EVCS. Hence optimization models could be developed to determine the optimal charging schedule for all the charging stations considering the proposed smart charging load model for each EVCS.
- The PEV customers may be interested in partial charging instead of full charging at the charging station. Moreover, a priority service may be possible at the charging station, so that the customer can opt for immediate charging by paying a high price instead of waiting. Including of these features can significantly affect the charging schedules at the charging station, which can be studied.
- In the optimal design model of EVCS, the initial costs of charging station for example, land costs, and chargers' costs could be included. Also, the analysis could be carried out to examine the impact of PEV charging environment, for example, the cost of CO_2 reduction be incorporated along with the renewable energy sources.

References

[1] Transport Canada. [Online]. Available: http://www.tc.gc.ca/environment/menu.htm#climatechange.

[2] Ontario Power Authority, "Ontario's Integrated Power System Plan: Scope and Overview," June 2006 [online]. Available: http://www.powerauthority.on.ca/Storage/24/1922_OPA__IPSP_Scope_and_Overview.pdf.

[3] Ontario Ministry of Energy, "Green Energy Act (GEA)" [Online]. Available: http://www.energy.gov.on.ca/en/green-energy-act/#.UyEZbvmSx1Y.

[4] Ontario Ministry of Transportation, "A plan for a greener Ontario" [Online]. Available:http://www.mto.gov.on.ca/english/dandv/vehicle/electric/plan-greener-ontario/ev-pub-en-june-2011.pdf.

[5] Ontario Ministry of Transportation, "Electric vehicle incentive and charging incentive programs"[Online].Available: https://news.ontario.ca/opo/en/2016/02/ontario-making-electric-vehicles-more-affordable.html?_ga=1.97598809.779842822.1463153117.

[6] D. Hurst, J. Gartner, "Electric vehicle geographic forecasts," Pike Research , 2012 [Online].Available:http://www.navigantresearch.com/wordpress/wpcontent/uploads/2012/09/EVGEO-12-Executive-Summary.pdf.

[7] A. Hajimiragha, C. A. Cañizares, M.W. Fowler, and A. Elkamel, "Optimal transition to plug-in hybrid electric vehicles in Ontario, Canada, considering the electricity-grid limitations," IEEE Transactions on Industrial Electronics, vol. 57, pp. 690–701, Feb. 2010.

[8] M. S. ElNozahy, and M. M. A. Salama, "A comprehensive study of the impacts of PHEVs on residential distribution networks," IEEE Transactions on Sustainable Energy, vol. 5, no. 1, Jan 2014.

[9] M. D. Galus, R. A. Waraich, F. Noembrini, K. Steurs, G. Georges, K. Boulouchos, K. W. Axhausen, and G. Andersson, "Integrating power systems, transport systems and vehicle technology for electric mobility impact assessment and efficient control," IEEE Transactions on Smart Grid, vol. 3, no. 2, Jun 2012.

[10] Z. Luo, Z. Hu, Y. Song, Z. Xu, and H. Lu, "Optimal coordination of plug-in electric vehicles in power grids with cost-benefit analysis—part I: enabling techniques," IEEE Transactions on Power Systems, vol. 28, no.4, Nov 2013.

[11] A. Ashtari, E. Bibeau, S. Shahidinejad, and T. Molinski, "PEV charging profile prediction and analysis based on vehicle usage data," IEEE Transactions on Smart Grid, vol. 3, no. 1, Mar 2012.

[12] Summary of travel trends: 2009 National Household Travel Survey, Federal Highway Administration, USA, 2012 [Online]. Available: http://nhts.ornl.gov/2009/pub/stt.pdf.

[13] D. Wu, D. C. Aliprantis, and K. Gkritza, "Electric energy and power consumption by light-duty plug-in electric vehicles," IEEE Transactions on Power Systems, vol. 26, no. 2, pp. 738-746, May 2011.

[14] A. Rautiainen, S. Repo, P. Järventausta, A. Mutanen, K. Vuorilehto, and K. Jalkanen, "Statistical charging load modeling of PHEVs in electricity distribution networks using national travel survey data,'' IEEE Transactions on Smart Grid, vol. 3, no. 4, Dec 2012.

[15] P. Grahn, J. Munkhammar, J. Widén, K. Alvehag, and L. Söder, "PHEV home-charging model based on residential activity patterns,'' IEEE Transactions on Power Systems, vol. 28, no. 3, Aug 2013.

[16] RELOAD database documentation and evaluation and use in NEMS" [Online]. Available: http://www.onlocationinc.com/LoadShapes- Reload2001.pdf.

[17] K. Zhou and L. Cai, “Randomized PHEV charging under distribution grid constraints,’’ IEEE Transactions on Smart Grid, vol. 5, no. 2, Mar 2014.

[18] A. O’Connell, D. Flynn, and A. Keane, “Rolling multi-period optimization to control electric vehicle charging in distribution networks,’’ IEEE Transactions on Power Systems, vol. 29, no. 1, Jan 2014.

[19] M. F. Shaaban, Y. M. Atwa, and E. F. El-Saadany, “PEVs modeling and impacts mitigation in distribution networks,” IEEE Transactions on Power Systems, vol. 28, no. 2, May 2013.

[20] C. Liu, J. Wang, A. Botterud, Y. Zhou, and A. Vyas, “Assessment of impacts of PHEV charging patterns on wind-thermal scheduling by stochastic unit commitment,” IEEE Transactions on Smart Grid, vol. 3, no. 2, Jun 2012.

[21] D. Steen, L. A. Tuan, O. Carlson, and L. Bertling, “Assessment of electric vehicle charging scenarios based on demographical data,” IEEE Transactions on Smart Grid, vol. 3, no. 3, Sep 2012.

[22] X. Xi and R. Sioshansi, “Using price-based signals to control plug-in electric vehicle fleet charging,” IEEE Transactions on Smart Grid, vol. 5, no. 3, May 2014.

[23] J. M. Foster, and M. C. Caramanis, “Optimal power market participation of plug-in electric vehicles pooled by distribution feeder,” IEEE Transactions on Power Systems, vol. 28, no. 3, Aug 2013.

[24] C. T. Li, C. Ahn, H. Peng, and J. Sun, “Synergistic control of plug-in vehicle charging and wind power scheduling,” IEEE Transactions on Power Systems, vol. 28, no. 2, May 2013.

[25] Q. Li, R. Negi, and M. D. Ili´c, "A queueing based scheduling approach to plug-in electric vehicle dispatch in distribution systems", [Online]. Available: http://arxiv.org/pdf/1203.5449v1.pdf

[26] J. G. Vlachogiannis, “Probabilistic constrained load flow considering integration of wind power generation and electric vehicles,” IEEE Transactions on Power Systems, vol. 24, no. 4, pp. 1808–1817, Nov 2009.

[27] S. Bae, and A. Kwasinski, “Spatial and temporal model of electric vehicle charging demand,” IEEE Transactions on Smart Grid, vol. 3, no. 1, Mar 2012.

[28] G. Li and X. Zhang, “Modeling of plug-in hybrid electric vehicle charging demand in probabilistic power flow calculations,” IEEE Transactions on Smart Grid, vol. 3, no. 1, Mar 2012.

[29] S. Deilami, A. S. Masoum, P. S. Moses, and M.A. S. Masoum, “Real-time coordination of plug-in electric vehicle charging in smart grids to minimize power losses and improve voltage profile,” IEEE Transactions on Smart Grid, vol. 2, no. 3, Sep 2011.

[30] Z. Li, Q. Guo, H. Sun, S. Xin, and J. Wang, "A new real-time smart-charging method considering expected electric vehicle fleet connections," IEEE Trans. Power Syst, vol. 29, no. 6, pp. 3114-3115, Nov. 2014.

[31] W. Su, J. Wang, K. Zhang, and A. Q. Huang, "Model predictive control-based power dispatch for distribution system considering plug-in electric vehicle uncertainty," Electr Pow Syst Res, vol. 106, pp. 29-35, 2014.

[32] L. Bremermann, M. Matos, J. Peças Lopes, M. Rosa, “Electric vehicle models for evaluating the security of supply,” Electric Power Systems Research, vol.111, pp.32-39, Fevereiro, 2014.

[33] S. Dhameja, “Electric Vehicle Battery Systems”, Newnes, 2001, ISBN 0750699167.

[34] A. L. Zhang, and Y. Li, “Optimal management for parking-lot electric vehicle charging by two-stage approximate dynamic programming”, IEEE Transactions on Smart Grid (in print).

[35] B. H. Zhang, Z. Hu, Z. Xu, and Y. Song, “Optimal planning of PEV charging station with single output multiple cables charging spots” IEEE Transactions on Smart Grid, (in print).

[36] C. E. Akhavan-Rezai, M. Shaaban, E. El-Saadany, and F. Karray, “Online intelligent demand management of plug-in electric vehicles in future smart parking lots”, IEEE Systems Journal (in print).

[37] C. K. Wen, J. C. Chen, J. H. Teng, and P. Ting, “Decentralized plug-in electric vehicle charging selection algorithm in power systems,” IEEE Transaction on Smart Grid, vol. 3, no. 4, pp. 1779 -1789, Dec. 2012.

[38] H. Liu, Z. Hu, Y. Song, J. Wang, and X. Xie, “Vehicle-to-grid control for supplementary frequency regulation considering charging demands,” IEEE Transaction on Power System, vol. 30, no. 6, pp. 3110-3119, November 2015.

[39] P. Richardson, D. Flynn, and A. Keane, “Local versus centralized charging strategies for electric vehicles in low voltage distribution systems,” IEEE Transaction on Smart Grid, vol. 3, no. 2, pp. 1020-1028, June 2012.

[40] J. A. P. Lopes, F. J. Soares and P. M. R. Almeida, “Integration of electric vehicles in the electric power system”, Proceedings of the IEEE, vol. 99, No. 1, pp. 168-183, 2011.

[41] G. T. Heydt, “The impact of electric vehicle deployment on load management strategies,” IEEE Transactions on Power Apparatus and Systems, vol. 1, no. 144, pp. 1253–1259, May 1983.

[42] K. Clement-Nyns, E. Haesen, and J. Driesen, “The impact of charging plug-in hybrid electric vehicles on a residential distribution grid,” IEEE Transactions on Power Systems, vol. 25, no.1, pp. 371–380, Feb 2010.

[43] E. Sortomme, M. M. Hindi, S. D. MacPherson, and S. S. Venkata, “Coordinated charging of plug-in hybrid electric vehicles to minimize distribution system losses,” IEEE Transactions on Smart Grid, vol. 2, no. 1, Mar 2011.

[44] C. Canizares, J. Nathwani, K. Bhattacharya, M. Fowler, M. Kazerani, R. Fraser, I. Rowlands, H. Gabbar, “Towards an Ontario action plan for plug-in-electric vehicles (PEVs),” Waterloo Institute for Sustainable Energy, University of Waterloo, May 17, 2010.

[45] D. Wu, D. C. Aliprantis, and L. Ying, “Load scheduling and dispatch for aggregators of plug-in electric vehicles,” IEEE Transactions on Smart Grid, vol. 3, no. 1, Mar 2012.

[46] I. Sharma, C. A. Cañizares, and K. Bhattacharya, “Smart charging of PEVs penetrating into residential distribution systems,” IEEE Transactions on Smart Grid, vol. 5, no. 3, May 2014.

[47] Q. Gong, S. Mohler, V. Marano, and G. Rizzoni, ” Study of PEV charging on residential distribution transformer life”, IEEE Transactions on Smart Grid, vol. 3, no. 1, Mar 2012.

[48] A. D. Hilshey, P. D. H.Hines, P. Rezaei, and J. R. Dowds, “Estimating the impact of electric vehicle smart charging on distribution transformer aging,” IEEE Transactions on Smart Grid, vol. 4, no. 2, Jun 2013.

[49] M. F. Shaaban, and E. F. El-Saadany,“Accommodating high penetrations of PEVs and renewable DG considering uncertainties in distribution systems,” IEEE Transactions on Power Systems, vol. 29, no.1, Jan 2014.

[50] W. Su, J. Wang, and J. Roh, “Stochastic energy scheduling in micro-grids with intermittent renewable energy resources,” IEEE Transactions on Smart Grid, vol. 5, no. 4, July 2014.

[51] M. E. Khodayar, L. Wu, and M. Shahidehpour, “Hourly coordination of electric vehicle operation and volatile wind power generation in SCUC,” IEEE Transactions on Smart Grid, vol. 3, no. 3, Sep 2012.

[52] S. J. Gunter, K. K. Afridi, and D. J. Perreault, “Optimal design of grid-connected PEV charging systems with integrated distributed resources,” IEEE Transactions on Smart Grid, vol. 4, no. 2, Jun 2013.

[53] J. M. Foster, G. Trevino, M. Kuss, and M. C. Caramanis, “Plug-in electric vehicle and voltage support for distributed solar: theory and application,” IEEE Systems Journal, vol. 7, no. 4, Dec 2013.

[54] F. Guo, E. Inoa,W. Choi, and J. Wang,“Study on global optimization and control strategy development for a PHEV charging facility,” IEEE Transactions on Vehicular Technology, vol. 61, no. 6, Jul 2012.

[55] J. H. Zhao, F. Wen, Z. Y. Dong, Y. Xue, and K. P. Wong, “Optimal dispatch of electric vehicles and wind power using enhanced particle swarm optimization,” IEEE Transactions on Industrial Informatics, vol. 8, no. 4, Nov 2012.

[56] W. Hu, C. Su, Z. Chen, and B. Bak-Jensen, "Optimal operation of plug-in electric vehicles in power systems with high wind power penetrations," IEEE Transactions on Sustainable Energy, vol. 4, no. 3, Jul 2013.

[57] C. X. Wu, C. Y. Chung, F. S. Wen, and D. Y. Du, "Reliability/cost evaluation with PEV and wind generation system," IEEE Transactions on Sustainable Energy, vol. 5, no. 1, Jan 2014.

[58] The 2011 Transportation Tomorrow Survey [Online]. Available: http://www.dmg.utoronto.ca/reports/ttsreports.html.

[59] Ontario hydro Time of use pricing rates [Online]. Available: http://www.ontario-hydro.com/index.php?page=current_rates.

[60] S. Onori, L. Serrao, and G. Rizzoni, Hybrid electric vehicles: energy management strategies, Springer, New York, 2016.

[61] A comprehensive guide to plug-in hybrid vehicles, Hybrid Cars, [Online] Available: http://www.hybridcars.com/plug-in-hybrid-cars#battery, (2011).

[62] S. W. Hadley, "Impact of plug-in hybrid vehicles on the electric grid", ORNL, [Online]Available:http://apps.ornl.gov/~pts/prod/pubs/ldoc3198_plug_in_paper_final.pdf, October, 2006.

[63] M. Duvall, "Grid integration of plug-in hybrid and electric vehicles," in PHEV Executive Summit, Electric Power Research Institute (EPRI), July 2009.

[64] T. Gonen, Electric Power Distribution System Engineering, McGraw Hill, 1986.

[65] W. H. Kersting, Distribution System Modeling and Analysis, Taylor & Francis Group, 2007.

[66] M. M. A. Salama, Lecture Notes on the Course, “Distribution Systems”, University of Waterloo, Winter 2010.

[67] D. Rajicic, and A. Bose, “A modification to the fast decoupled power flow for networks with high R/X ratios,” IEEE Transactions on Power Systems, vol. 3, no. 2, pp. 743-746, 1988.

[68] U. Narayan Bhat, An Introduction to Queueing Theory: Modeling and Analysis in Applications, Birkhauser Boston USA, 2008.

[69] D. Gross, J. F. Shortle, J. M. Thompson, and C. M. Harris, Fundamentals of Queuing Theory, Hoboken New Jersey, 2008.

[70] K. Gurney, An Introduction to Neural Networks, 1st ed. UCL Press Limited, 1997.

[71] D. Chen and R. Mohler, “Neural-network-based load modeling and its use in voltage stability analysis,” IEEE Transactions on Control Systems Technology, vol. 11, no. 4,pp. 460–470, July 2003.

[72] D. Park, M. El-Sharkawi, I. Marks, R.J., L. Atlas, and M. Damborg, “Electric load forecasting using an artificial neural network,” IEEE Transactions on Power Systems, vol. 6, no. 2, pp. 442–449, May 1991.

[73] H. C. Tijms, A First Course in Stochastic Models, John Wiley & Sons Ltd, The Netherlands, 2003.

[74] GAMS: The Solver Mannuals. GAMS Development Corporation, [Online] Available: www.gams.com.

[75] Y. Cao, Y. Tan, C. Li, and C. Rehtanz, "Chance-constrained optimization-based unbalanced optimal power flow for radial distribution networks," IEEE Trans. Power Del, vol. 28, no. 3, July 2013.

[76] F. Allgöwer, R. Findeisen, and Z. Nagy, “Nonlinear model predictive control: from theory to application”, J. Chin. Inst. Chem. Engrs., Vol. 35, No. 3, 299-315, 2004.

[77] M. E. Baran and F. F. Wu, “Optimal sizing of capacitor placed on radial distribution systems,” IEEE Trans. Power Del. , vol. 4, no. 1, pp. 735–743, Jan. 1989.

[78] EasyFit Software [Online].Available: http://www.mathwave.com/en/home.html.

[79] I. Adan, and J. Resing, “Queueing system”, Dept. Math. Comput. Sci., Eindhoven Univ. Technol., Eindhoven, The Netherlands, 2015. [Online] Available: http://www.win.tue.nl/~iadan/queueing.pdf.

[80] G.M. Kisacikoglu, B. Ozpineci, and L. Tolbert, “EV/PHEV bidirectional charger assessment for V2G reactive power operation,” IEEE Trans. Power Electron., vol. 28, no. 12, pp. 5717-5727, 2013.

[81] H.M. Falahi, H. Chou, M. Ehsani, L. Xie, and K. Purry, “Potential power quality benefits of electric vehicles,” IEEE Trans. Sustainable Energy, vol. 4, no. 4, pp. 1016-1023, 2013.

[82] HOMER analysis. [Online] Available: https://analysis.nrel.gov/homer/.

[83] R. Panneerselvam, Engineering Economics, 2nd edition, PHI Learning Private Limited, New Delhi, 2013.

[84] Independent Electricity System Operator FIT program [Online] Available: http://fit.powerauthority.on.ca/.

[85] Drive-4-Data University of Waterloo. [Online] Available: https://wise.uwaterloo.ca/drive4data.

[86] NASA Surface meteorology and solar energy. [Online] Available: http://eosweb.larc.nasa.gov/sse/.

[87] O. Hafez, and K. Bhattacharya, “Optimal planning and design of a renewable energy based supply system for micro-grids,” International Journal of Renewable Energy, Vol. 45, 2012, pp.7-15.